

**EFFECTS OF FUNCTIONALIZED CARBON NANOTUBES WITH
SURFACTANTS ON THE MECHANICAL AND THERMAL PROPERTIES
OF HIGH DENSITY POLYETHYLENE (HDPE) NANOCOMPOSITES**

BY

AHMAD AKANBI ADEWUNMI

A Thesis Presented to the
DEANSHIP OF GRADUATE STUDIES

KING FAHD UNIVERSITY OF PETROLEUM & MINERALS

DHAHRAN, SAUDI ARABIA

In Partial Fulfillment of the
Requirements for the Degree of

MASTER OF SCIENCE

In
CHEMICAL ENGINEERING

JUNE 2011

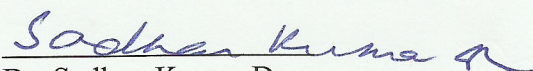
KING FAHD UNIVERSITY OF PETROLEUM & MINERALS
DHAHRAN 31261, SAUDI ARABIA
DEANSHIP OF GRADUATE STUDIES

This thesis, written by Ahmad Akanbi Adewunmi, under the direction of his thesis advisor and approved by his thesis committee, has been presented to and accepted by the Dean of Graduate Studies, in partial fulfillment of the requirements for the degree of **MASTER OF SCIENCE IN CHEMICAL ENGINEERING.**

Thesis Committee



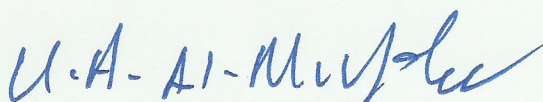
Dr. Muataz Ali Atieh
(Advisor)



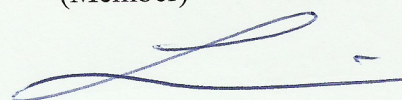
Dr. Sadhan Kumar De
(Co-Advisor)



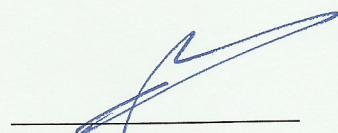
Dr. Abdulhadi A. Al-Juhani
(Member)



Dr. Usamah Al-Mubaiyedh
(Departmental Chairman)



Dr. Tahar Laoui
(Member)



Dr. Salam A. Zummo
(Dean of Graduate Studies)



Dr. Rachid Sougrat
(Member)

26/9/11

Date

DEDICATION

This thesis work is dedicated to my loving father, Imam Tajudeen Mustafa Adewunmi, Al-Ilaaro. May Allah (SWT) continue to protect and shower His endless bliss on him.

ACKNOWLEDGEMENT

All praise and adoration is due to Almighty Allah (SWT) the Lord of the worlds. May the peace and blessing of Almighty Allah (SWT) be upon the noble prophet Muhammad (SAW), his companion and family till the day of reckoning.

I give thanks to Almighty Allah (SWT) for sparing my life from the inception of my master degree program up till this moment. He is worthy of my praise and immense gratitude.

I wholeheartedly thank my humble advisor, Dr. Muataz Ali Atieh, for his moral and technical support throughout this work. He always assists whenever the need arises. May Allah (SWT) bestow upon him and his family His pleasure. My appreciation also goes to my co-advisor, Dr. Sadhan Kumar De, for his meaningful suggestions and having time to correct this manuscript. My sincere gratitude goes to all my committee members: Dr. Abdulhadi A. Al-Juhani, Dr. Tahar Laoui and Dr. Rachid Sougrat for their assistance, suggestions and time to scrutinize and correct the original manuscript. Without your efforts, this work would not have got to this stage. I appreciate you all.

Special thanks to the Departmental Chairman, Staff, Faculty members for providing me conducive learning atmosphere. Also, to the entire Nigerian community in KFUPM, I really enjoy your company. I ask Allah (SWT) to strengthen our relationship.

My deep appreciation also extend to my parents; Imam Tajudeen Mustafa Adewunmi Al-Ilaaro, Hajia Fatima Adenike Adewunmi of blessed memory and Hajia Khadijat Adewunmi. Also, to a loving father, Sheikh (Engr) Abdur-Razaq Shittu; Umm

Aqiqiyah, Alhaji Rahman Idowu, Ustaz Saheed Sanni, my fiancée and all my siblings. I thank you all for your words of encouragement and prayers.

Lastly, my acknowledgement goes to the governing council of King Fahd University of Petroleum & Minerals (KFUPM) for providing me scholarship throughout my master degree program in Chemical Engineering.

TABLE OF CONTENTS

DEDICATION.....	iii
ACKNOWLEDGEMENT.....	iv
TABLE OF CONTENTS.....	vi
LIST OF TABLES.....	ix
LIST OF FIGURES.....	x
THESIS ABSTRACT.....	xiv
THESIS ABSTRACT (ARABIC).....	xvi
CHAPTER 1.....	1
1.0 INTRODUCTION.....	1
1.1 BACKGROUND.....	1
1.2 STATEMENT OF THE PROBLEM.....	3
1.3 RESEARCH OBJECTIVES AND SIGNIFICANCE.....	4
CHAPTER 2.....	6
2.0 LITERATURE REVIEW.....	6
2.1 BACKGROUND.....	6
2.2 POLYETHYLENE, HIGH DENSITY (HDPE).....	7
2.3 HISTORY OF POLYETHYLENE.....	7
2.4 PROPERTIES OF POLYETHYLENE.....	8
2.4.1 Molecular Structure and Morphology.....	8
2.4.2 General Properties.....	10
2.5 CARBON NANOTUBES.....	12
2.5.1 Structure and properties of carbon nanotubes.....	13
2.5.2 Dispersion of CNTs (Nature of dispersion for CNTs).....	20
2.6 MECHANICAL DISPERSION OF CNTs.....	22
2.6.1 Ultrasonication.....	22

2.6.2 Calendering process.....	24
2.6.3 Ball milling.....	28
2.6.4 Stir and extrusion.....	32
2.7 CNT/POLYMER NANOCOMPOSITES.....	34
2.7.1 Classification of CNT/ polymer nanocomposites.....	34
2.8 FABRICATION FOR CNT POLYMER/COMPOSITES.....	35
2.8.1. Solution mixing.....	35
2.8.2.Melt blending.....	36
2.8.3.In situ polymerization.....	36
2.8.4.Latex technology.....	37
2.8.5.Other methods.....	38
2.9. FUNCTIONALIZATION OF CNTs.....	38
2.9.1 Chemical functionalization.....	39
2.9.2 Physical functionalization.....	40
2.9.3 Applications of surfactants for dispersing carbon nanotubes.....	41
CHAPTER 3.....	43
3.0 EXPERIMENTAL METHODOLOGIES.....	43
3.1 MATERIALS.....	43
3.1.1 Acid Modification of MWCNT.....	44
3.1.2 Substitution of Carboxylic (-COOH) group with different Surfactants.....	46
3.1.3 Sample preparation.....	50
3.1.4 Tensile properties.....	50

3.1.5 Thermal analysis of the samples.....	50
3.1.6 Rheological characterization.....	51
CHAPTER 4.....	52
4.0 RESULTS AND DISCUSSION.....	52
4.1 THE FOURIER TRANSFORM INFRARED SPECTROSCOPY CHARACTERIZATION.....	52
4.2 CARBON NANOTUBES DISPERSION.....	61
4.3 TENSILE PROPERTIES OF HDPE NANOCOMPOSITES.....	64
4.4 EFFECT OF CNTs ON THE ENERGY ABSORPTION OF HDPE NANOCOMPOSITES.....	70
4.5 THERMAL ANALYSIS OF HDPE NANOCOMPOSITES.....	72
4.6 RHEOLOGICAL PROPERTIES.....	105
CHAPTER 5.....	121
5.0 CONCLUSIONS AND RECOMMENDATIONS.....	121
5.1 CONCLUSIONS.....	121
5.2 RECOMMENDATIONS.....	122
APPENDIX A: Stress-Strain curves of HDPE nanocomposites.....	124
APPENDIX B: Percentage increase and decrease in mechanical properties of HDPE nanocomposites	128
APPENDIX C: Nomenclatures.....	129
REFERENCES.....	131
VITAE	140

LIST OF TABLES

Table 1.Properties of some typical polyethylene	11
Table 2.Dimension and corresponding number of particles in composites for different fillers.	21
Table 3.Comparison of various techniques for CNT dispersion in polymer composites.....	33
Table 4.Mechanical properties of MWCNT-HDPE nanocomposites.....	57
Table 5.Crystallization temperatures, melting temperatures and enthalpies.....	65
Table 6.The onset temperatures and degradation temperatures.....	94

LIST OF FIGURES

Figure.1.Computer-generated image of carbon nanotubes.....	15
Figure.2 It is possible to create a single wall carbon nanotube by rolling-up a graphene sheet. 16	
Figure.3.The conductivity of HDPE filled with SDS-coated SWNT.....	19
Figure.4.Sonicator with different modes for CNT dispersion (A: water bath sonicator; B:probe/horn sonicator), and the effect of sonication on the structure of CNTs.....	23
Figure.5.Calendering (or three roll mills) machine used for particle dispersion into a polymer matrix (A) and corresponding schematic showing the general configuration and its working mechanism (B).....	26
Figure.6.TEM image of CNTs dispersed by calendaring machine in an epoxy matrix. Note that dispersed CNTs and the aggregated ones co-existed in the nanocomposites.....	27
Figure.7. Schematics of ball milling technique (A) and container (B).....	30
Figure.8.TEM images of pristine CNTs and those milled after 9h (A: pristine; B: milled with NH_4CO_3 ; C: milled without NH_4CO_3). CNTs milled with NH_4CO_3) were more effectively disentangled and shortened than those without the chemical. After (Ma PC, Wang SQ, et al 2009).....	31
Figure.9. Chemical modification multiwall of carbon nanotubes (MWCNTs) through thermal oxidation.....	44
Figure.10. Mechanism of C_{18} modification of MWCNT (MWCNT- C_{18}).....	45
Figure.11. Mechanism of phenol modification of MWCNT (MWCNT-phenol).....	46

Figure.12. FTIR of multiwalled carbon nanotubes (MWCNT).....	50
Figure.13. FTIR of MWCNT modified with COOH.....	51
Figure.14. FTIR of MWCNT-C ₁₈	52
Figure.15. FTIR of MWCNT-phenol.....	53
Figure.16.SEM images (a)Neat HDPE; (b) HDPE/MWCNT-C ₁₈ 1wt%.....	54
Figure.17. SEM images (c) HDPE/MWCNT-C ₁₈ 3%; (d) HDPE/MWCNT-C ₁₈ 5wt%.....	55
Figure.18.Ultimate Strength of HDPE nanocomposites.....	58
Figure.19.Young's modulus of HDPE nanocomposites.....	53
Figure.20.Strain at break of HDPE nanocomposites.....	60
Figure.21.The toughness as a function of wt% for HDPE nanocomposites.....	62
Figure.22.Melting temperature curves of MWCNT/HPDE nanocomposites.....	66
Figure.23.Crystallization temperature curves of MWCNT-HPDE nanocomposites.....	67
Figure.24.Melting temperature curves of MWCNT/COOH-HPDE nanocomposites.....	68
Figure.25.Crystallization temperature curves of MWCNT/COOH-HPDE nanocomposites....	69
Figure.26 Melting temperature curves of MWCNT/C ₁₈ -HPDE nanocomposites	70
Figure.27.Crystallization temperature curves of MWCNT/C ₁₈ -HPDE nanocomposites.....	71
Figure.28.Melting temperature curves of MWCNT/PHENOL-HPDE nanocomposites.....	72
Figure.29.Crystallization temperature curves of MWCNT/PHENOL-HPDE nanocomposites...	73
Figure.30.Influence of MWCNT content on peak crystallization and melting temperature ($T_{c, peak}$ and $T_{m, peak}$) for HDPE/MWCNT nanocomposites.....	75
Figure.31.Influence of MWCNT content on peak crystallization and melting temperature ($T_{c, peak}$ and $T_{m, peak}$) for MWCNT-COOH/HDPE nanocomposites.....	76
Figure.32. Influence of MWCNT content on peak crystallization and melting temperature	

($T_{c, \text{ peak}}$ and $T_{m, \text{ peak}}$) for MWCNT-C ₁₈ /HDPE nanocomposites.....	77
Figure.33.Influence of MWCNT content on peak crystallization and melting temperature ($T_{c, \text{ peak}}$ and $T_{m, \text{ peak}}$) for MWCNT-phenol/HDPE nanocomposites.....	78
Figure.34.Influence of MWCNT content on the degree of crystallinity (X_c) for MWCNT/HDPE nanocomposites.....	80
Figure.35.Influence of MWCNT content on the degree of crystallinity (X_c) for MWCNT-COOH/HDPE nanocomposites.....	81
Figure.36.Influence of MWCNT content on the degree of crystallinity (X_c) for MWCNT-C ₁₈ /HDPE nanocomposites.....	82
Figure.37.Influence of MWCNT content on the degree of crystallinity (X_c) for MWCNT-phenol/HDPE nanocomposites.	83
Figure.38.TGA curves of MWCNT-HDPE nanocomposites.....	85
Figure.39.TGA curves of MWCNT-COOH/HDPE nanocomposites.....	86
Figure.40.TGA curves of MWCNT-C ₁₈ /HDPE nanocomposites.....	87
Figure.41.TGA curves of MWCNT-phenol/HDPE nanocomposites.....	88
Figure.42.DTG curves of MWCNT/HDPE nanocomposites.....	89
Figure.43.DTG curves of MWCNT-COOH/HDPE nanocomposites.....	90
Figure.44.DTG curves of MWCNT-C ₁₈ /HDPE nanocomposites	91
Figure.45.DTG curves of MWCNT-phenol/HDPE nanocomposites.....	92
Figure 46.Rheological response: complex viscosity of MWCNT/HDPE nanocomposites as a function of frequency at 200 °C.....	97
Figure 47.Rheological response: complex viscosity of MWCNT-COOH/HDPE nanocomposites as a function of frequency at 200 °C.....	98
Figure 48.Rheological response: complex viscosity of MWCNT-C ₁₈ /HDPE nanocomposites as a function of frequency at 200 °C	99

Figure.49.Rheological response: complex viscosity of MWCNT-PHENOL/HDPE nanocomposites as a function of frequency at 200 °C.....	100
Figure.50.Rheological response: storage modulus of MWCNT/HDPE nanocomposites as a function of frequency at 200 °C.....	102
Figure 51. Rheological response: storage modulus of MWCNT-COOH/HDPE nanocomposites as a function of frequency at 200 °C.....	103
Figure 52. Rheological response: storage modulus of MWCNT-C ₁₈ /HDPE nanocomposites as a function of frequency at 200 °C.....	104
Figure 53. Rheological response: storage modulus of MWCNT-PHENOL/HDPE nanocomposites as a function of frequency at 200 °C.....	105
Figure 54. Rheological response: loss modulus of MWCNT/HDPE nanocomposites as a function of frequency at 200 °C.....	107
Figure 55. Rheological response: loss modulus of MWCNT-COOH/HDPE nanocomposites as a function of frequency at 200 °C.....	108
Figure 56. Rheological response: loss modulus of MWCNT-C ₁₈ /HDPE nanocomposites as a function of frequency at 200 °C.....	109
Figure 57. Rheological response: loss modulus of MWCNT-PHENOL/HDPE nanocomposites as a function of frequency at 200 °C.....	110

THESIS ABSTRACT

Full Name: Ahmad Akanbi Adewunmi

Thesis Title: Effects of functionalized carbon nanotubes with surfactants on the mechanical and thermal properties of High Density Polyethylene (HDPE) nanocomposites.

Major Field: Chemical Engineering

Date of Degree: June, 2011

Multiwalled carbon nanotubes (CNTs) have been used with polymers from date of their inception to make composites having remarkable properties and materials. In this work, the nanocomposites were prepared by blending the CNTs with high density polyethylene (HDPE) using brabender mixing machine at various loadings (1 wt%, 3 wt%, and 5 wt%). The blending was repeated for the surfactants (CNTs/COOH, CNTs/C₁₈, and CNTs/PHENOL). The surface morphology of CNTs and their functional groups were characterized using Fourier Transform Infrared (FTIR) and Scanning Electron Microscopy (SEM). A significant improvement on mechanical properties of HDPE/CNTs nanocomposites were observed by increasing the loading of raw and functionalized CNTs. From thermal analysis study, it was found that the melting and crystallization temperatures of the composites are slightly affected by the addition of raw and functionalized CNTs. However, clear enhancements on the degree of crystallization of the nanocompopsites by adding 1 wt% of CNTs while further increase in the amounts of raw and functionalized CNTs caused a clear reduction in the degree of crystallization. From rheological characterization, the complex viscosity (η') was lowered at 1wt% loading and increased with addition of

raw and functionalized CNTs. Likewise, the storage modulus (G') was found to be increased in all the nanocomposites with the increasing in the CNTs contents. The corresponding increase in the loss moduli (G'') in all HDPE nanocomposites is much lower than for the storage moduli and there is no evidence for the formation of a plateau.

ملخص

الاسم: احمد اكانبي ادويني

عنوان الدراسة: تأثير خلط انابيب الكربون متناهيه الصغر علي الخصائص الحراريه والميكانيكية للبولي ايثلين

عالي الكثافه

التخصص: الهندسه الكيميائيه

التاريخ: يونيو ٢٠١١

تم استخدام الأنابيب الكربونية المتناهيّة الصغر منذ اكتشافها في تطبيقات البوليمرات وذلك لزيادة خصائصها الفيزيائية لتكون مواد ذات مواصفات وجودة عالية جداً. في هذه الدراسة تم خلط الأنابيب الكربونية المتناهيّة الصغر عند نسب وزنية مختلفه (1-5 wt %) باستخدام طريقة الخلط الميكانيكي. عملية خلط الأنابيب الكربونية المتناهيّة الصغر باستخدام طريقة الخلط الميكانيكي تمت أيضاً باستخدام أنواع مختلفه من الأنابيب الكربونية مثل (CNTS-COOH ، CNTS-C18 و CNTS-Phenol). تم تحليل أسطح الأنابيب الكربونية و المواد الكيميائية المطعمة على سطحها باستخدام جهازي FTIR و SEM. تم تحسين الخصائص الميكانيكية للخلط النانوي للأنابيب الكربونية المتناهيّة الصغر المطعمة والغير مطعمة مع البولي ايثلين العالي الكثافة. في حين لا يوجد تأثير كبير لهذه الأنابيب على الخصائص الحرارية للخلط النانوي. بالإضافة إلى ذلك هناك تحسن واضح في درجة البلورية عند خلط 1 wt % من الأنابيب الكربونية المطعمة والغير مطعمة وينقص هذا التأثير بزيادة نسبة الأنابيب الكربونية أعلى من 1 wt % . أما من الناحية الريولوجية فإنه ظهر واضحاً أن اللزوجة انخفضت عند إضافة 1 wt % من الأنابيب الكربونية إلى البولي ايثلين عالي الكثافة. بالعكس من ذلك فإن زيادة واضحة في خاصية التخزين ظهرت عند إضافة هذه الأنابيب إلى البولي ايثلين.

CHAPTER 1

1 INTRODUCTION

1.1 BACKGROUND

Since the landmark paper by Iijima in 1991 (Iijima, 1991), CNTs have generated huge activity in most areas of science and engineering due to their high flexibility, low mass density, and high aspect ratio (300-1000) in addition to their excellent mechanical, thermal, and electrical properties. The latter also highlighted their potential in the production of advanced composites with great interest for several applications. From the preparation of the first polymeric nanocomposite incorporating CNT by (Ajayan et al. in 1994), several researchers have explored the potentiality of such nanocomposites. This has been reflected in the growing number of patents and publications to date (Moniruzzaman, M. Winey 2006). Although several studies have been focused on producing nanocomposites, many practical challenges concerning their fabrication still remain, compromising the full realization of their enormous potential. One of the problems with the preparation of polymeric nanocomposites with CNT is the difficulty of dispersing them. Their small size, large superficial area, and the presence of π electrons highly delocalized in their surface make them susceptible to van der Waals forces that promote aggregation (Ajayan, 2000; Wang, C et al. 2004). Many techniques have been applied to attempt the dispersion of CNT in polymeric matrices, for example, the application of ultrasound and chemical modification of the CNT

surface (Wang, C et al 2004; Moniruzzaman,M. Winey 2006; Gojny et al 2003). Another method involves the dispersion in solvents of the CNT with surfactants and high frequency ultrasound. In this way, suspensions are achieved in which a polymer is later dissolved, and the nanocomposite is prepared by solvent evaporation. Because of the problems associated with the fabrication of CNT composites, the literature reports several techniques to achieve homogeneous distribution of CNTs into the polymer matrix. Those techniques include: constant stirring (Sandler et. al.1999); surfactant-assisted processing (Shaffer MSP, et al. 1999); solution evaporation methods with high energy sonication (Qian D, et al. 2000); and covalent functionalization of nanotubes with a polymer matrix (Bratcher M, et al. 2001). Gong et al. reported the role of surfactants as processing aid in CNT-polymer composites and found their enormous influence on mechanical and thermal properties of composites. Ji et al have discussed the difficulties obtained to get uniform dispersion of CNTs in a polymer matrix. Zou et al. found that HDPE/CNT composites fabricated at higher screw speed give uniform dispersion of CNT in HDPE. Thostenson and Chou studied the mechanical properties of aligned and random oriented nanocomposites using DMA and observed an improvement on Young's Modulus with an addition of CNTs. Moreover, in the aligned composites, Young Modulus could be observed five times greater than that of randomly oriented composites. Gorga and Cohen (Gorga R E; Cohen R.E, et al. 2004) found that in addition to a good dispersion of CNTs in polymer, their orientation and an interface between CNT and polymer also play a critical role to improve the mechanical properties of composites.

Edidin and Kurtz et al.2001 showed that toughness of the material is strongly correlated to the wear resistance of polymers. Cadek et al. 2002 studied mechanical and thermal properties of amorphous and crystalline polymers with MWCNT and observed significant improvement in their properties. Gorga et al.2006 prepared MWCNT-PMMA composites using melt processing and melt drawing method and studied their mechanical properties as a function of CNT concentration and surface treatment on CNTs. Tang et al. 2003 used melt processing technique to make MWCNT/HDPE composite films and observed an enhancement of mechanical properties.

Although research in the field of CNT/polymer composites has been conducted on thermoplastics such as ABS, PC, PMMA, PP and PS, to our knowledge, not much mechanical properties of CNT/HDPE have been reported. Conversely, HDPE provides excellent chemical resistance, high impact strength, good fatigue and abrasive wear resistance, low coefficient of friction and moderate stiffness and rigidity. It has a very wide of applications including orthopedic implants, distribution pipes and auto parts. To utilize and enhance these properties of HDPE, especially to improve its stiffness and rigidity, CNTs can be used to make CNT/HDPE composites.

1.2 STATEMENT OF THE PROBLEM

Despite the outstanding thermal, electrical and mechanical properties of CNTs and their increasing potential as fillers for large variety of polymers (Lin et al., 2007; Du 2007 et al., and Coleman et al., 2006) CNTs tend to aggregate into bundles and hence they are difficult to be dispersed homogeneously in polymer

matrices. Likewise, the strong intermolecular van der Waals interactions among the nanotubes in addition to weak polymer CNTs interfacial adhesion prevents efficient load transfer from the polymer matrix to the CNTs. As a result of poor dispersion and inefficient load transfer, the mechanical properties of polymer/CNTs are not as good as expected. In view of this, it became necessary to carry out research that will be more suitable, efficient and also enhance the dispersion of CNTs into polymer matrices. From the forgoing literature surveyed, it follows that chemical functionalization of CNTs with organic moieties or polymers proves promising in reducing agglomeration and load transfer problems associated with polymer/CNT nanocomposites.

1.3 RESEARCH OBJECTIVES AND SIGNIFICANCE

The salient feature of this work is to study the effect of functionalized carbon nanotubes with surfactants on the mechanical, thermal and rheological properties of polyethylene (HDPE) based nanocomposites. Furthermore, characterization of the composite matrix dispersion will be investigated in a qualitative manner in order to ascertain the structure-property relationship of this composite. Thus, the objectives of this research are enumerated as follows:

1. To functionalize MWCNT with different surfactants (carboxylic group, phenol and C_{18}) followed by surface characterization of the functionalized nanotubes using Fourier Transform Infrared Spectroscopy (FTIR).
2. To develop MWCNT/Polyethylene (HDPE) nanocomposites by using Brabender blending machine.

3. To study the dispersion behavior, thermal, mechanical and rheological properties of the nanocomposites developed by using Scanning Electron Microscopy (SEM), Differential Scanning Calorimetry (DSC), Thermogravimetric analyzer (TGA), Instron Tensile Machine and Advanced Rheometric Expansion System (ARES) respectively.

CHAPTER 2

2.0 LITERATURE REVIEW

2.1 BACKGROUND

Research on new materials technology is attracting the attention of researchers all over the world. Developments are being made to improve the properties of the materials and to find alternative precursor that can bestow desirable properties on the materials. Great interest has recently developed in the area nanostructured carbon materials. Carbon nanostructures are becoming of considerable commercial importance with interest growing rapidly over the years or since the discovery of buckminsterfullerene, carbon nanotubes and carbon nanofibers. Carbon nanotubes (CNTs) exhibit unique mechanical, electronic and magnetic properties, which have caused them to be widely studied. CNTs are probably the strongest substance that will ever exist with a tensile strength greater than steel, but only one sixth the weight of the steel. Iijima (1991) was first discovered carbon nanotubes using arc discharge method. Following this discovery a number of scientific researchers have been initiated and variable methods have been used to synthesis CNTs and reported to be able to produce them, namely arc discharge, laser vaporization and catalytic chemical vapor deposition of hydrocarbon. Since carbon – carbon are one of the strongest in nature, a structure based on a perfect arrangement of these bonds oriented along the axis of nanotubes would produce an exceedingly strong material. Nanotubes are strong and resilient structures that

can be bent and stretched into shapes without catastrophic structural failure in the nanotube.

2.2 POLYETHYLENE, HIGH DENSITY (HDPE)

Polyethylene (PE) is the most widely used plastic throughout the world, and high density polyethylene is the most widely used type of polyethylene. High density polyethylene has generally been taken to mean the product of ethylene polymerization having density greater than ~ 0.935 (or 0.94). It includes both ethylene homopolymers and copolymers of ethylene and alpha-olefins, such as 1-butene, 1-hexene, 1-octane, or 4-methyl-1-pentene. Other types of PE include low density PE (LDPE) made through a free radical process, and linear low density PE (LLDPE).

2.3 HISTORY OF POLYETHYLENE

The history of (HDPE) (and polyolefins in general) actually began in the 1890s with the synthesis of “polymethylene” from the decomposition of diazomethane. Between 1897 and 1938 numerous reports of such polymers appear in the literature (1-6). Catalysts such as unglazed china, amorphous boron, and boric acid esters were used for the decomposition. The empirical formula of such products was found to be CH_2 . Later, reproductions of the work of Werle (6) and Bamberger and Techiner (3) established that the polymethylene thus obtained was a high molecular weight linear polymer having a melting point of 134-137°C, and a density of 0.964-0.970 g/cm³ (7). Thus it can be stated that, although no commercial use was initially made of it, HDPE was discovered long before the

well known LDPE was introduced (8, 9). In another early approach, Pichler (10) and Pichler and Buffleb (11) describe in 1938-1940 the preparation of high molecular weight ($M_n=23,000$) polymers from the hydrogenation of carbon monoxide over ruthenium and cobalt catalysts. The reported melting point of 132-134 °C and density of 0.980 g/cm³ indicate that linear, HDPE was obtained.

2.4 PROPERTIES OF POLYETHYLENE

2.4.1 Molecular Structure and Morphology

LDPE has a random long branching structure, with branches on branches. The short branches are not uniform in length but are mainly four or two carbon atoms long. The ethyl branches probably occur in pairs and there may be some clustering of other branches. The molecular mass distribution (MMD) is moderately broad. LLDPE has branching of uniform length which is randomly distributed along a given chain, but there is a spread of average concentrations of branches being generally in the shorter chain. The catalysts used to minimize this effect generally also produce fairly narrow MMDs. HDPE is essentially free of both long and short chain branching, although very small amounts may be deliberately incorporated to achieve specific product targets. The MMS depends on the catalyst type but is typically of medium width.

Polyethylene crystallizes in the form of platelets (lamellae) with a unit cell similar to that of low molecular mass paraffin waxes. Due to chain folding, the molecular axes are oriented perpendicular to the longest dimension of the lamella and not parallel to it as might be expected. The thickness of the lamellae is determined by the crystallization conditions and the concentration of branches and is typically in

the range of 8-20nm. Thicker lamellae are associated with higher melting points and higher overall crystallinities. Slow cooling from the melt or annealing just below the melting point produces thicker lamellae. Where long molecules emerge from the lamella they may either loop back elsewhere into the same lamella or crystallize in one or more adjacent lamellae, thereby forming “tie molecules”. Thermodynamically the side branches are excluded from the crystalline region because their geometry is too different from that of the main chains to enter the crystalline lamellae. Therefore, the branches initiate chain folding, which results in thinner lamellae with the branches mainly situated on the chain folds on the surface of the lamellae. However, on rapid cooling these energetically preferred placements may not always occur, and some branches may become incorporated as crystal defects in the crystalline regions. Detailed measurement by solid-state NMR and Raman spectroscopy show that the categorization into crystalline and amorphous phases is too simplistic and a significant fraction of the polymer is present in the form of an “interfacial” fraction which has neither the freedom of motion of a liquid nor the well defined order of a crystal.

Under moderately slow cooling conditions, crystallization may be nucleated at a comparatively small number of sites. Crystallization then propagates outwards from these centers until the surfaces of the growing sphere meet. The resulting spherulites show a characteristic banded structure under a polarizing optical microscope.

2.4.2 General Properties

LDPE and LLDPE are translucent whitish solids and are fairly flexible. In the form of films they have a limp feel and are transparent with only a slight milkiness. HDPE on the other hand is a white opaque solid that is more rigid and forms films which have a more turbid appearance and a crisp feel. Polyethylene does not dissolve in any solvent at room temperature, but dissolves readily in aromatic and chlorinated hydrocarbon hydrocarbons above its melting point. On cooling, the solutions tend to form gels which are difficult to filter. Although LDPE and LLDPE do not dissolve at room temperature they may swell in certain solvents with deterioration in mechanical strength.

Some properties of typical LDPE, HDPE, and LLDPE are listed in Table 1. Polyethylenes are routinely characterized by their density and melt flow index (MFI). The MFI test was originally chosen for LDPE to give a measurement of the melt characteristics under conditions related to its processing. It is carried out by applying a standard force to a piston and measuring the rate of extrusion (in g/10min) of the polyethylene through a standard die. The short parallel section of the standard die introduces errors which mean that the MFI cannot be accurately related to viscosity (it would be an inverse relationship). For LDPE and HDPE, the MFI increases disproportionately with the applied load. The ratio of the two MFIs gives a measure of the ease of flow at high shear and is sometimes known as the flow ratio.

Table 1. Properties of some typical polyethylene (data from Repsol Quimica)

Property	LDPE	HDPE	LLDPE	Method	Standard
Polymer grade	Repsol PE077/A	Hoechst GD-4755	BP LL 0209		
Melt flow index(MFI),g/600s	1.1	1.1	0.85	190°C/2.16kg	ASTM D1238
High load MFI, g/600s	57.9	50.3	24.2	190°C/2.16kg	ASTM D1238
Die swell ratio (SR)	1.43	1.46	1.11		
Density, kg/m^3	924.3	961.0	922.0	Slow annealed	ASTM D1505
Crystallinity, %	40	67	40	DSC	
Temperature of fusion (max), °C	110	131	122	DSC	
Vicat softening point, °C	93	127	101	5°C/h	ASTM D1525
Short branches **	23	1.2	26	IR	ASTM D2238
Comonomer		butene	butene	NMR	
Molecular mass*					
M_w	200 000	136 300	158 100	SEC	
M_n	44 200	18 400	35 800	SEC	
Tensile yield strength, MPa	12.4	26.5	10.3	50mm/min	ASTM D638
Tensile rupture strength, MPa	12.0	21.1	25.3		
Elongation at rupture, %	653	906	811		
Modulus of elasticity, MPa	240	885	199	flexure	ASTM D790
Impact Energy, Unnotched, kJ/m^2	74	187	72		ASTM D256
Notched, kJ/m^2	61	5	63		ASTM D256
Permittivity at 1MHz	2.28				ASTM D1531
Loss tangent at 1MHz	100×10^{-6}				ASTM D1531
Volume resistivity, $\Omega \cdot m$	10^{16}				
Dielectric strength, kV/mm	20				

* Corrected for effects of long branching by on-line viscometry

** Number of methyl groups per 1000 carbon atoms

2.5 CARBON NANOTUBES

Carbon nanotubes have been attracting great interest due to their wide scope of possible applications, such as composite reinforcement material (Tai NH, et al 2004; Ogasawara T, et al 2004; Gojny FH, 2004), hydrogen container (Liu C, et al 1999), field emission sources (Sugie H et al 2001), super capacitor (Frackowiak E, et al 2002), molecular sensors (Kong J, Franklin NR, et al 2000) and scanning probe tips (Dai HJ, et al 1996). Offering attractive mechanical/electric/thermal properties, carbon nanotubes could constitute a model system for evaluation of the potential to achieve a significant improvement in bulk properties by adding nanoscale modulators at low weight percents. Carbon nanotubes (CNT) have a unique set of properties that position them for a wide scope of possible applications in suspensions and polymer based solutions, melts and composites (Assouline E, et al 2003; Potschke P et al 2002; Haggemueller R, et al 200; Wang H, et al 2003). Their outstanding characteristics include high mechanical properties, namely tensile strength and elastic modulus, and still remarkable flexibility, excellent thermal and electric conductivities, low percolation thresholds (loading weight at which a sharp drop in resistivity occurs) and high aspect ratio (length to diameter ratio, L/D), while the latter provides the nanotubes with additional advantage over spherical fillers to obtain high property composites (Thostenson ET, et al 2005).

Main challenges for integration of this unique nano-material include: (1) uniform dispersion; (2) preferential alignment in liquid and melt phases; and (3) mass production of high- purity materials at low costs.

2.5.1 Structure and properties of carbon nanotubes

The discovery of the C_{60} molecules in 1985 by a group of chemist from Rice University (Texas, US) has evoked a tremendous interest among the world scientific community and led to the development of a completely novel branch of chemistry called *Fullerene-Chemistry* (Kroto HW, et al 1985). Fullerenes are geometric cage-like structures of carbon atoms that are composed of hexagonal carbon (graphite-like structure), and the end caps contain pentagonal rings (Fig. 1). CNTs were observed for the first time by Sumio Iijima in 1991 (Iijima, 1991). Theoretically, it is possible to construct carbon tubules by rolling up a hexagonal graphene sheet as shown in figure 2 (Odom TW, et al 2000). In graphite, sp^2 hybridization occurs, where each atom is connected evenly to three carbons (120°) in the xy plane, and a weak π bond is present in the z axis. The sp^2 set forms the hexagonal (honeycomb) lattice typical of a sheet of graphite. The p_z orbital is responsible for van der Waals interactions. The free electrons in the p_z orbital move within this cloud and are no more longer local to a single carbon atom (Terrones M, et al 2003). This phenomenon lies behind the reason why graphite (and CNT, accordingly) can conduct electricity, as opposed to diamond, which behaves as insulator because all electrons are localized in the bonds within the sp^3 framework (Knupher M, et al 2001). Besides being responsible for high conductivity, the delocalized π -electrons of carbon nanotubes could be utilized to promote adsorption of various moieties on the CNT surface via π - π stacking interactions.

The exact properties of CNT are extremely sensitive to their degree of graphitization, diameter (or chirality), and whether they are single wall or multi wall form (Fig. 2a and b, respectively). Single wall carbon nanotubes (SWCNT), which are seamless cylinders, each made of a single graphene sheet, were first reported in 1993 (Iijima S, et al 1993). Multi wall carbon nanotubes (MWCNT), consisting of two or more seamless grapheme cylinders concentrically arranged, were discovered two years previously (Iijima S, 1991). The production method is often aimed at processing a particular type of carbon nanotubes, thus MWCNTs are most commonly produced via non catalytic means, whereas SWCNTs are usually dominant products under catalytic growth conditions. Furthermore, the production method dictates the quality of the generated tubes (as do their properties) viz., distribution of diameters and lengths, degree of entanglement, and the amount of impurities (encapsulated catalyst particles, amorphous carbon, polyhedral graphite particles etc.) (Baughman RH, et al 2002). Among various processing techniques, such as arc discharge, laser vaporization, or electrolysis, according to Refs (Ge M, et al 1994; Li WZ et al 1996; Che G et al 1998) it appears that the chemical vapor deposition (CVD) method has the highest potential for growing large quantities of pure and crystalline carbon nanotubes.

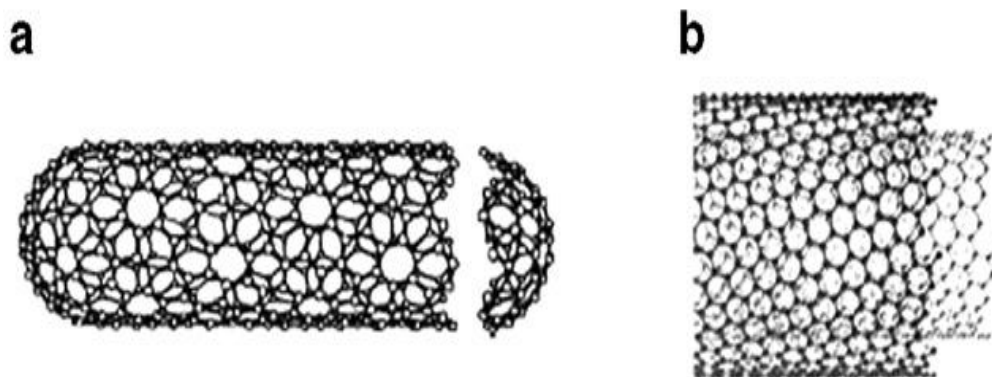


Fig1. Computer-generated image of carbon nanotubes.

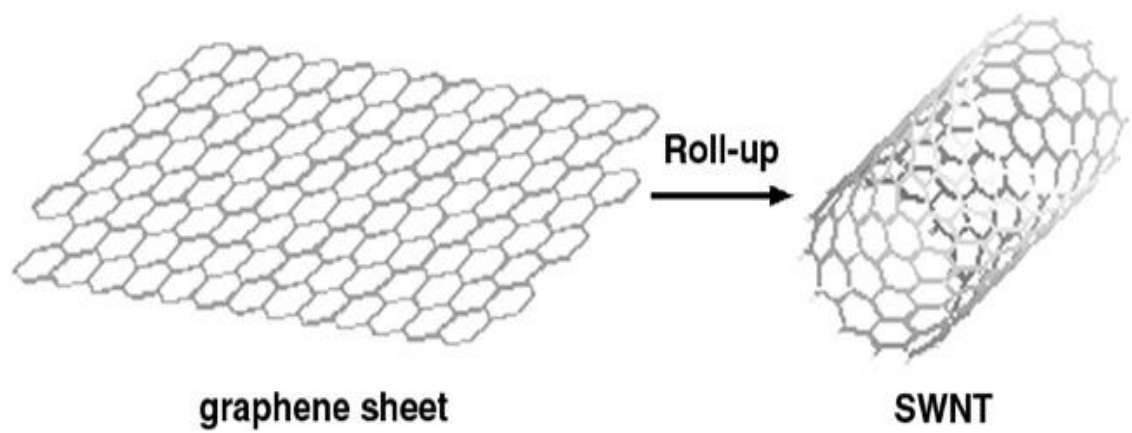


Fig.2 It is possible to create a single wall carbon nanotube by rolling-up a graphene sheet.

Among various attractive characteristics, it was mainly the electric properties of carbon nanotubes that stimulated large scale industrial production of CNT-based materials. However, the electronic response of individual nanotubes is reported to be sensitive to various parameters, such as the synthesis method, defects, chirality, diameter and degree of crystallinity (Roche S, et al 2000). Generally, the thermal and electric conductivities (TC and EC, respectively) of single nanotubes are thought to be higher than graphite. For example, the TC of graphite along its planar direction is 1000W/m K, while the TC of SWNT and MWNT is 2400 and 1980W/m K, respectively (Che J, et al 2000; Berber S, et al 2000). However, the reported values for bundles of CNT resemble those of in-plane and cross-plane graphite. It is known that solids with high aspect ratios can produce three dimensional networks when incorporated into polymer materials. When added as well dispersed fillers, they provide a conductive path through the composite. Therefore, carbon nanotubes ($L/D > 1000$) were shown to increase both thermal (Ounaies Z, et al 2003; Biercuk MJ, et al 2002) and electric (Andrew R, et al 1999; Grunlan JC, et al 2004; Kim B, et al 2003) conductivities of polymers at low percolation thresholds (up to a few weight percents). Nevertheless, the strong dependence of percolation limits on the CNT state of dispersion has to be emphasized. Thus, to improve SWCNT dispersion in high density polyethylene (HDPE), the tubes were dispersed with the aid of sodium dodecyl sulfate (SDS) surfactant (Zhang Q, et al 2006). The percolation threshold for this system was reported at about 4wt% CNT loading, as demonstrated in Fig.3. Even lower percolation limits were obtained with polystyrene and epoxy filled CNT

composites, thus 0.5 vol.% and 0.04wt.% loadings, respectively, were reported (Safadi B, et al 2002; Sandler J, et al 1999). Because the carbon-carbon bond observed in graphite is one of the strongest in nature, carbon nanotubes are excellent candidates for the stiffest and strongest material ever synthesized. Despite large variation in the reported values, carbon nanotubes were shown to exhibit mechanical performance higher than that of classic advanced fibers, like carbon and Kevlar. As with electric properties, the mechanical strength of the tubes depends on the crystallinity of the material, number of defects (often controlled by the synthesis method), diameter, etc. Mechanical properties of SWNT usually exceed those of MWCNT, thus measurement of Young's modulus give results in the range of 10^3 GPa and 500 GPa, respectively (Krishman A, et al 1998; Popov VN, et al 2000; Yu M-F, et al 2000; Xie S, et al 2000). Smaller size and massive arrangement in ropes make the measurement of the mechanical properties of SWNT more complex and less precise (Belin T, et al 2005).

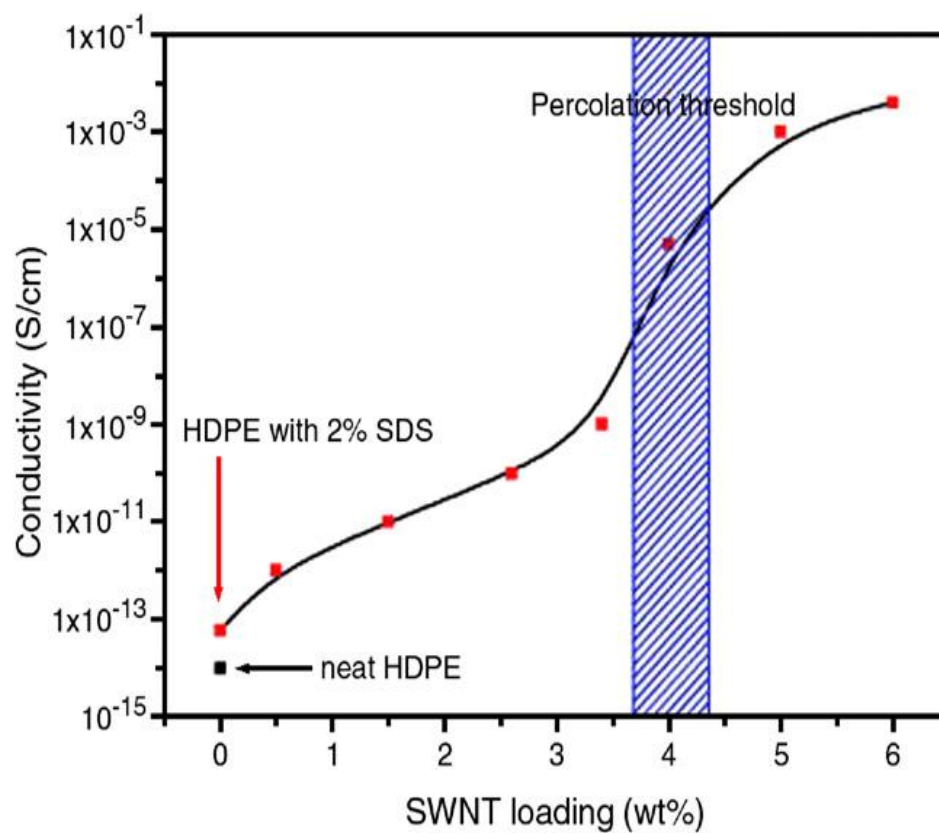


Fig.3 The conductivity of HDPE filled with SDS-coated SWCNT.
(Zhang Q, et al. 2006)

2.5.2 Dispersion of CNTs (Nature of dispersion for CNTs)

Many research efforts have been directed towards producing CNT/polymer composites for functional and structural applications (Thostenson ET, et al 2001; Ajayan PM, et al 2003; Coleman JN, et al 2006). However, even after a decade of research, the full potential of employing CNTs as reinforcements has been severely limited because of the difficulties associated with dispersion of entangled CNT during processing and poor interfacial interaction between CNTs and polymer matrix. The nature of dispersion problem for CNTs is rather different from other conventional fillers, such as spherical particles and carbon fibers, because CNTs are characteristic of small diameter in nanometer scale with high aspect ratio (>1000) and thus extremely large surface area. In addition, the commercialized CNTs are supplied in the form of heavily entangled bundles, resulting in inherent difficulties in dispersion. Table 2 compares the dimension of commonly used fillers, including Al_2O_3 particles, carbon fibers, graphite nanoplatelets (GNPs) and CNTs and the number of particles corresponding to a uniform fillers volume fraction of 0.1% in a composite of 1.0mm^3 cube. Because there are large differences in dimension and geometry of these four different reinforcements, the number of fillers contained for a given filler volume fraction will also be largely varying.

Table 2. Dimension and corresponding number of particles in composites for different fillers (^a N : number of particles in 1.0mm^3 with 0.1 vol% filler content, ^b S : surface area of individual particles)

Filler	Description		Density (g/cm^3)	N^a	S^b
	Average dimension of filler				
Al_2O_3 particle	100 μm in diameter (d)		4.0	1.9	πd^2
Carbon fiber	5 μm in diameter (d) \times 200 μm in length (l)		2.25	255	$S = \pi dl + \frac{\pi d^2}{2}$
GNP	45 μm in length (square, l), 7.5nm in thickness (t)		2.2	6.58×10^4	$S = 4l^2 + 2lt$
CNT	12nm in diameter (d) \times 20 μm in length (l)		1.8	4.42×10^8	$S = \pi dl + \frac{\pi d^2}{2}$

2.6 MECHANICAL DISPERSION OF CNTs

As discussed previously, the incorporation of CNTs into a polymer matrix leads to an exceptionally large quantity of particles and high surface area of fillers, resulting in the difficulties to uniformly disperse these particles. There is a sizable volume of literature reported on the techniques developed for CNT dispersion in polymer matrix (Breuer O, et al 2004; Xie XL, et al 2005; Moniruzzaman M, et al, 2006; Fiedler B, et al 2006; Gibso RF, et al 2007; Bal S, et al 2007). However, little information has been hitherto reported on the principle and features of these dispersion techniques. Therefore, the basis of CNT dispersion methods are introduced here, some typical results on CNT dispersion in polymers by employing these methods are demonstrated, and a general guideline for selecting proper techniques for CNT dispersion is provided.

2.6.1 Ultrasonication

Ultrasonication is the act of applying ultrasound energy to agitate particles in a solution for various purposes. In the laboratory, it is usually achieved using an ultrasonic bath or an ultrasonic probe/horn (A and B in Fig.4), also known as sonicator. It is the most frequent used method for nanoparticle dispersion. The principle of this technique is that when ultrasound propagates via a series of compression, attenuated waves are induced in the molecules of the medium through which it passes. The production of these shock waves promotes the “peeling off” of individual nanoparticles located at the outer part of the nanoparticle bundles, or agglomerates, and thus results in the separation of individualized nanoparticles from the bundles.

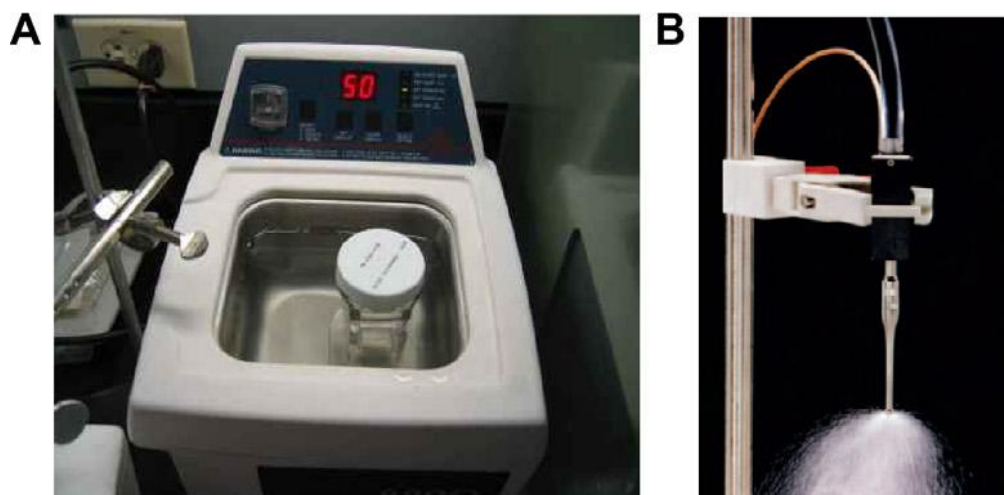


Fig.4. Sonicator with different modes for CNT dispersion (A: water bath sonicator; B: probe/horn sonicator), and the effect of sonication on the structure of CNTs. (Lu KL, et al. 1996)

Ultrasonication is an effective method to disperse CNTs in liquids having a low viscosity, such as water, acetone and ethanol. However, most polymers are either in a solid or viscous liquid state, which requires the polymer to be dissolved or diluted using a solvent to reduce the viscosity before dispersion of CNTs.

2.6.2 Calendering process

The calendar, or commonly known as three roll mills, is a machine tool that employs the shear force created by rollers to mix, disperse or homogenize viscous materials. This method has also been used to disperse color pigments for cosmetics and lacquers. The general configuration of a calendaring machine consists of three adjacent cylindrical rollers each of which runs at a different velocity (Fig. 5A) (Gojny FH, et al 2004; Thostenson ET, et al 2006). The first and third roller, called the feeding and apron rollers (n_1 and n_3 in Fig. 5B), rotate in the same direction while the center roller rotates in the opposite direction. The material to be mixed is fed into the hopper, where it is drawn between the feed and center rollers. When pre-dispersed, the material sticks to the bottom of the center roller, which transport it into second the gap. In this gap, the material is dispersed to the desired degree of fineness. Upon exiting, the material that remains on the center roller moves through the second nip between the second roller and apron roller, which subjects it to even higher shear force due to the higher speed of the apron roller. A knife blade then scrapes the processed material off the apron roller and transfers it to the apron. Calendering is widely used to mix electronic thick film inks, high performance ceramics, carbon/graphite, paints, printing inks, pharmaceuticals, chemicals, glass coatings, dental composites,

pigment, coatings, adhesives, sealants, and foods. Typical calendaring machine and the principle are shown schematically in Fig 6. The employment of a calendar to disperse CNTs in a polymer matrix has become a very promising approach to achieve a relatively good CNT dispersion according to some recent reports (Gojny FH, et al 2004; Thostenson ET, et al 2006). A high shear stress is required to apply to disentangle CNT bundles and distribute the dispersed CNT into polymer matrix, while a short residence time will likely limit the breakage of individual nanotubes (Thostenson ET, et al 2006). However, there are several concerns in using this technique for CNT dispersion: for example, the minimum gap between the rollers is about 1-5 μm , which is comparable to the length of CNTs, but is much larger than the diameter of individual CNTs. These dimensional disparities between the roller gap and the CNT dimensions may suggest that calendaring can better disperse the large agglomerated CNTs into small ones at sub-micron level, although some individual CNTs may be disentangled out from the agglomerates (Fig.6). In addition, the feeding materials should be in the viscous state when mixing with nanoparticles, thus this tool may not be applied for dispersing CNTs into thermoplastic matrices, such as polyethylene, polypropylene and polystyrene. In contrast, CNTs can be conveniently dispersed into the liquid monomer or oligomer of thermosetting matrices, and nanocomposites can be obtained via the in situ polymerization.

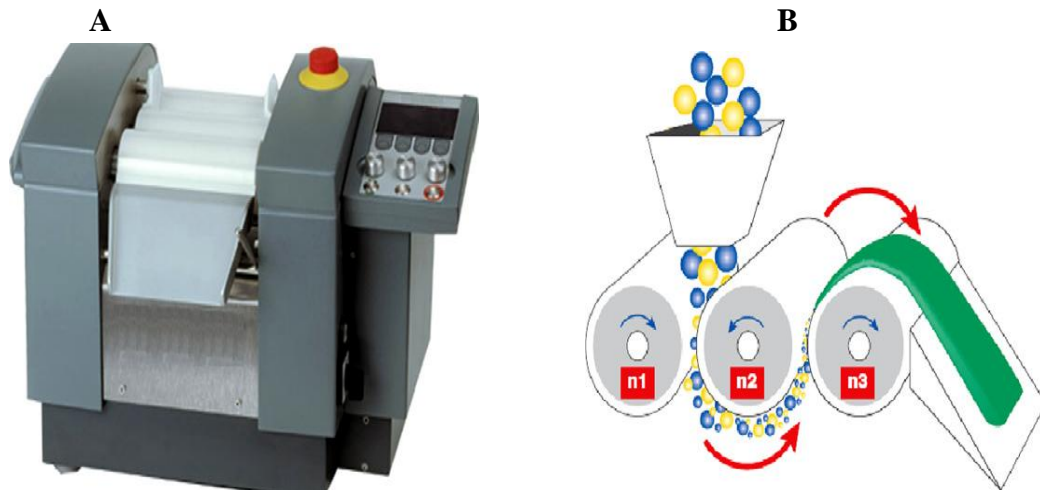


Fig.5. Calendering (or three roll mills) machine used for particle dispersion into a polymer matrix (A) and corresponding schematic showing the general configuration and its working mechanism (B). (< <http://www.exakt.com>>, three roll mill, EXAKT company)

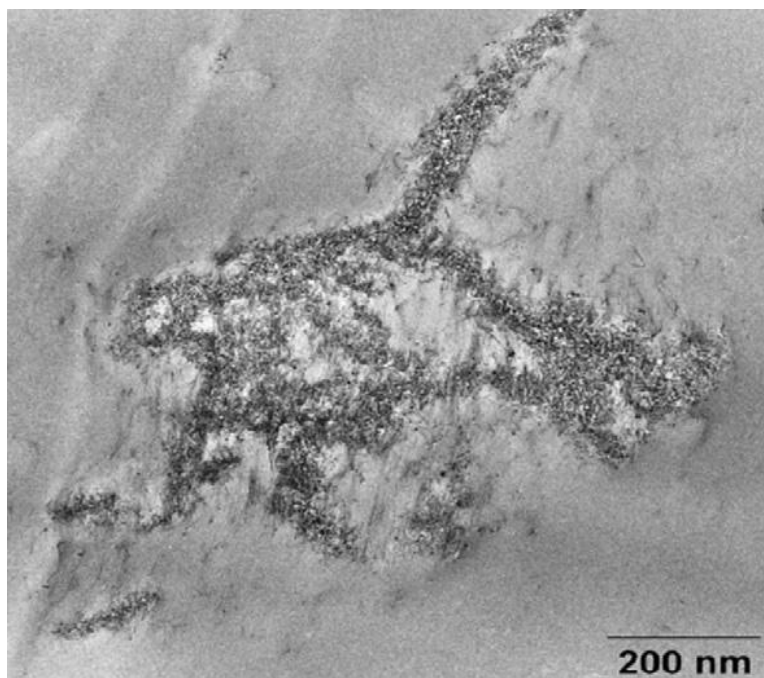


Fig.6.TEM image of CNTs dispersed by calendaring machine in an epoxy matrix. (Thostenson ET, et al. 2006)

2.6.3 Ball milling

Ball milling is a type of grinding method used to grind materials into extremely fine powder for use in paints, pyrotechnics and ceramics. During the milling, a high pressure is generated locally due to the collision between the tiny, rigid balls in a concealed container, which is schematically shown in Fig. 7. An internal cascading effect of balls reduces the material to fine powder. Different materials, including ceramic, flint pebbles and stainless steel, are used as balls. Industrial ball mills can operate continuously to feed materials at one end and discharge them at the other end. High-quality ball mills can grind mixture particles to as small as 100nm, enormously increasing the surface area of the materials. Balling milling has been successfully applied to carbon materials for a variety of purposes, e.g. to transform CNTs into nanopaticles (Li YB, et al 1999) to generate highly curved or closed shell carbon nanostructures from graphite (Gao B, et al 2000), to enhance the saturation of lithium composition in SWNTs (Huang JY, et al 1999), to modify the morphologies of cup-stacked CNTs (Kim YA, et al 2002), and to generate different carbon nanoparticles from graphitic carbon for hydrogen storage applications (Awasthi k, et al 2002).

Ball milling of CNTs in the presence of chemicals not only enhances their dispersibility, but also introduces some functional groups onto the CNT surface. A simple chemo-mechanical method was used to achieve in situ amino functionalization of CNTs using ball milling (Ma PC, et al 2008; Ma PC, Wang SQ, et al 2009). The result showed that the CNTs milled with ammonium bicarbonate (NH_4CO_3) were more effectively disentangled and shortened than those

without the chemical (Fig. 8, and the CNT length was controlled by choosing an appropriate milling time. Some useful functional groups, like amine and amide terminals, were attached onto the CNT surface after milling, allowing covalent bonding to polymers and biological systems. These nitrogen atoms introduced on CNT surface function as the electron donors in the material, resulting in the conversion of the semiconducting behavior of CNTs from p-type to n-type (Ma PC, Wang SQ, et al 2009).

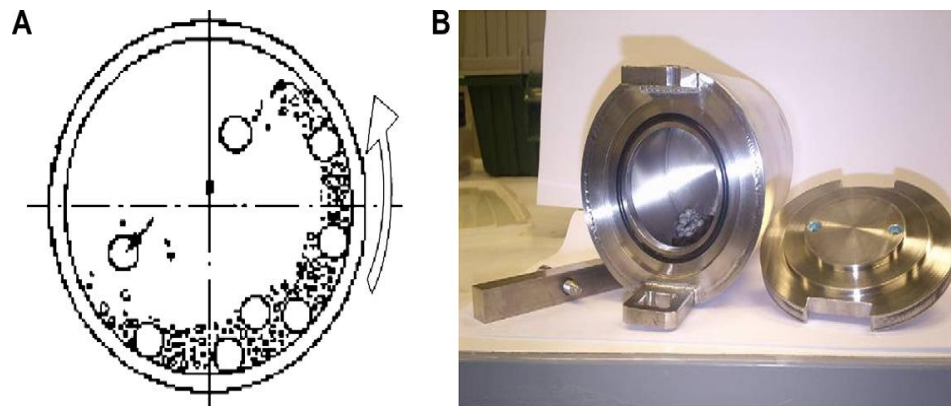


Fig.7.Schematics of ball milling technique (A) and container (B)

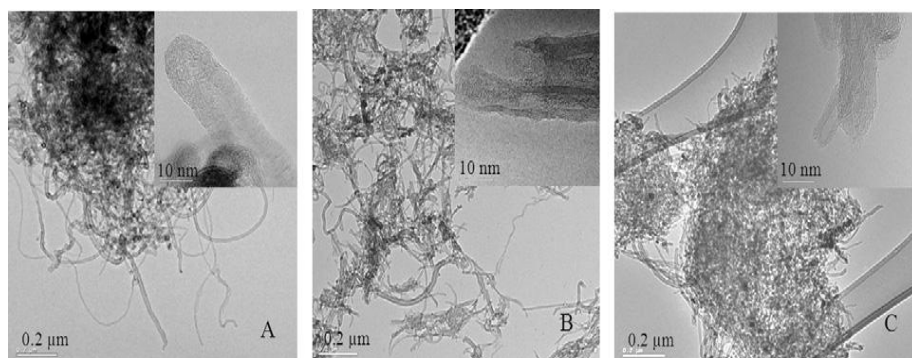


Fig.8. TEM images of pristine CNTs and those milled after 9h (A: pristine; B: milled with NH_4CO_3 ; C: milled without NH_4CO_3). CNTs milled with NH_4CO_3 were more effectively disentangled and shortened than those without the chemical. After (Ma PC, Wang SQ, et al 2009)

2.6.4 Stir and extrusion

Stir is a common technique to disperse particles in liquid systems and can be used as well to disperse CNT in a polymer matrix. Size and shape of the propeller and the mixing speed control the dispersion results. After intensive stirring of CNTs in polymer matrix, a relatively fine dispersion can be achieved (Sandler JKW, et al 1999). MWCNTs can be dispersed more easily than SWNTs by employing this technique, although the MWCNTs tend to re-agglomerate. This experimentally observed behavior is mainly caused by frictional contacts and elastic interlocking mechanisms (Schmid CF, et al 2000). Other parameters, like sliding forces and weak attractive forces have only little effect on this tendency during stir; however, the agglomeration becomes spontaneous under static conduction. For some thermosetting polymers, such as epoxy, obvious CNT re-agglomeration was observed after several hours of curing reaction (Li J., et al 2007). In case of severally agglomerated CNTs, higher shear forces are needed to achieve a fine dispersion in the polymer matrix, this can be accomplished by employing high speed shear mixer at a speed up to 10,000rpm.

Extrusion is a popular technique to disperse CNTs into solid polymers like most thermoplastics, where thermoplastic pellet mixed with CNTs are fed into the extruder hopper. Twin screws rotate at a high speed create shear flow resulting in dispersion of CNT agglomerate and mixing them with the polymer melt. This technique is particularly useful to produce CNT/polymer nanocomposites with high filler content (Villmow T, et al 2008).

Table 3. Comparison of various techniques for CNT dispersion in polymer composites

Technique	Factor				
	Damage to CNTs	Suitable matrix	polymer	Governing factors	Availability
Ultrasonication	Yes	Soluble low polymer or oligomer,	polymer, viscous or monomer	Power and mode of sonicator, sonication time	Commonly used in lab, easy operation and cleaning after use
Calendering	No, CNTs may be aligned in matrix	Liquid polymer or oligomer, monomer		Rotation speed, distance between adjacent rolls	Operation training is necessary, hard to clean after use
Balling milling	Yes	Powder (polymer or monomer)		Milling time, rotation speed, size of balls, balls/CNT ratio	Easy operation, need to clean after use
Shear mixing	No	Soluble low polymer or oligomer,	polymer, viscous or monomer	Size and shape of the propeller, mixing speed and time	Commonly used in lab, easy operation and cleaning after use
Extrusion	No	Thermoplastics		Temperature, configuration and rotation speed the screw	Large scale production, hard to clean after use

2.7 CNT/POLYMER NANOCOMPOSITES

2.7.1 Classification of CNT/ polymer nanocomposites

Polymer composites, consisting of additives and polymer matrices, including thermoplastics, thermosets and elastomers, are considered to be an important group of relatively inexpensive materials for many engineering applications. Two or more materials that are combined to produce composites that possess properties that are unique and cannot be obtained each material acting alone. For example, high modulus carbon fibers or silica particles are added into a polymer to produce reinforced polymer composites that exhibit significantly enhanced mechanical properties including strength, modulus and fracture toughness. However, there are some bottlenecks in optimizing the properties of polymer composites by employing traditional micron-scale fillers. The conventional filler content in polymer composites is generally in the range of 10-70%, which in turn results in a composite with a high density and high material cost. In addition, the modulus and strength of composites are often traded for high fracture toughness (Ajayan PM, et al 2003). Unlike traditional polymer composites containing micro-scale fillers, the incorporation of nano-scale CNTs into polymer system results in very short distance between the filler, thus the properties of composites can be largely modified even at extremely low content filler. For example, the electrical conductivity of CNT/epoxy nanocomposites can be enhanced several orders of magnitude with less than 0.5wt% of CNTs (Li J, et al 2007). As described previously, CNTs are amongst the strongest and stiffest fibers ever known. These excellent mechanical properties combined with other physical properties of CNTs

exemplify huge potential applications of CNT/polymer nanocomposites. Ongoing experimental works in this area have shown some exciting results, although the much anticipated commercial success has yet to be realized in the years ahead. In addition, CNT/polymer nanocomposites are one of the most studied systems because of the fact that polymer matrix can be easily fabricated without damaging CNTs based on conventional manufacturing techniques, a potential advantage of reduced cost for mass production of nanocomposites in the future.

2.8 FABRICATION FOR CNT/POLYMER COMPOSITES

2.8.1. Solution mixing

Solution mixing is the most common method for the fabrication of CNT/polymer nanocomposites because it is amenable to small sample sizes (Moniruzzaman M, et al 2006; Grossiord N, et al 2006; Du JH, et al 2007). Typically, solution blending involves three major steps: dispersion of CNT in a suitable solvent by mechanical mixing, magnetic agitation or sonication. The solvent can also dissolve polymer resins. Subsequently, the dispersed CNTs are mixed with the polymer matrix at room elevated temperatures. The nanocomposites are finally obtained by precipitating or casting the mixture. This method is often used to prepare composite films.

2.8.2. Melt blending

Melt blending is another commonly used method to fabricate CNT/polymer nanocomposites. Thermoplastic polymers, such as polypropylene (Zhang QH, et al 2004), polystyrene (Hill DE et al 2002), poly(ethylene 2,6-naphthalate) (Kim JY, et al 2006), can be processed as matrix materials in this method. The major advantage of this method is that no solvent is employed to disperse CNTs. Melt blending uses a high temperature and a high shear force to disperse CNTs in a polymer matrix, and is most compatible with current industrial practices. Special equipments, such as extruder, injection machine, which are capable of being operated at an elevated temperature and generating high shear forces, are employed to disperse CNTs. Melt blending or variants of this technique are frequently used to produce CNT/polymer composite fibers. Compared with the solution mixing methods, this technique is generally considered less effective to disperse CNTs in polymers than that of solution mixing, and its application is also limited to low filler concentrations in thermoplastic matrices (Moniruzzaman M, et al 2006).

2.8.3. In situ polymerization

In situ polymerization is an efficient method to realize uniform dispersion of CNTs in a thermosetting polymer. In this method, CNTs are mixed with monomers, either in the presence or absence of a solvent, and then these monomers are polymerized via addition or condensation reactions with a hardener or curing agents at an elevated temperature. One of the major

advantages of this method is that covalent bonding can be formed between the functionalized CNTs and polymer matrix, resulting in much improved mechanical properties of composites through strong interfacial bonds.

2.8.4. Latex technology

A relatively new approach to incorporate CNTs into a polymer matrix is based on the use of latex technology (Moniruzzaman M, et al 2006; Grossiord N, et al 2006; Du JH, et al 2007). Latex is a colloidal dispersion of discrete polymer particles, usually in an aqueous medium. By using this technology, it is possible to disperse single and multi-walled CNTs in most of polymers that are produced by emulsion polymerization, or that can be brought into the form of an emulsion. Contrary to in situ polymerization system, the addition of CNTs in this technique takes place after the polymer has been synthesized. The first step of the process consists of exfoliation (for SWNT bundles) or dispersion/stabilization (for MWCNT entanglements) of CNTs in an aqueous surfactant solution. This is followed by mixing the stable dispersion of surfactant treated CNTs with a polymer latex. After freeze-drying and subsequent melt-processing, a nanocomposite consisting of dispersed CNTs in a polymer matrix can be obtained. The advantages of this technique are obvious (Grossiord N, et al 2006; Du JH, et al 2007): the whole process is easy (because it basically consists of a simple mixing of two aqueous components), versatile, reproducible, and reliable, and allow incorporation of individual CNTs into a highly viscous polymer matrix. The solvent used for CNT dispersion is water, thus the process is a safe,

environmentally friendly and low-cost method. Nowadays, polymer latex is industrially produced on a large scale and this industry is matured. Since the process is relatively easy, the prospect for scale up fabrication of CNT/polymer nanocomposites using this technique is very bright.

2.8.5. Other methods

To obtain CNT/polymer nanocomposites with a very high CNT content or for some specific applications, new methods have been developed in recent years: they include densification, spinning of coagulant, layer-by-layer deposition and pulverization. It should be noted that as nanocomposite materials are an emerging field, many studies are being made to devise new processing methods that can produce nanocomposites with unique structures and properties for specialty end applications.

2.9. FUNCTIONALIZATION OF CNTs

The performance of a CNT/polymer nanocomposite depends on the dispersion of CNTs in the matrix and interfacial interactions between the CNT and the polymer. However, the carbon atoms on CNT walls are chemically stable because of the aromatic nature of the bond. As a result, the reinforcing CNTs are inert and can interact with the surrounding matrix mainly through van der Waals interactions, unable to provide an efficient load transfer across the CNT/matrix interface. Therefore, significant efforts have been directed towards developing methods to

modify surface properties of CNTs. There are several comprehensive review papers that describe the chemistry of functionalized CNTs and the reaction mechanism between the CNTs and functional group (Hirsch A, et al 2002; Balasubramanian K, et al 2005; Hirsch A, Vostrowsky O, et al 2005; Tasis D, et al 2006). These methods can be conveniently divided into chemical functionalization and physical methods based on the interactions between the active molecules and carbon atoms on the CNTs.

2.9.1 Chemical functionalization

Chemical functionalization is based on the covalent linkage of functional entities onto carbon scaffold of CNTs. It can be performed at the termini of the tubes or at their sidewalls. Direct covalent sidewall functionalization is associated with a change of hybridization from sp^2 to sp^3 and a simultaneous loss of π -conjugation system on graphene layer. This process can be made by reaction with some molecules of a high chemical reactivity, such as fluorine. It was shown that the fluorination of purified SWNEs occurred at temperature up to 325°C and the process was reversible using anhydrous hydrazine that could remove the fluorine (Mickelson ET, et al 1998). The fluorinated CNTs have C-F bonds that are weaker than those in alkyl fluoride (Kelly KF, et al 1999) and thus providing substitution sites for additional functionalization (Touhara H, et al 2002). Besides sidewall fluorination of CNTs, other similar methods, including cycloaddition, such as Diels-Alder reaction, carbene and nitrene addition (Chen J, et al 1998; Hu H, et al 2003; Holzinger M, et al 2004), chlorination bromination (Unger E, et al 2002),

hydrogenation (Kim KS, et al 2002), azomethine ylides (Tagmatarchis N, et al 2004) have also been successfully employed in recent years. All these methods can be regarded as the derivative of sidewall functionalization.

Defect functionalization is another method for covalent functionalization of CNTs. This process takes advantage of chemical transformation of defect sites on CNTs. Defect sites can be the open ends and /or holes in the sidewalls, pentagon or heptagon irregularities in the hexagon graphene framework. Oxygenated sites can also to be considered as defects. Defects can be created on the sidewalls as well as the open ends of CNTs by an oxidative process with strong acids such as HNO_3 , H_2SO_4 or a mixture of them (Esumi K, et al 1996), or with strong oxidants such as $KMnO_4$ (Yu R, et al 1998), ozone (Sham ML, et al 2006; Ma PC, et al 2006), reactive plasma (Wang SC, et al 2009; Avila-Orta CA, et al 2009). The defect on CNTs created by oxidants are stabilized by bonding with carboxylic acid (-COOH) hydroxyl (-OH) groups. The chemically functionalized CNTs can produce strong interfacial bonds with many polymers, allowing CNT based nanocomposites to possess high mechanical and functional properties.

2.9.2. Physical functionalization

Functionalization of CNTs using covalent method can provide useful functional groups onto the CNT surface. However, these methods have two major drawbacks: firstly, during the functionalization reaction, especially along with damaging ultrasonication process, a large number of defects are inevitably created on the CNT sidewalls, and in some extreme cases, CNTs are fragmented into

smaller pieces. These damaging effects results in severe degradation in mechanical properties of CNTs as well as disruption of π electro system in nanotubes. The disruption of π electrons is detrimental to transport properties of CNTs because defect sites scatter electrons and phonons that are responsible for the electrical and thermal conductions of CNTs, respectively. Secondly, concentrated acids or strong oxidants are often used for CNT functionalization, which are environmentally unfriendly. Therefore, many efforts have been put forward to developing methods that are convenient to use, of low cost and less damage to CNT structure.

2.9.3 Applications of surfactants for dispersing carbon nanotubes

It is extremely important to learn how to manipulate the surface properties in order to achieve a product with the desired properties. A surfactant's property of accumulation at surfaces or interfaces has been widely utilized to promote stable dispersion of solids in different media (Lee BI, et al 1991; Seelenmeyer S, et al 2000; Clarke JG, et al 1993; Green JH, et al 1988; Singh BP, et al 2005). Two important features which characterize surfactants, namely adsorption at interface and self accumulation into supramolecular structures, are advantageously used in processing stable colloidal dispersions. Naturally, the addition of the surfactant has an effect on the wetting behavior, and on the interfacial adhesion, which in return has an impact on the surfactant's ability to disperse the nanotubes. More detailed study of the interfacial chemistry of carbon nanotubes should be an important subject for future research in this area. However, on the basis of previous adsorption studies of hydrocarbon molecules on carbeneous materials, it

may be suggested that the surfactant interact with carbon through the hydrophobic segment. It should be pointed out that even with the addition of the surfactants to carbon nanotubes/polymer nanocomposites, complete homogeneous dispersion of the nanotubes cannot be achieved.

CHAPTER 3

3.0 EXPERIMENTAL METHODOLOGIES

This section demonstrates the step by step methods employed in obtaining the results to be discussed in Chapter 4. It highlights the methods and procedures for surface modification of CNTs and the Fourier Infrared Spectroscopy FTIR characterization techniques. The later sections discuss nanocomposites preparation and its characterization through the use of Transmission Electron Microscopy (TEM), Instron Tensile Testing machine, Differential Scanning Calorimetry (DSC), Thermogravimetric Analysis (TGA) and Rheology.

3.1 MATERIALS

The MWCNTs were purchased from Cheap Tube Inc, 112 Mercury Drive, Brattleboro, VT 05301 USA. The specifications of MWNTs are as follows: range of diameter 20-30nm, length of the tube 10-30 μ m, and purity >95wt%. The density of MWCNT is 2.1 g/cm^3 . The HDPE pallets were obtained from ExxonMobil Corporation and their grades are HDPE HMA 014. The melt index and density of the HDPE pallets are 4.0g/10 min and 0.960 g/cm^3 , respectively.

3.1.1 Acid Modification of MWCNT

The CNTs were mixed with concentrated nitric acid at a ratio of 1:10 in a round bottom flask and refluxed for 48hours at 120°C under continuous stirring (using magnetic stirrer) to obtain CNT-COOH modified MWCNTs (Bae JH, et al 2007). Upon cooling, the mixture was thoroughly filtered, washed continuously with deionized water to remove last traces of unreacted acid until the pH value was almost 7 which signifies zero acidity. The modified multiwall carbon nanotubes, henceforth MWCNT-COOH was filtered and dried at 60°C (Bae JH, et al 2007).

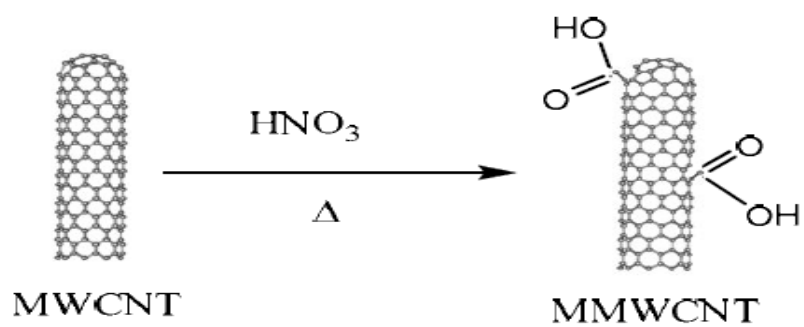


Fig 9: Chemical modification multiwall of carbon nanotubes (MWCNTs) through thermal oxidation.

3.1.2 Substitution of Carboxylic (-COOH) group with different Surfactants

Surface functionalization of CNTs with surfactants was achieved by substitution of the MWCNT-COOH with appropriate surfactants: 1-Octadecanol (C18) and phenol at the surfactant melting temperature (Huges M., et al 2002). The first functionalization carried out was the substitution of carboxylic group in MWCNT-COOH with 1-Octadecanol ($C_{18}H_{38}O$). For this purpose, 4g of MWCNT-COOH nanotubes was collected from the bulk samples of the acid modified CNTs and reacted with C_{18} in a few drops of sulfuric acid at a MWCNT-COOH to C_{18} ratio of ratio 1:10 and a temperature of 59.8°C for six (6) hrs under continuous stirring. The reaction takes place as shown in the scheme below

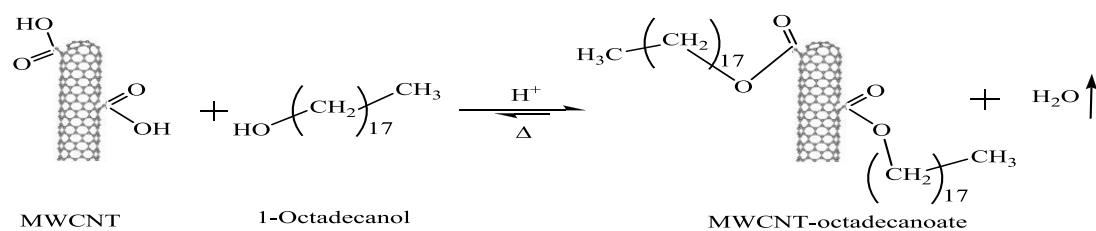


Fig.10. Mechanism of C_{18} modification of MWCNT (MWCNT- C_{18})

The resulting mixture was allowed to cool down, then washed and filtered in excess toluene solution.

For the substitution of MWCNT-COOH with phenol group, phenol was mixed with MWCNT-COOH in a few drops of sulfuric acid at a ratio 10:1. The mixture was then heated at 42°C with continuous stirring for about six (6) hrs to obtain phenol modified CNTs. The content was allowed to cool as with the previous substitution process, and then washed with toluene solution.

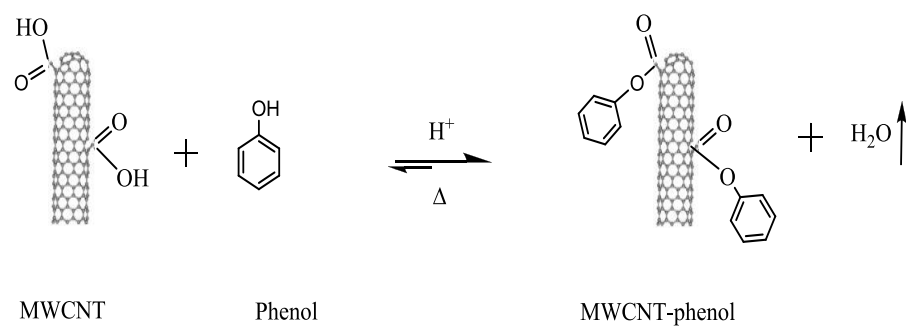


Fig.11. Mechanism of phenol modification of MWCNT (MWCNT- phenol)

3.1.3 Sample preparation

High Density Polyethylene (HDPE) was melt blended with 1wt%, 3wt%, and 5wt% MWCNTs using a Brabender mixer. To disperse MWCNTs powder into HDPE matrix more uniformly and to avoid thermal degradation of HDPE, HDPE and various amounts of MWCNTs were mixed at 150°C for 10min using Brabender mixer at the speed of 120rpm. The blended mixtures were then hot pressed at 150°C under 9MPa into plates using Carver hot-press. The same procedure was repeated for the MWCNTs with different surfactants.

3.1.4 Tensile properties

Tensile properties of the molded dog bone specimens were tested according to the ASTM-D638 standard, using an Instron machine (Model 5567) at room temperature and a crosshead speed of 50mm/min. The average test specimen dimensions were 15mm × 3mm × 1mm. A minimum of five samples were tested for each MWCNTs/HDPE nanocomposites.

3.1.5 Thermal analysis of the samples

The literature highlights the crystallinity as having a relative influence on the mechanical properties of composites, therefore thermal analysis of the MWCNT-HDPE sample and MWCNTs with different surfactants was carried out using DSC and TGA.

The thermal transition of the composites was evaluated using non-isothermal DSC analysis. The analysis was performed by using TA Q1000 instrument equipped

with liquid nitrogen cooling system and auto sampler. The samples (sample size was around 6mg) in non-hermetic pan were heated and cooled at the rate 10°C/min, and the temperature range of 30-170°C. The measurement process was as follows: first the sample was heated to 170°C, stayed for 5 minutes to eliminate the thermal history and then was cooled to observe the crystallinity behavior. The thermal stability of the nanocomposites was studied using thermogravimetric analysis (TGA). TGA measurements were carried out using TA Instrument Hi-Res SDT Q600 thermogravimetric analyzer from 25 to 800°C with the heating rate of 10°C/min and a nitrogen gas flow rate of 50 cm^3/min .

3.1.6 Rheological characterization

The rheological behavior of the composites was studied using an ARES (Rheometrics, Inc.) cone plate rheometer at 200°C, using dynamic oscillation frequency sweep of 0.015-100 rad/s and back, in the linear viscoelastic range (2%) under a nitrogen atmosphere.

CHAPTER 4

4.0 RESULTS AND DISCUSSIONS

In this chapter, experimental results are presented and discussed. The experimental results of the effects of functionalized carbon nanotubes with different types of surfactants on mechanical and thermal properties of polyethylene (HDPE) were designed in four stages. The first section covers characterization of surface chemistry of the modified carbon nanotubes using Fourier Infrared Spectroscopy (FTIR). The remaining three stages involve discussion on the mechanical and thermal properties of polyethylene/CNT with the aid of Instron Testing Machine, Differential Scanning Calorimetry (DSC) and thermogravimetric analyzer (TGA) respectively.

4.1 THE FOURIER TRANSFORM INFRARED SPECTROSCOPY (FTIR) CHARACTERIZATION

Infrared spectroscopy is an extremely powerful analytical technique for both qualitative and quantitative analysis. In order to identify the existence of functional group on the MWCNTs surface, Fourier Transform Infrared Spectroscopy (FTIR) performed for all the nanotubes in the range of 400 - 4000 cm^{-1} . FTIR spectroscopy has been widely used in the determination of structure of molecules (Socrates G. 1980). Its application in the study of surface chemistry has

provided one of the direct means of observing the interaction and perturbations that occur at the surface during adsorption and in determining the structure of the absorbed species. Fig 12 shows the spectra of MWCNT.

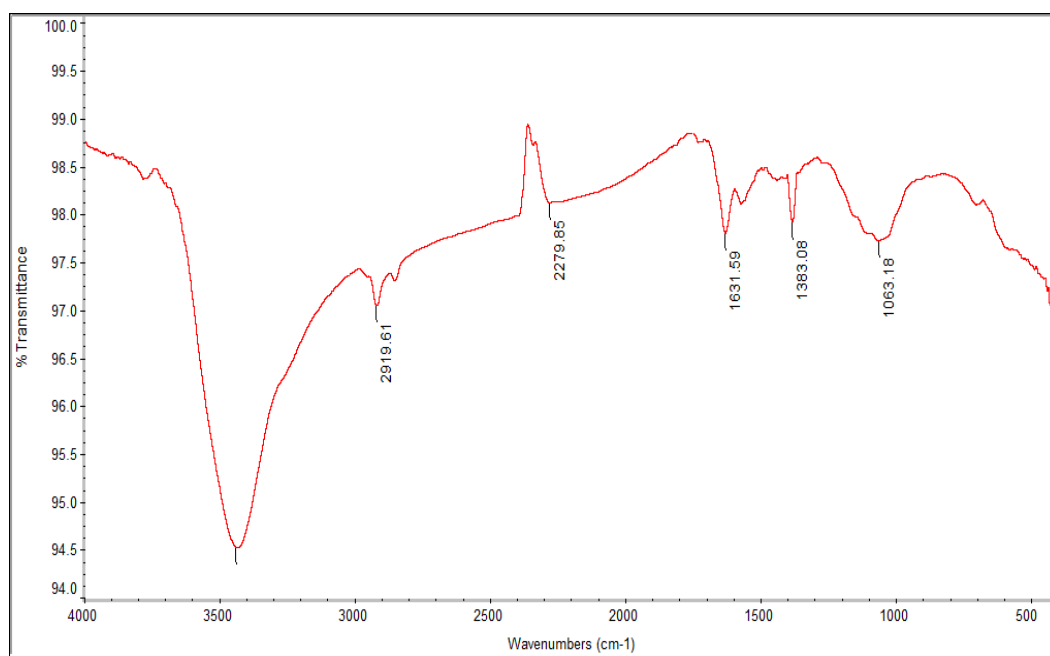


Fig 12: FTIR of multiwalled carbon nanotubes (MWCNT)

The IR spectrum for the MWCNT shows absorption band at 3447cm^{-1} (hydrogen bonded O-H stretch) which is ascribed to the characteristic spectrum of carboxylic acid. As can be seen from Fig 12 above, this particular peak is usually broad and can obscure other peaks within the entire region of 3500 to 2500cm^{-1} . Moreover, carboxylic peak C=O stretching peak is observed from 2279 to 1631cm^{-1} . It should be noticed that the as received MWCNTs were purified and a part of catalytic metallic nanoparticles were possibly eliminated during the purification process cutting the nanotube cap. Thus, the presence of carboxylic groups in these MWCNTs is expectable. The peak at 1383cm^{-1} can be associated with the stretching of carbon nanotubes backbone. Following the chemical modification of the carbon nanotubes with concentrated nitric acid (HNO_3), a new spectrum was obtained as shown in the Fig. 13 below:

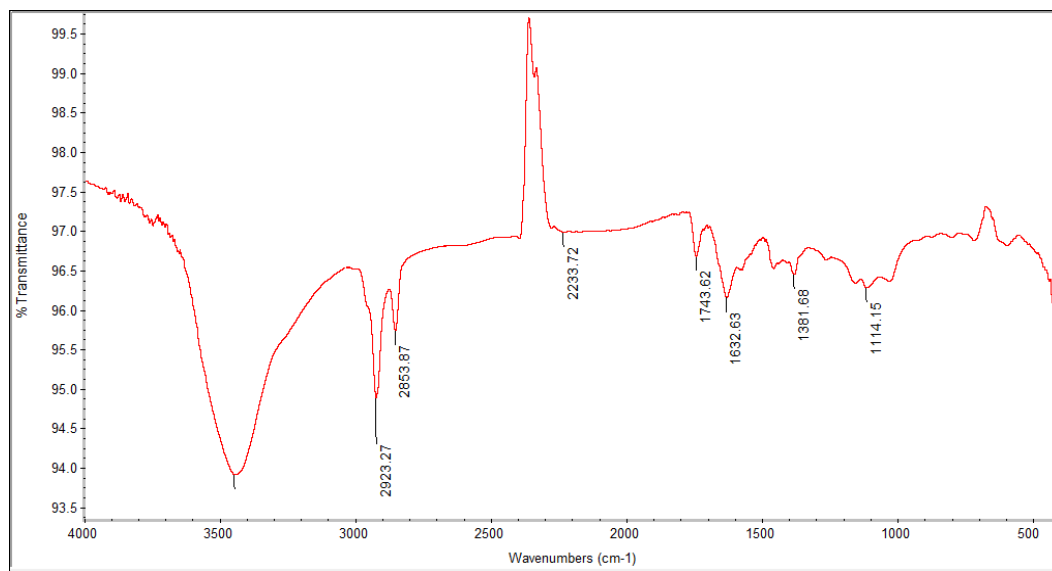


Fig.13: FTIR of MWCNT modified with COOH

The spectrum shows absorption band at 3447cm^{-1} attributed to hydrogen bonded O-H stretching, $2923\text{-}2233\text{cm}^{-1}$ which is attributed to symmetric and asymmetric CH_2 and a peak at 1632cm^{-1} ascribed to the oscillation of carboxylic groups C=O which moves to 1743cm^{-1} associated with the stretch mode of carboxylic groups stretching of carbon nanotubes backbone. The existence of these peaks signified the success of surface modification of the CNTs with carboxylic acid group. The peak at 1381cm^{-1} can be associated with the stretching of carbon nanotubes backbone. Similarly, substitution of MWCNT-COOH with 1- Octadecanol shown in Fig 14 below gives an indicative peak at 2920cm^{-1} corresponding to CH_2 stretching of long alkyl molecule of 1- Octadecanol emanates upon modification of MWCNT-COOH to MWCNT- C_{18} .

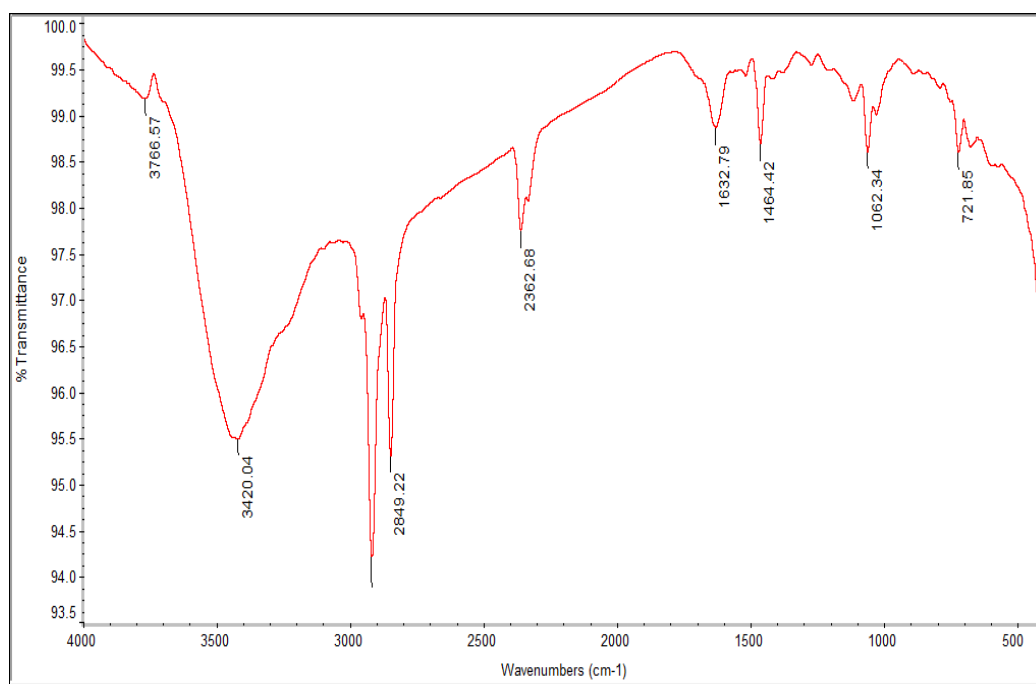


Fig 14: FTIR of MWCNT-C₁₈.

Besides, modification with Octadecanol gives a medium C-H stretch and C-H bend of alkenes' at 2849cm^{-1} and 1464cm^{-1} respectively. An indicative of long chain alkyl ester at 1062cm^{-1} generated from esterification reaction of OH group of Octadecanol COOH group of acid modified carbon nanotubes was also identified. Finally, a peak showing C-H bend at 721cm^{-1} also depicts the success of MWCNT-COOH modification with Octadecanol. Hence, we have MWCNT-C₁₈ modified carbon nanotubes. Likewise, Fig 15 shows the FTIR spectrum of MWCNT-phenol. The substitution of MWCNT-COOH with phenolic group gives an indicative peak at 1120cm^{-1} due to C-O stretching of phenolic ester. Moreover, strong peak at 622cm^{-1} indicate the existence of phenoxide groups generated from the reaction between carboxylic COOH and phenyl alcohol was also identified.

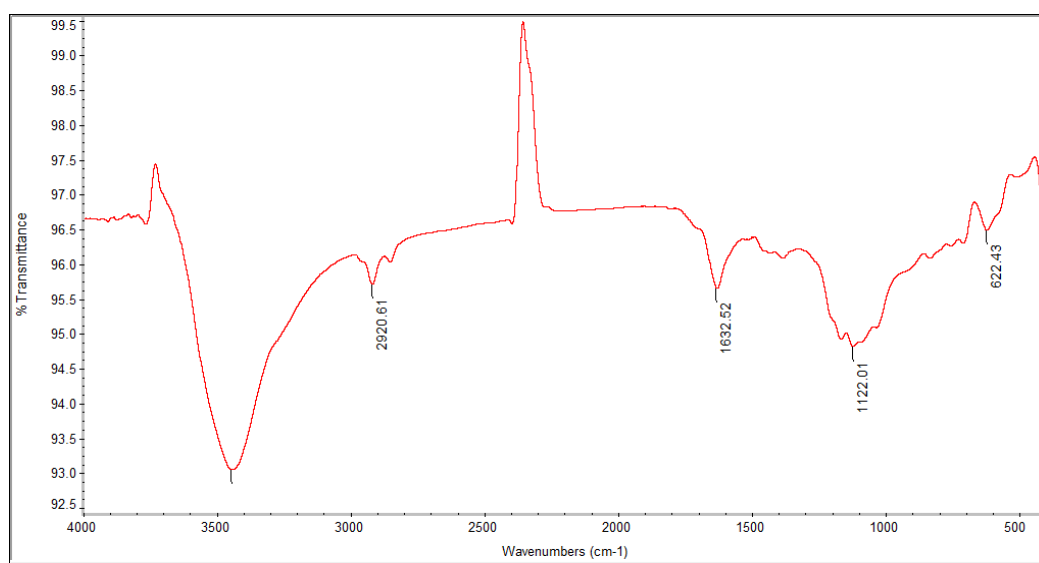


Fig 15: FTIR of MWCNT-phenol.

4.2 CARBON NANOTUBES DISPERSION

To analyze the dispersion of MWCNTs within the HDPE nanocomposites, neat HDPE and HDPE/MWCNT-C₁₈ nanocomposites were submerged in liquid N₂ for 3-4 min followed by fracturing, upon which the fractured surfaces were analyzed using SEM. Figs 16-17 show SEM micrographs of the fracture surfaces obtained upon cryofracturing. Such images of the nanocomposites indicate a relatively homogeneous dispersion of the MWCNTs in HDPE/MWCNT-C₁₈ nanocomposites.

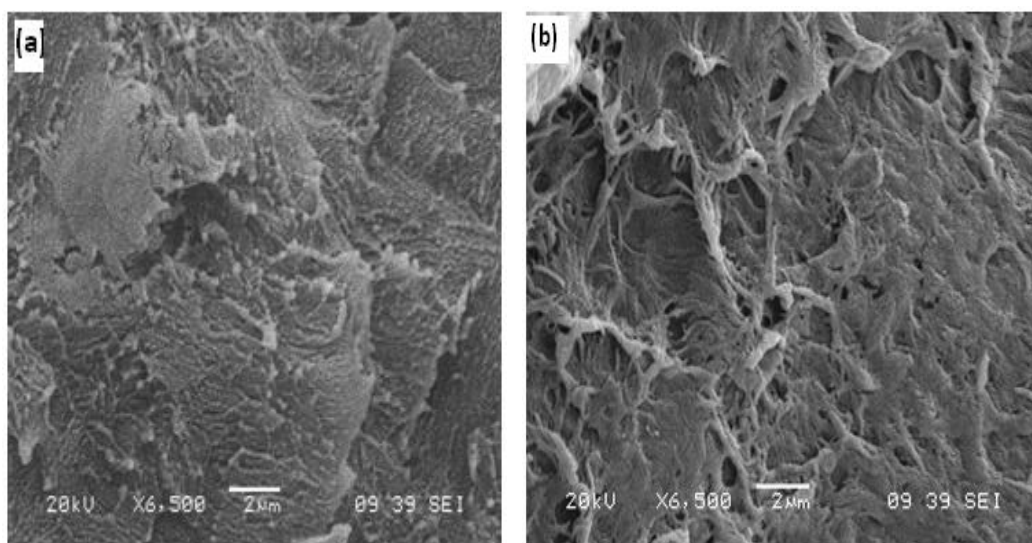


Figure 16: SEM images of (a) neat HDPE; (b) HDPE/MWCNT-C₁₈ 1wt%

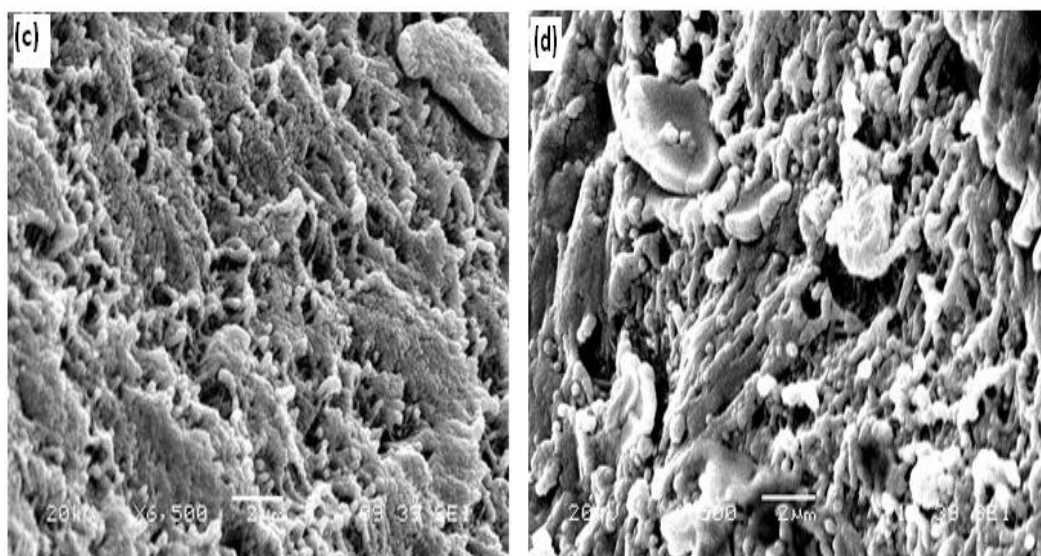


Figure 17: SEM images of (c) HDPE/MWCNT-C₁₈ 3wt%; (d) HDPE/MWCNT-C₁₈ 5wt%

4.3 TENSILE PROPERTIES OF HDPE NANOCOMPOSITES

Table 4 gives the overall view of mechanical properties of nanocomposites, i.e. elastic modulus, ultimate strength, toughness, strain at fracture, percentage increase in elastic modulus, percentage increase in ultimate strength, percentage decrease in strain at fracture and percentage decrease in toughness with an addition of MWCNTs and the surfactants (COOH, C₁₈ and phenol). In each case, minimum of five samples were tested and the tabulated values are the average of these results. It can be observed from figures 18-19 that the ultimate strength and elastic modulus show good enhancement with an increase in MWCNTs concentration and surfactants, which is believed to be due to good interface between polymer and MWCNT thus transferring load from polymer to MWCNT. However, not much improvement was achieved in HDPE-MWCNT/C₁₈ and HDPE-MWCNT/phenol. This could be as a result of inhomogeneous dispersion of CNT (i.e. agglomeration). The percentage increase of Young's modulus starts from 14.4% to 49.7%, 31% to 50.5%, 1.0% to 8.1%, and 9.7% to 37.7% with an increase of MWCNT, HDPE-MWCNT/COOH, HDPE-MWCNT/C₁₈, and HDPE-MWCNT/phenol concentrations respectively. Likewise, the percentage increase of ultimate strength starts from 5.5% to 21.6%, 24.0% to 26.5%, 0.9% to 9.0% and 0.8% to 19.0% with an increase of MWCNT, HDPE-MWCNT/COOH, HDPE-MWCNT/C₁₈, and HDPE-MWCNT/phenol loadings respectively. In case of strain at fracture as shown in figure 20, it decreases with addition of MWCNTs and the surfactants. Moreover, the neck formation of composite samples starts to occur between 10% to 15% of fracture strain. This is followed by a plateau region till its breaking point

which is due to strain induced crystallization of the polymer resulting into material hardening. In case of toughness, it is calculated from the area under the stress versus strain curve. It is also decreasing with an addition of MWCNT and the surfactants.

Table 4. Mechanical properties of MWCNT-HDPE nanocomposites

Composites	Ultimate Strength (MPa)	Young's modulus (MPa)	Toughness (MJ/m³)	% Strain @ fracture
Neat HDPE	26.50	515.43	35.10	1938
HDPE-MWCNT 1%	27.97	589.77	32.80	1745
HDPE-MWCNT 3%	31.65	743.89	8.73	443
HDPE-MWCNT 5%	32.23	771.96	3.30	175
HDPE-MWCNT/COOH 1%	32.87	676.94	14.82	664
HDPE-MWCNT/COOH 3%	32.89	682.56	6.77	351
HDPE-MWCNT/COOH 5%	33.53	776.24	1.58	77
HDPE-MWCNT/C₁₈ 1%	26.70	521.07	34.01	1865
HDPE-MWCNT/C₁₈ 3%	28.67	555.52	32.24	1629
HDPE-MWCNT/C₁₈ 5%	28.89	557.47	25.19	1333
HDPE-MWCNT/PHENOL1%	26.72	565.53	18.61	1003
HDPE-MWCNT/PHENOL3%	29.31	648.20	6.40	346
HDPE-MWCNT/PHENOL5%	31.56	710.13	5.92	299

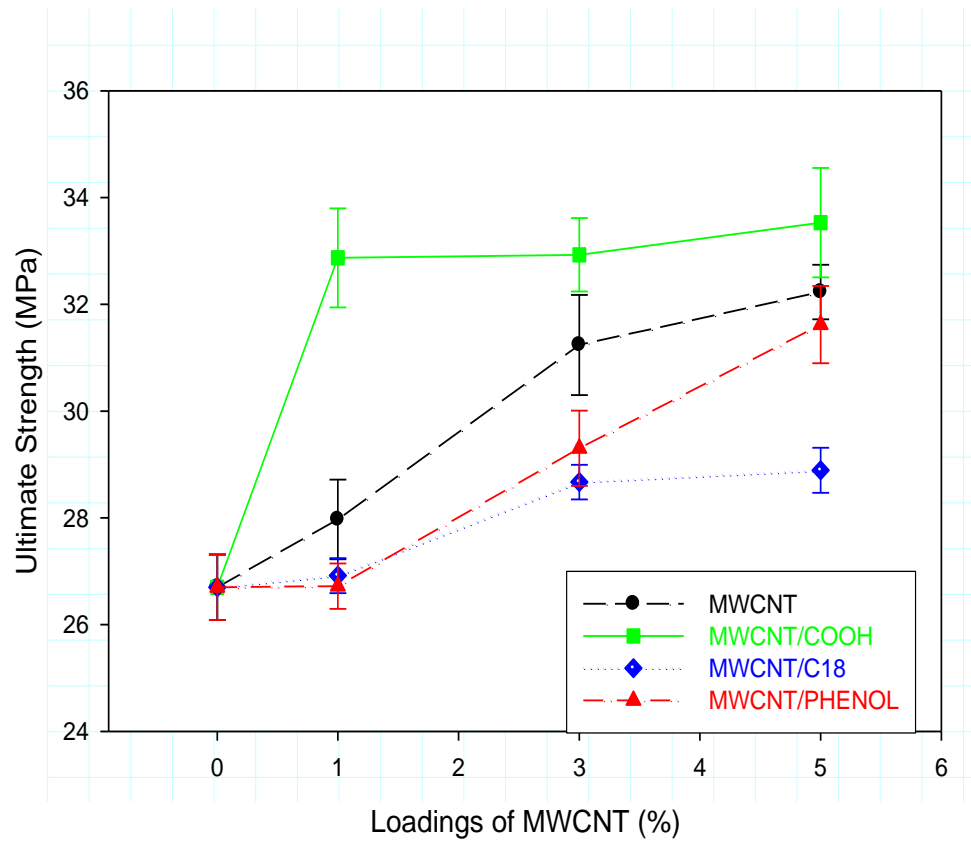


Figure.18. Ultimate strength of HDPE nanocomposites

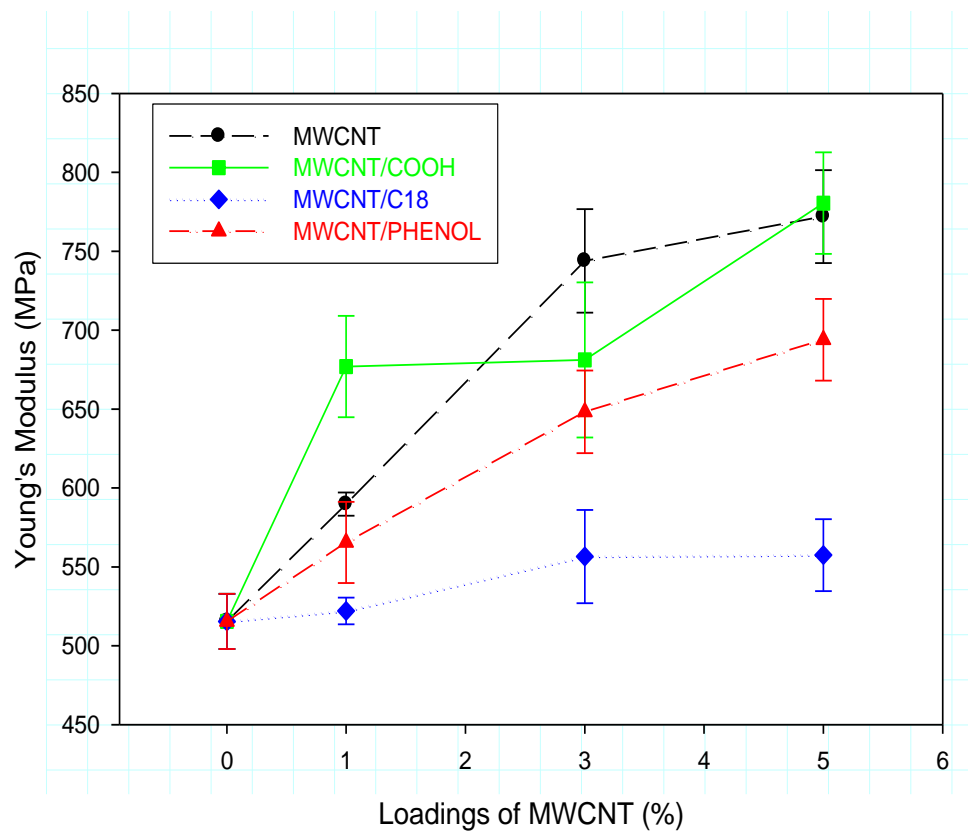


Figure.19.Young's modulus of HDPE nanocomposites.

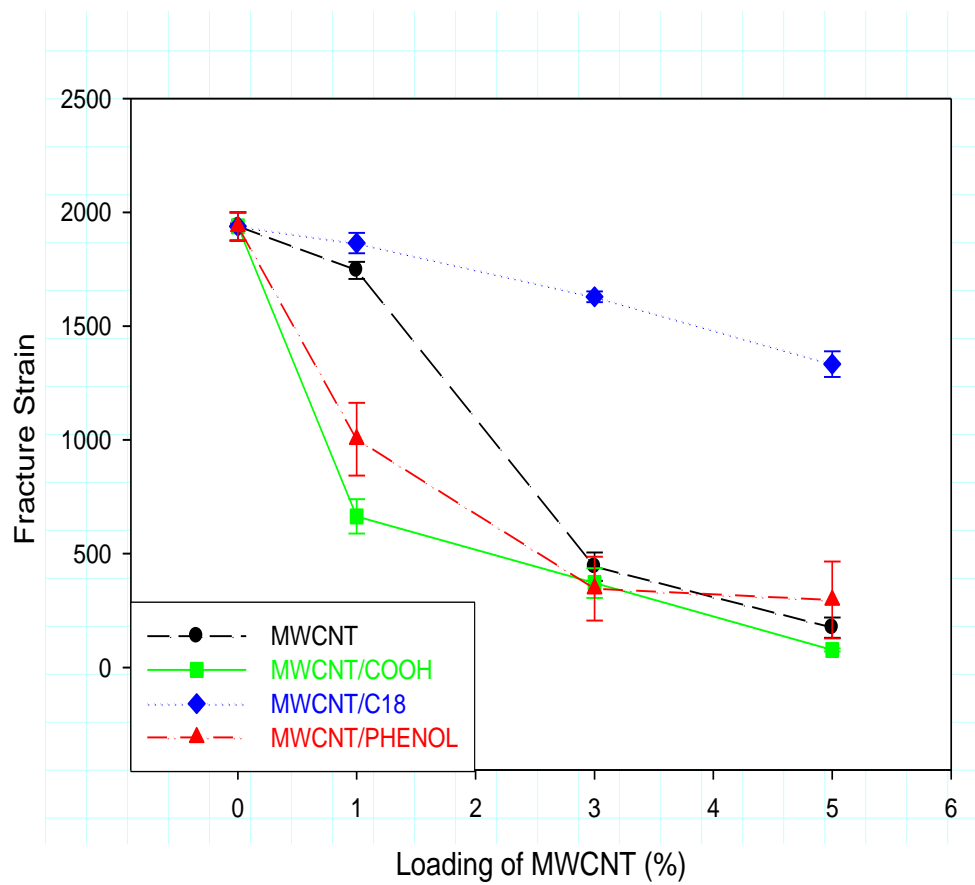


Figure 20. Strain at break of HDPE nanocomposites.

4.4 EFFECT OF CNTs ON THE ENERGY ABSORPTION OF HDPE-NANOCOMPOSITES

Figure 21 shows the toughness of MWCNTs and surfactants on HDPE nanocomposites and also considers the amount of energy required to fracture a material. From the analysis of figure 21, it was evident that increasing the amount of MWCNTs and surfactants in the HDPE matrices, the energy of absorption needed to fracture these samples decreased. Since the strength is proportional to the force needed to break the sample, and strain is measured in units of distance (i.e the distance the sample is stretched), then strength times strain is proportional to force times distance which in turn equals energy given by:

$$(\text{Strength} \times \text{Strain}) \propto (\text{Force} \times \text{Distance}) = \text{Energy}$$

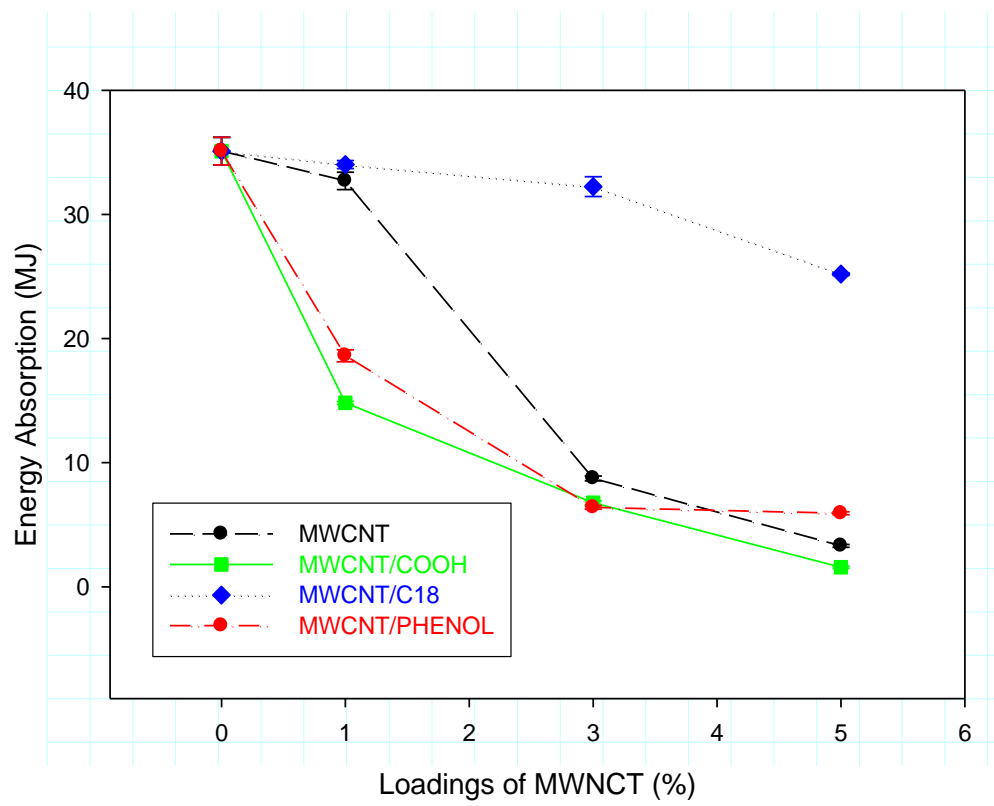


Fig.21: The toughness as a function of wt% for HPDE nanocomposites.

In general, the ultimate strength and stiffness increased with the amount of MWCNTs and surfactants concentration from 1-5%. Whereas, the energy required to fracture these samples decreased with an increase in MWCNTs and surfactants concentrations. The decrease can be observed from the fact that the strain decreases in all the samples with the addition of MWCNTs and surfactants.

4.5 THERMAL ANALYSIS OF HDPE NANOCOMPOSITES

As the crystallinity of the polymer composites is having influence on Young's modulus and toughness, it was decided to study thermal analysis of the composites, i.e. DSC (Differential Scanning Calorimetry) and TGA (thermogravimetric analysis). Figs 22-29 show the DSC curves of HDPE nanocomposites. In DSC analysis, the addition of MWCNTs and surfactants in HDPE decrease the total enthalpy of crystallization from 1% to 5% loading for all the composites. The melting temperature of composites occurred within the range of 133.7 °C to 136.8 °C indicating the degree of polymer crystallinity in all composites. The reinforcement of MWCNTs and surfactants in HDPE slightly affect the melting point of the composites. Table 5 shows all the characteristic temperatures and enthalpy values, where 100% pure crystalline HDPE polymer gives enthalpy of 293J/g, from literature. The nucleation and growth of individual crystallites are so rapid that a very large number of crystallites are formed together thus the large amount of heat is liberated during the crystallization of HDPE by adding MWCNTs and surfactants. The degree of crystallization was

evaluated from heat generated during crystallization (ΔH_c) using the relationship:

$$X_c = \frac{\Delta H_c}{(1-wt\%)\Delta H} \times 100$$

Where ΔH is the theoretical enthalpy of fusion for 100% pure crystalline HDPE (293J/g) and wt% is the weight fraction of MWCNTs in the nanocomposites (Mark J. E. 1996).

Table 5. Crystallization Temperatures, Melting Temperatures, and Enthalpies

Composites	T _{m, onset} °C	T _{m, peak} °C	ΔH _m J/g	T _{c, onset} °C	T _{c, peak} °C	ΔH _c J/g	% X _c
Neat HDPE	126.5	135.1	161.5	121.9	120.0	173.8	59.9
HDPE-MWCNT1%	126.7	135.8	221.9	124.7	121.9	249.2	85.9
HDPE-MWCNT3%	126.5	136.5	211.2	125.0	121.8	240.9	84.8
HDPE-MWCNT5%	127.2	136.2	194.7	125.0	121.9	228.0	81.9
HDPE-MWCNT/COOH1%	126.9	136.0	197.5	124.6	121.0	248.2	85.6
HDPE-MWCNT/COOH3%	127.1	135.2	220.3	125.0	122.8	240.2	84.5
HDPE-MWCNT/COOH5%	126.9	136.4	202.3	125.1	121.8	231.1	83.8
HDPE-MWCNT/ C ₁₈ 1%	126.9	135.5	217.5	124.5	121.8	249.6	86.0
HDPE-MWCNT/ C ₁₈ 3%	126.8	134.4	217.6	124.6	122.3	243.1	85.5
HDPE-MWCNT/ C ₁₈ 5%	126.9	133.7	211.0	124.6	122.5	231.1	83.0
HDPE-MWCNT/phenol 1%	129.2	136.8	208.0	124.4	121.2	249.2	85.9
HDPE-MWCNT/phenol 3%	126.8	135.7	210.2	124.8	122.2	242.5	85.3
HDPE-MWCNT/ phenol 5%	126.5	135.9	199.2	124.9	121.6	227.3	81.7

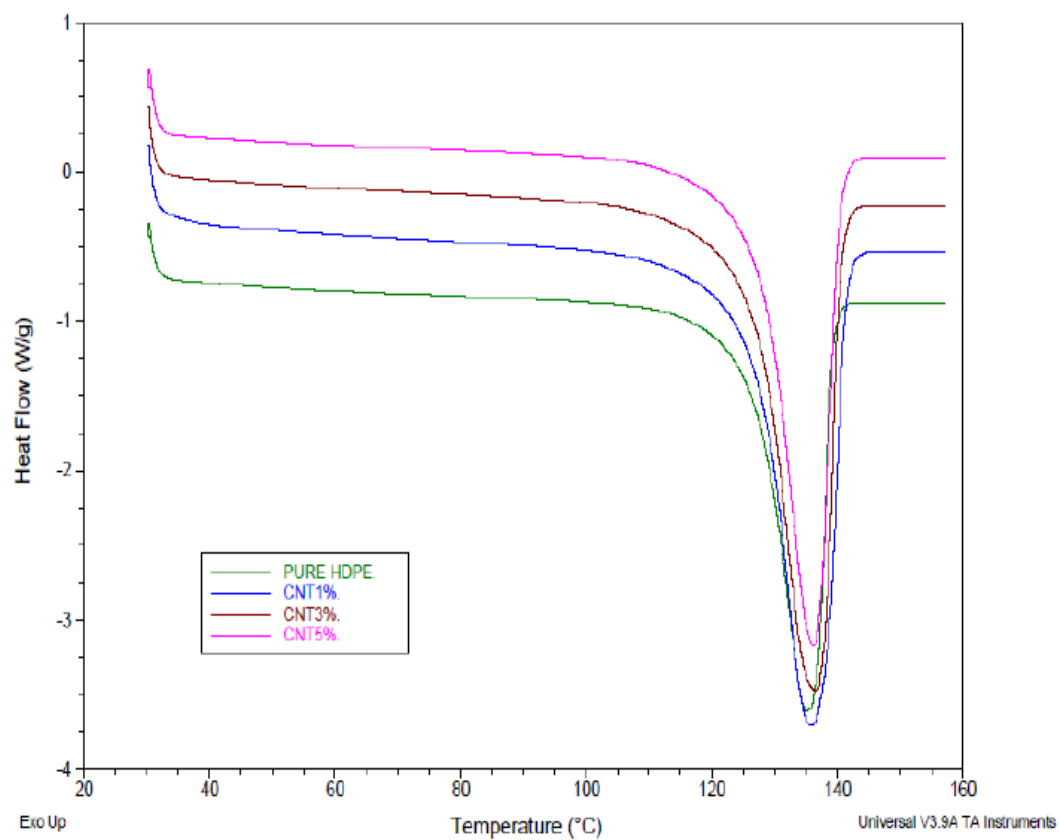


Figure.22.Melting temperature curves of MWCNT-HPDE nanocomposites

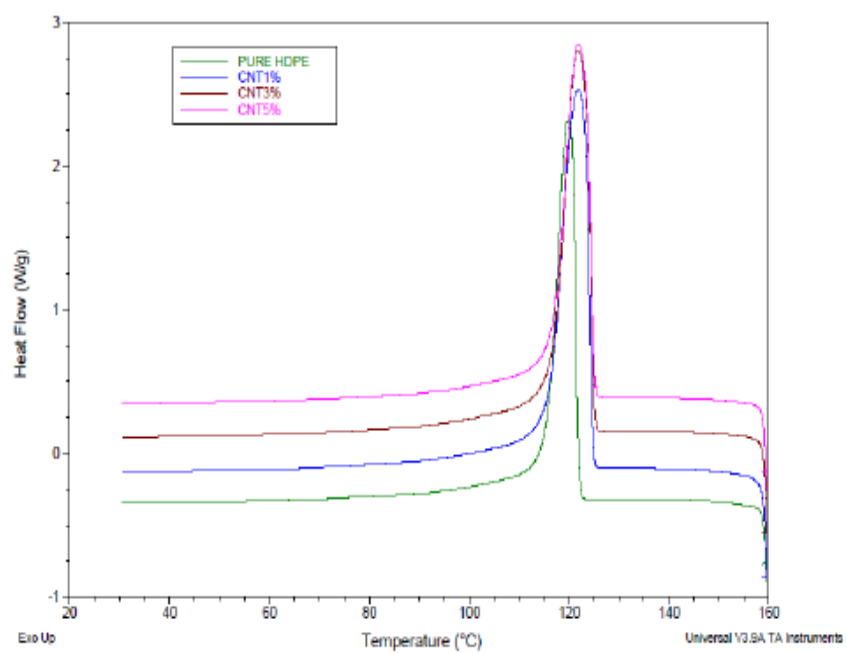


Figure.23. Crystallization temperature curves of MWCNT-HPDE nanocomposites

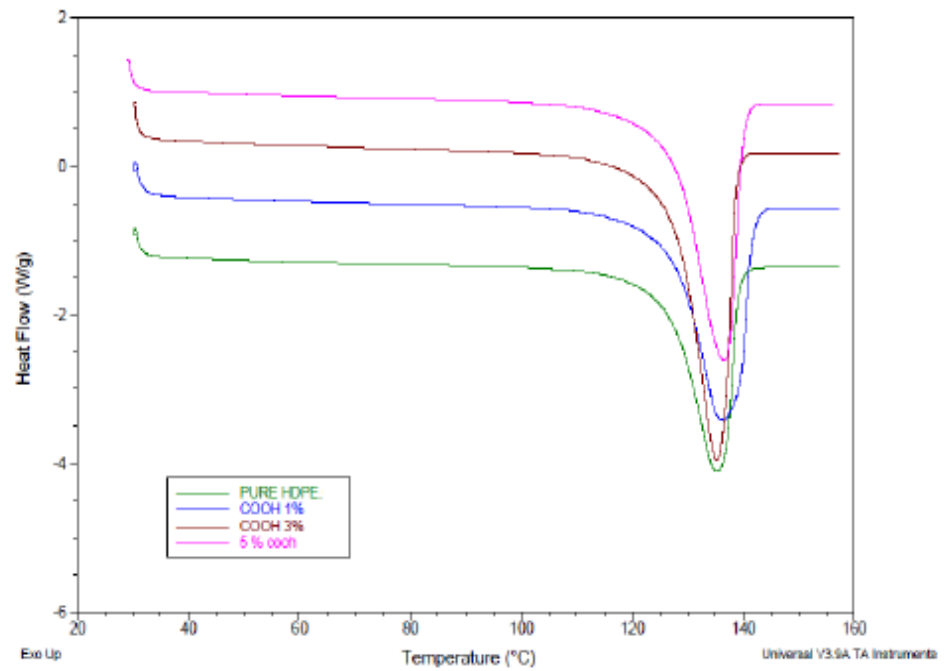


Figure.24. Melting temperature curves of MWCNT/COOH-HPDE nanocomposites

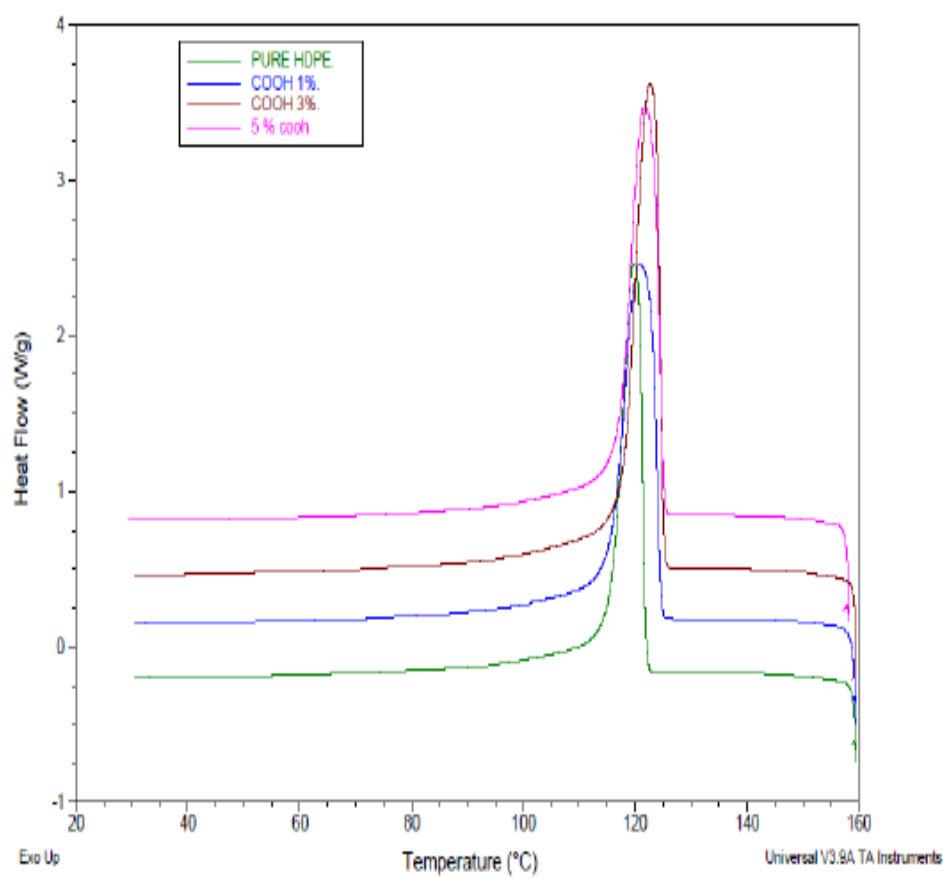


Figure 25. Crystallization temperature curves of MWCNT/COOH-HPDE nanocomposites.

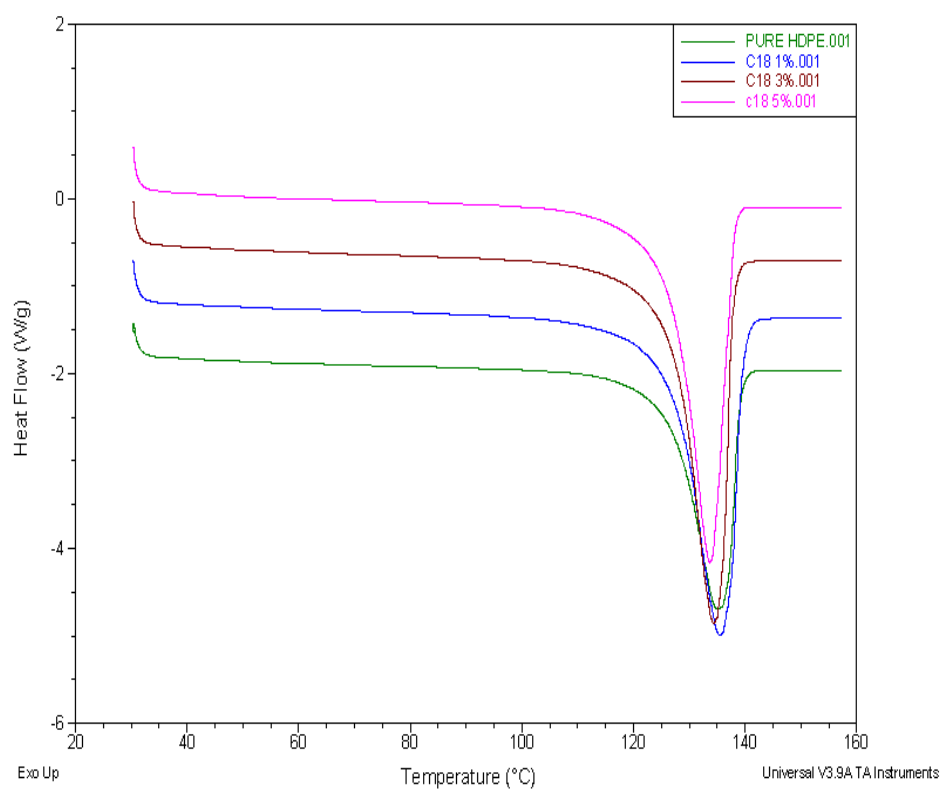


Figure.26.Melting temperature curves of MWCNT/C₁₈-HPDE nanocomposites

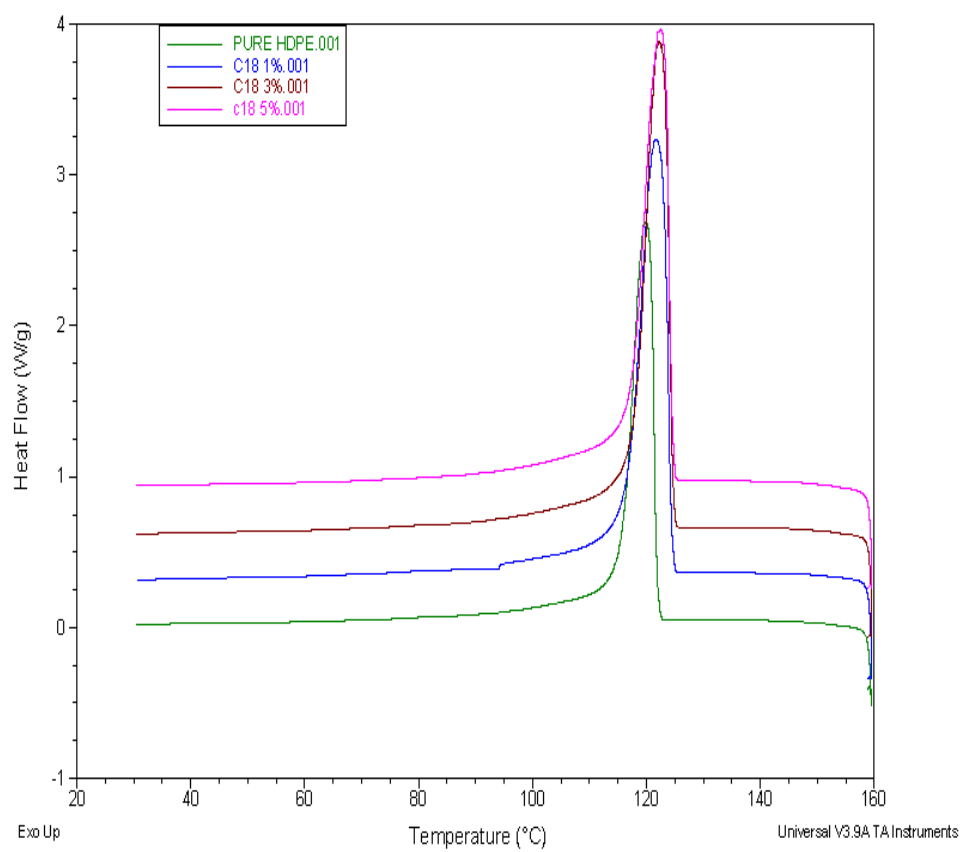


Figure.27.Crystallization temperature curves of MWCNT/C₁₈-HPDE nanocomposites

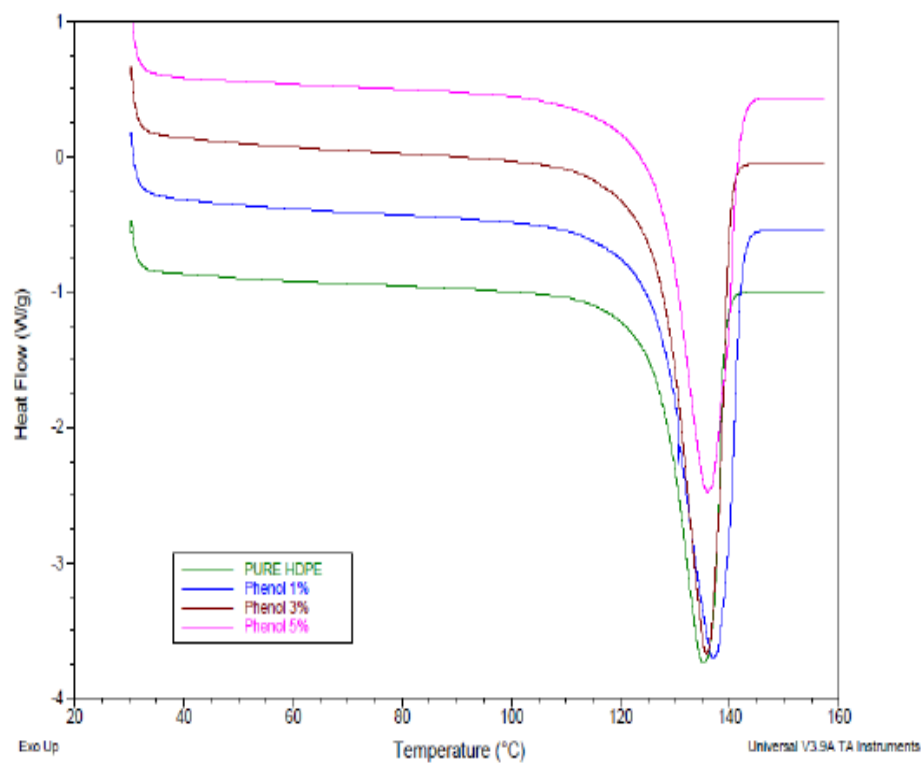


Figure28. Melting temperature curves of MWCNT/PHENOL-HPDE nanocomposites

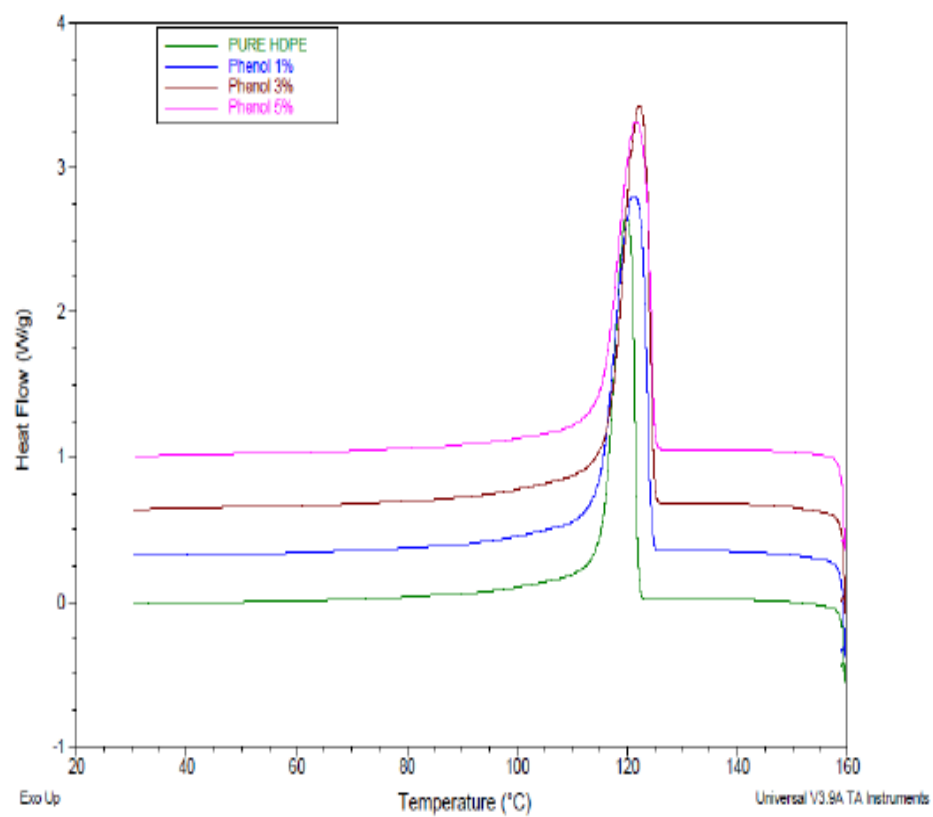


Figure.29.Crystallization temperature curves of MWCNT/PHENOL-HPDE nanocomposites.

An interesting phenomenon shown in Figure 30-33 are the slight variation in the melting temperature, $T_{m,peak}$, (133.7 °C to 136.8 °C) as a function of MWCNT in samples as compared to neat HDPE. One is tempted to explain the trends shown in Figure 13-16 on the basis of a simple nucleating agent action. However, HDPE is a polymer with an already high nuclei density; therefore, normally, even when it is nucleated by an external agent, its melting point should not be greatly affected. Moreover, little variation was also observed in the crystallization temperature, $T_{c,peak}$, (121.0 °C to 122.8).

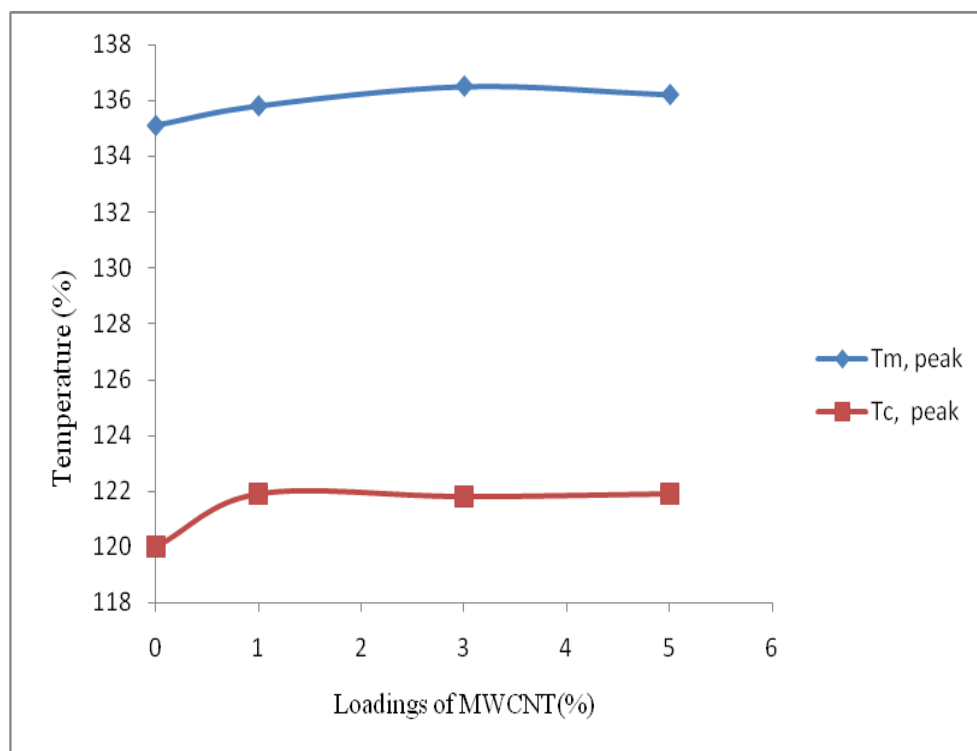


Figure.30. Influence of MWCNT content on peak crystallization and melting temperature ($T_{c, peak}$ and $T_{m, peak}$) for HDPE/MWCNT nanocomposites.

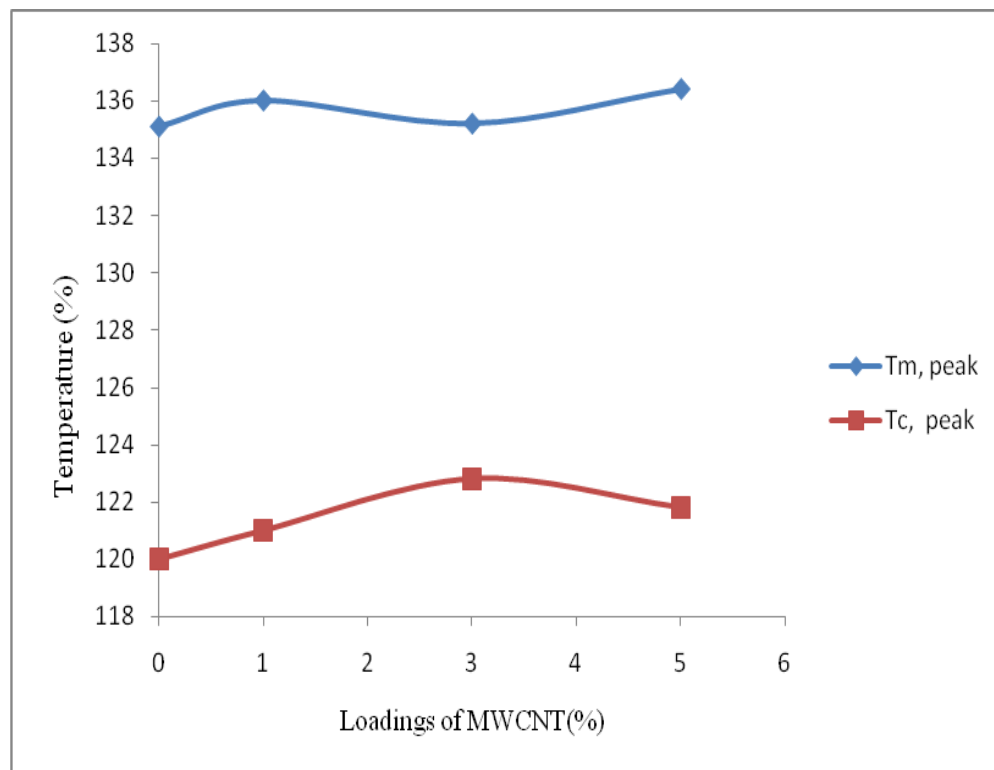


Figure.31. Influence of MWCNT content on peak crystallization and melting temperature ($T_{c, \text{peak}}$ and $T_{m, \text{peak}}$) for MWCNT-COOH/HDPE nanocomposites.

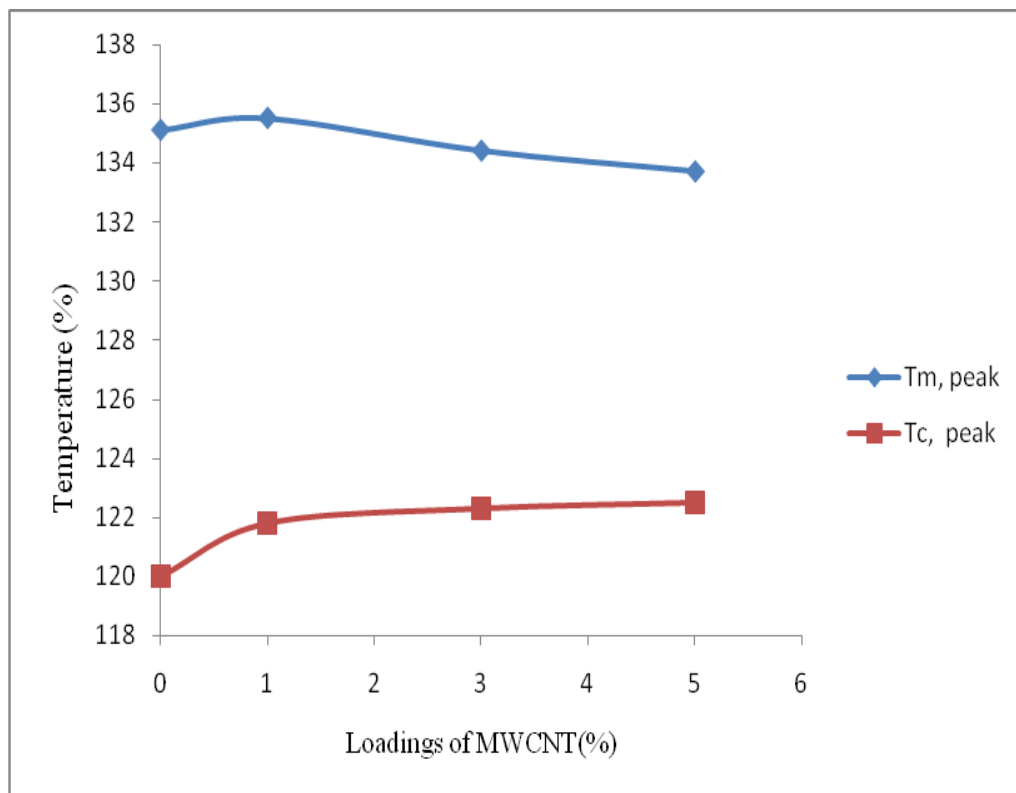


Figure.32. Influence of MWCNT content on peak crystallization and melting temperature ($T_{c, peak}$ and $T_{m, peak}$) for MWCNT-C₁₈/HDPE nanocomposites

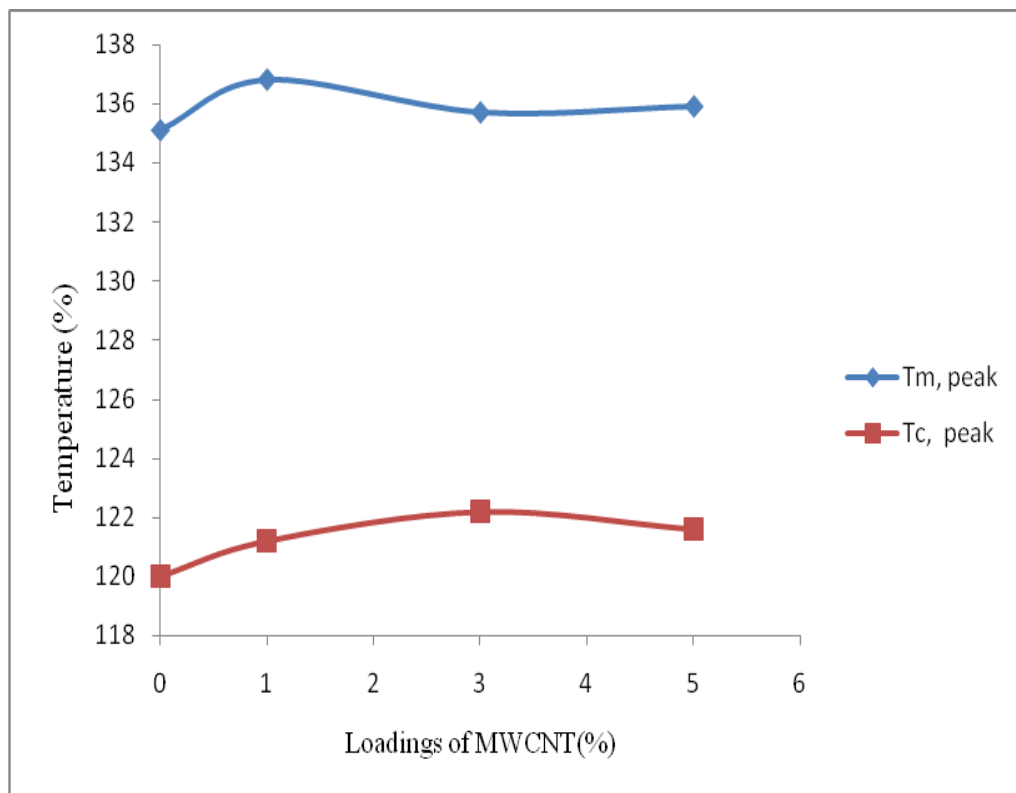


Figure.33. Influence of MWCNT content on peak crystallization and melting temperature ($T_{c, peak}$ and $T_{m, peak}$) for MWCNT-phenol/HDPE nanocomposites.

Moreover, Figs 34-37 show the influence of MWCNT and surfactants (COOH, C₁₈, and phenol) content on the degree of crystallinity (X_c) for all the nanocomposites. The tendency of degree of crystallinity to slightly decrease upon increasing the MWCNTs and surfactants content may be attributed as reported for HDPE/CNT nanocomposites (Trujillo M, et al. 2008), to the probable interference of the MWCNTs with the crystal growth.

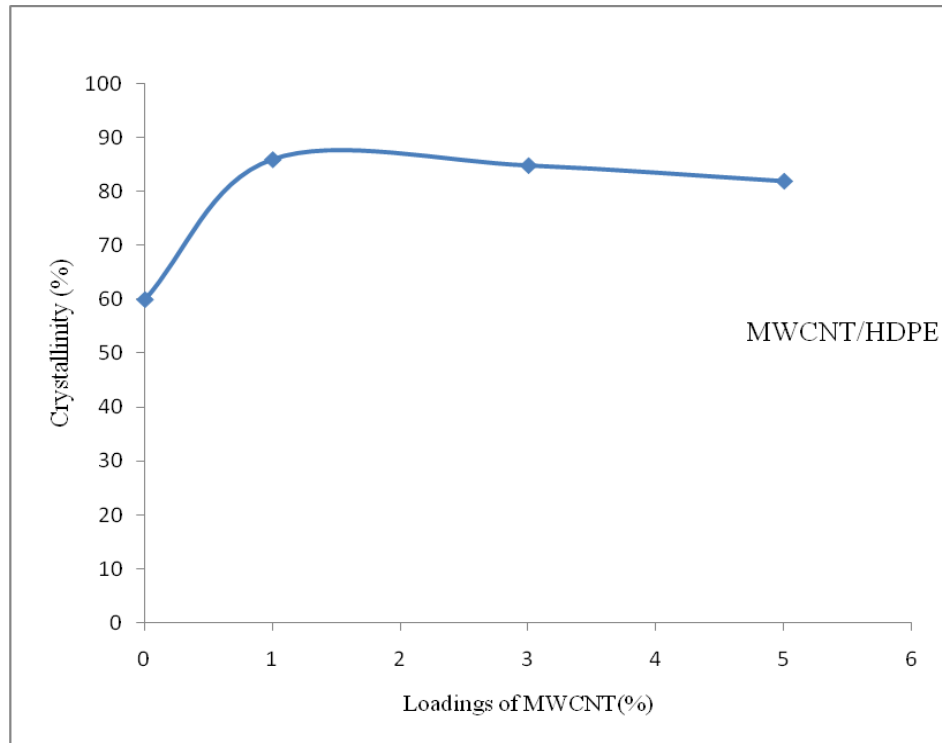


Figure.34. Influence of MWCNT content on the degree of crystallinity (X_c) for MWCNT/HDPE nanocomposites.

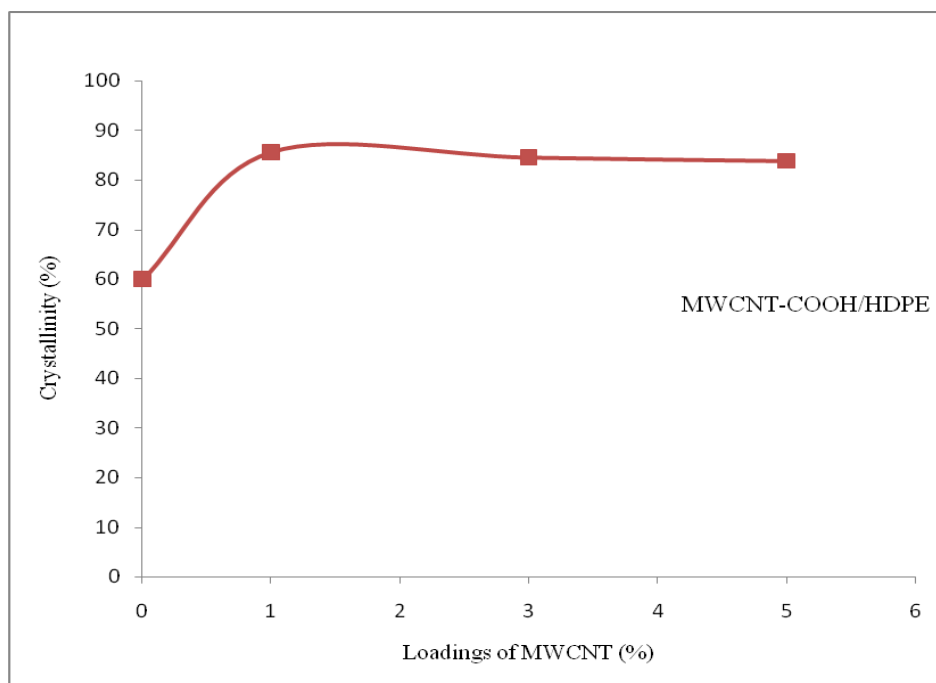


Figure 35. Influence of MWCNT content on the degree of crystallinity (X_c) for MWCNT-COOH/HDPE nanocomposites.

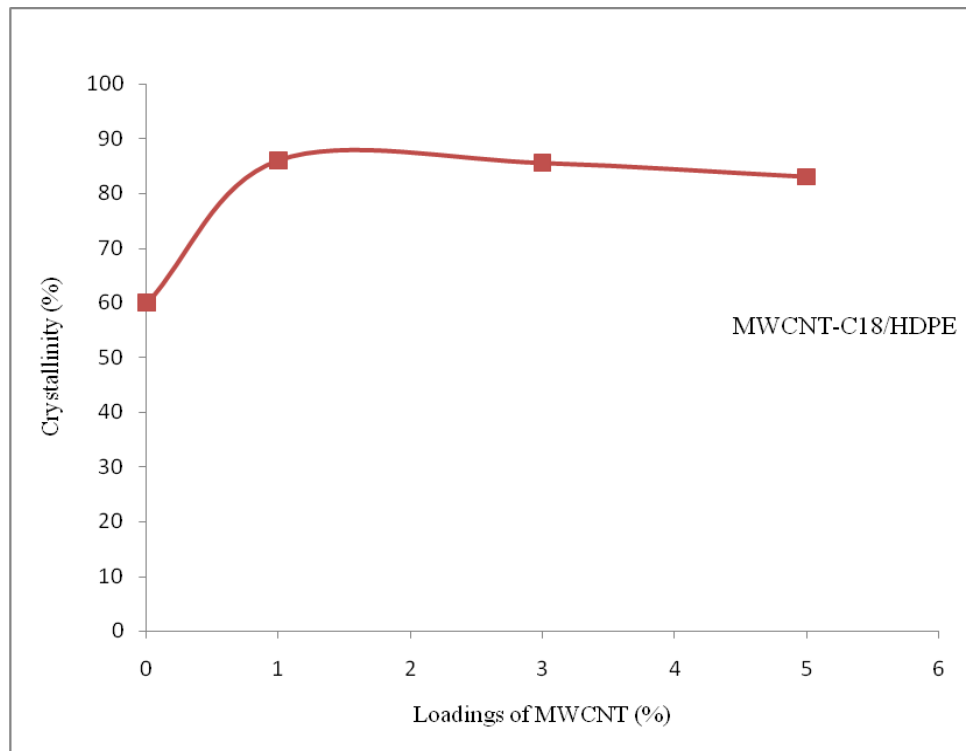


Figure 36. Influence of MWCNT content on the degree of crystallinity (X_c) for MWCNT-C₁₈/HDPE nanocomposites.

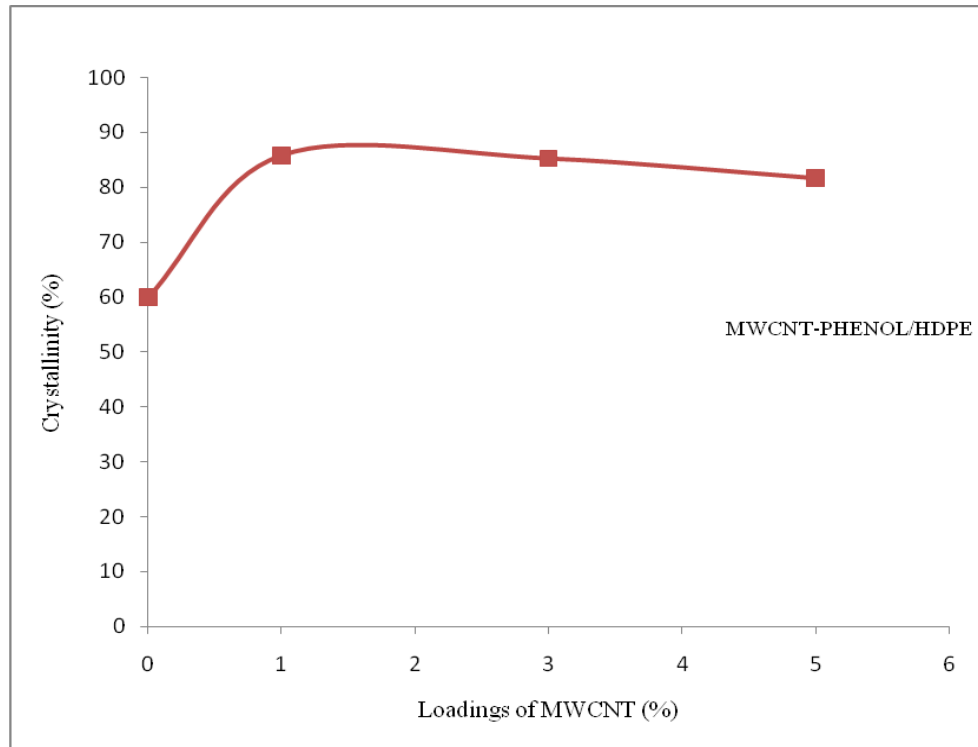


Figure 37. Influence of MWCNT content on the degree of crystallinity (X_c) for MWCNT-phenol/HDPE nanocomposites.

In case of TGA curves which are shown in Figs 38-41, thermal stabilization of all the nanocomposites and the fraction of volatile components are observed under inert nitrogen atmosphere. It is observed that the onset temperatures are 408 °C, 427 °C, 431 °C, and 438 °C for neat HDPE, 1%, 3% and 5% MWCNT, respectively. It is observed that onset temperatures increase with an addition of carbon nanotubes. This could be attributed to the high fractions of MWCNTs in the nanocomposites. Similarly, the onset temperatures of MWCNT-COOH/HDPE nanocomposites are 428 °C, 420 °C, and 440 °C for 1%, 3% and 5% respectively. The onset temperatures of MWCNT-COOH/HDPE composites decrease at 3% and then increase at 5% loading. This could be as a result of surface modification of carbon nanotubes. Moreover, the onset temperatures of MWCNT-C₁₈ decreased at 3% and increased at 5% loading. This could also be attributed to the surface modification of carbon nanotubes with Octadecanol. Also, the onset temperatures of MWCNT-phenol/HDPE nanocomposites are 422 °C, 430 °C and 420 °C for 1%, 3% and 5% respectively.

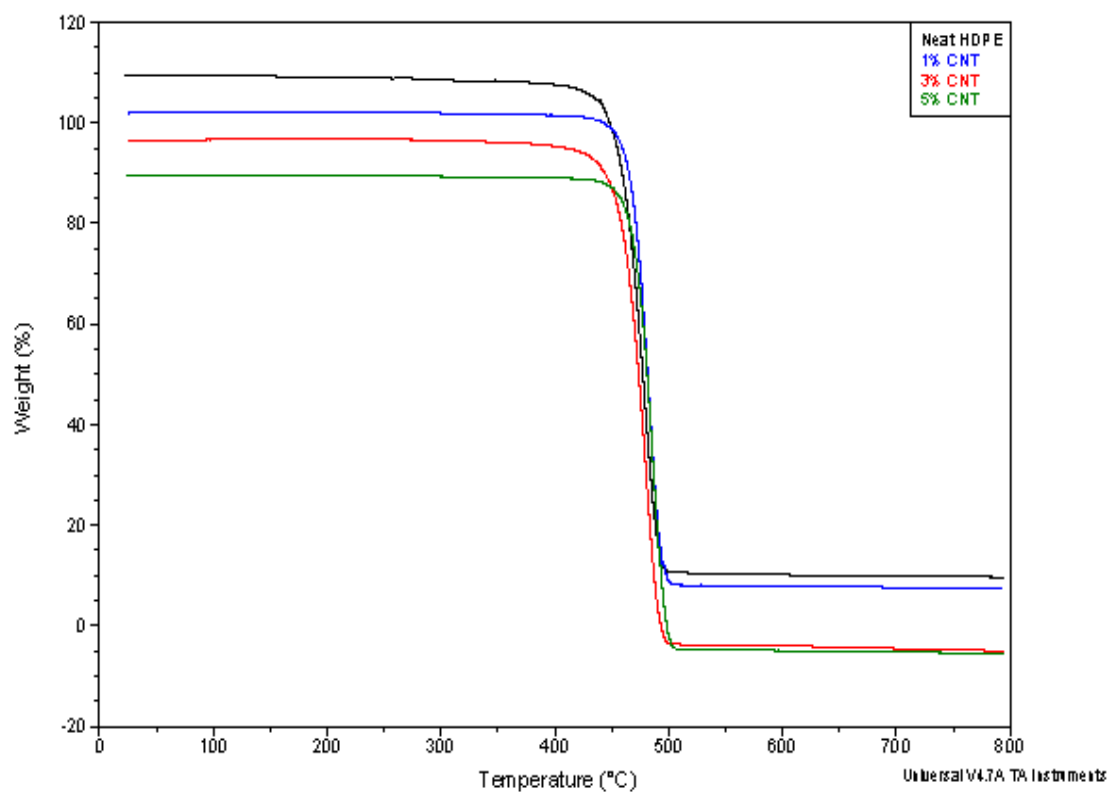


Figure.38: TGA curves of MWCNT-HDPE nanocomposites.

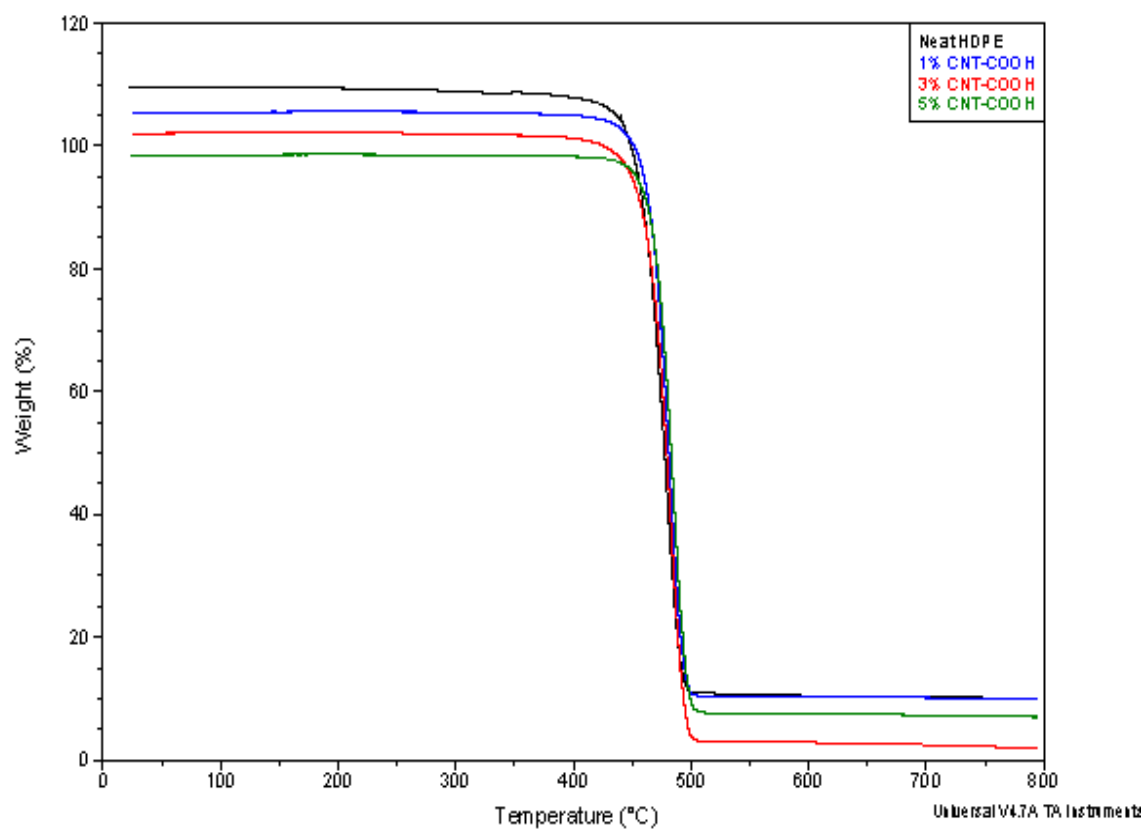


Figure.39: TGA curves of MWCNT-COOH/HDPE nanocomposites.

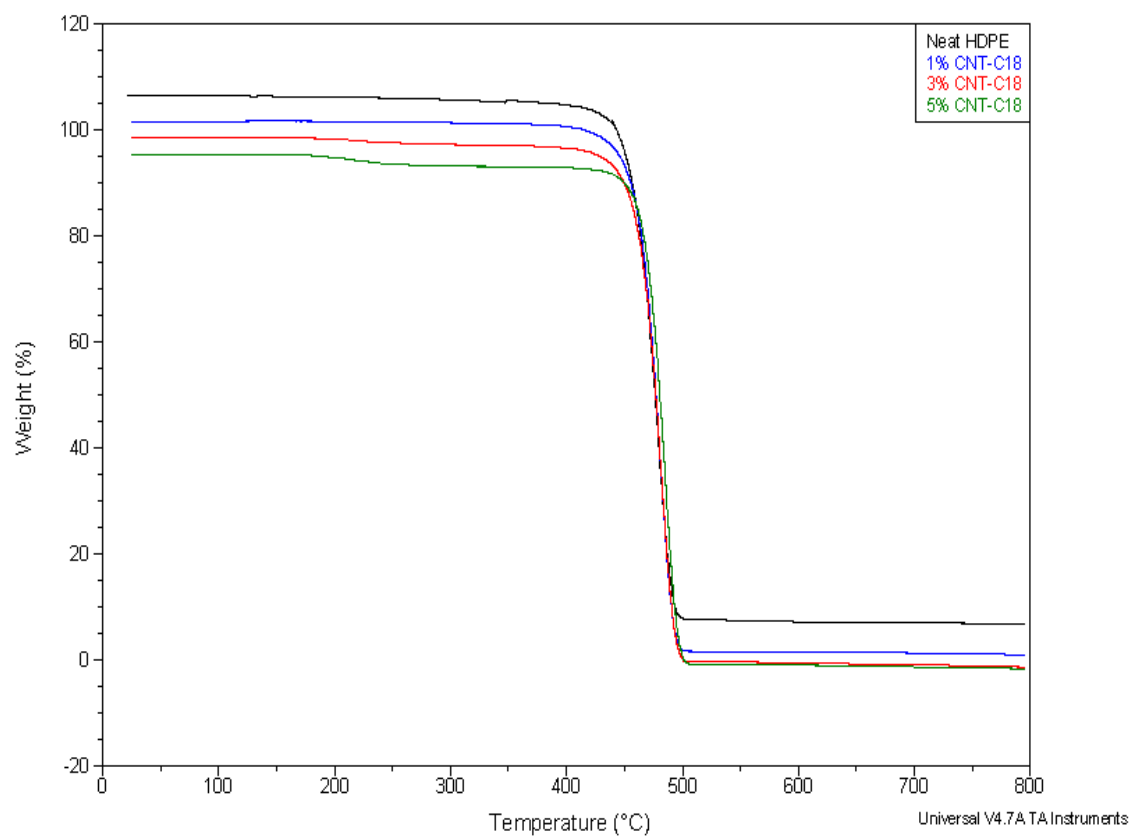


Figure.40: TGA curves of MWCNT-C₁₈/HDPE nanocomposites.

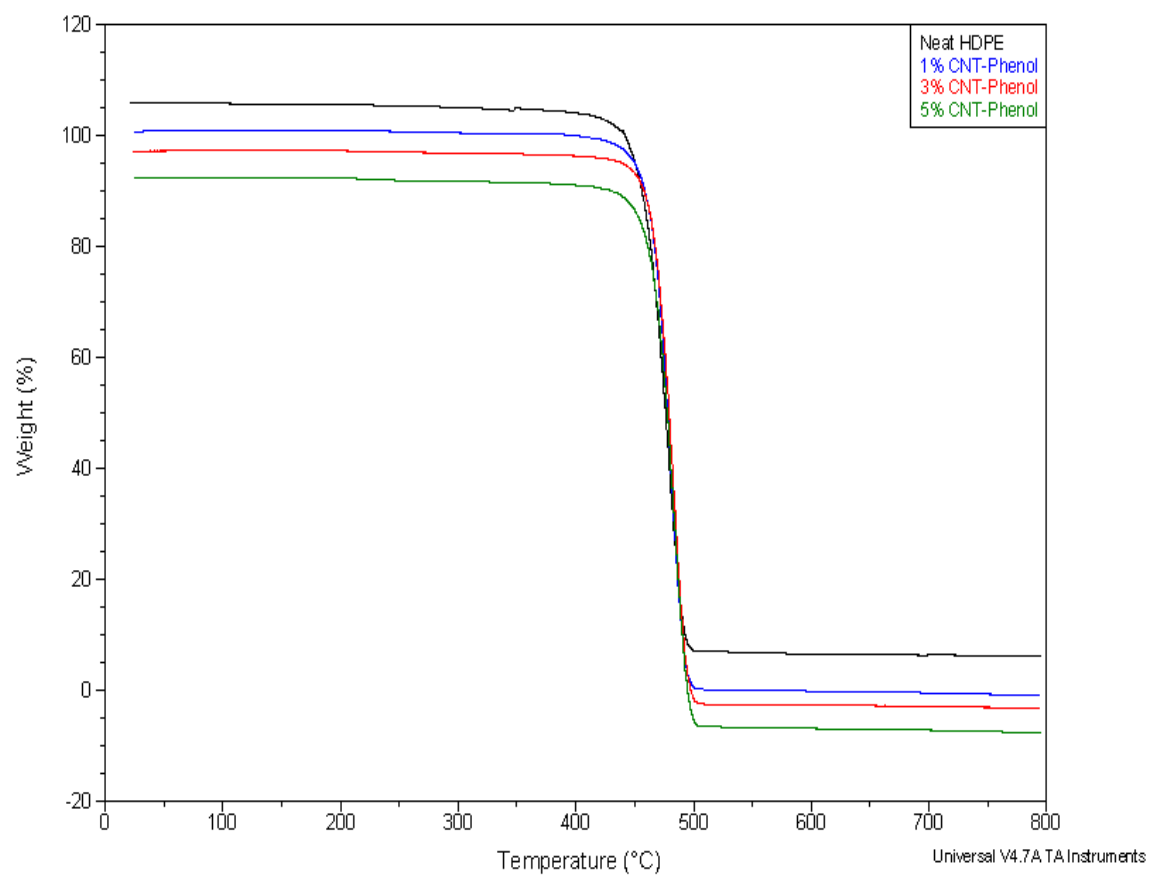


Figure.41: TGA curves of MWCNT-phenol/HDPE nanocomposites.

Similarly, Figs 42- 45 show the derivative weight loss as a function of temperature in all the nanocomposites. Each of the samples exhibited a very sharp peak which corresponds to the maximum weight loss and the temperature at this peak is termed degradation temperature.

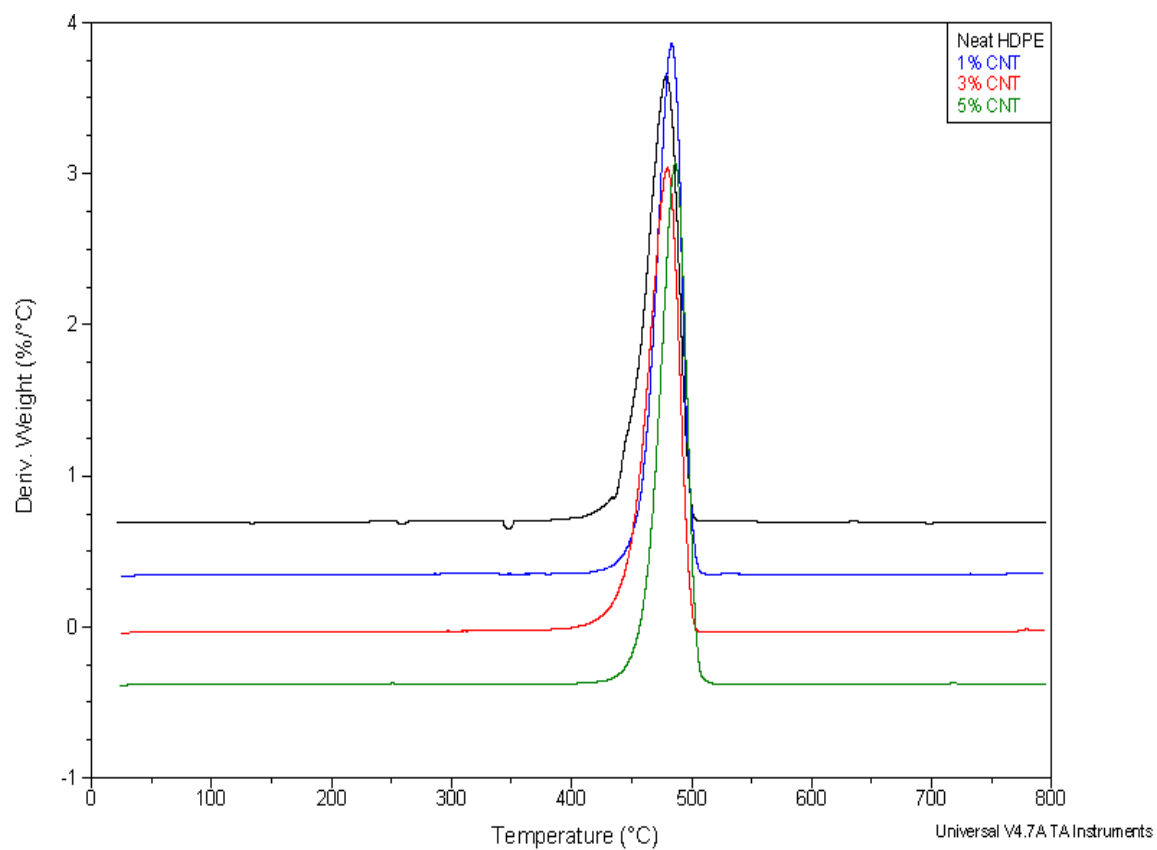


Figure.42.DTG curves of MWCNT/HDPE nanocomposites .

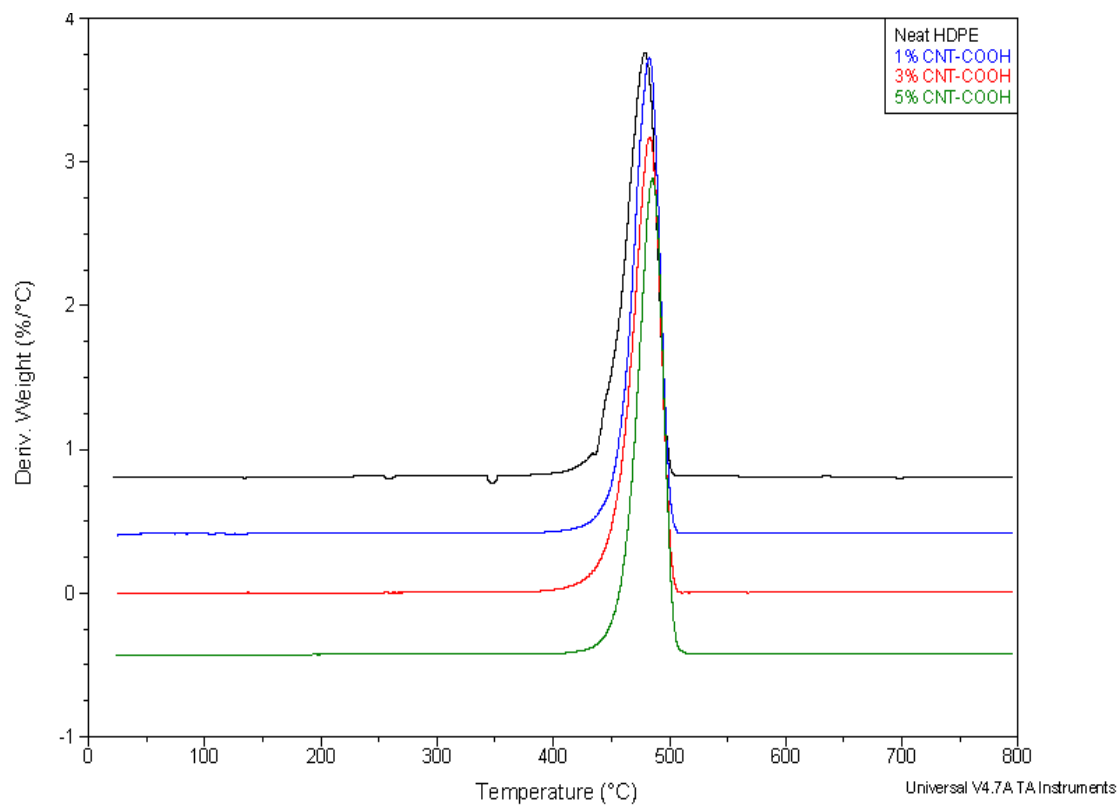


Figure.43.DTG curves of MWCNT-COOH/HDPE nanocomposites .

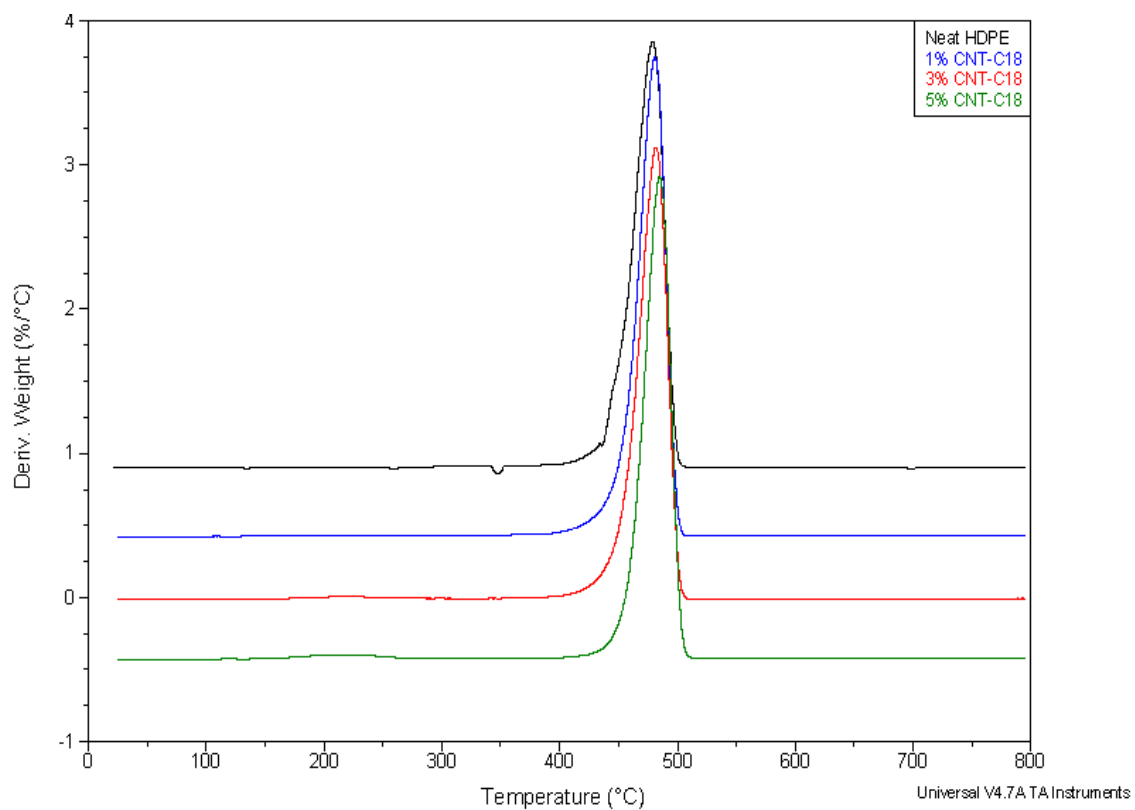


Figure.44.DTG curves of MWCNT-C₁₈/HDPE nanocomposites .

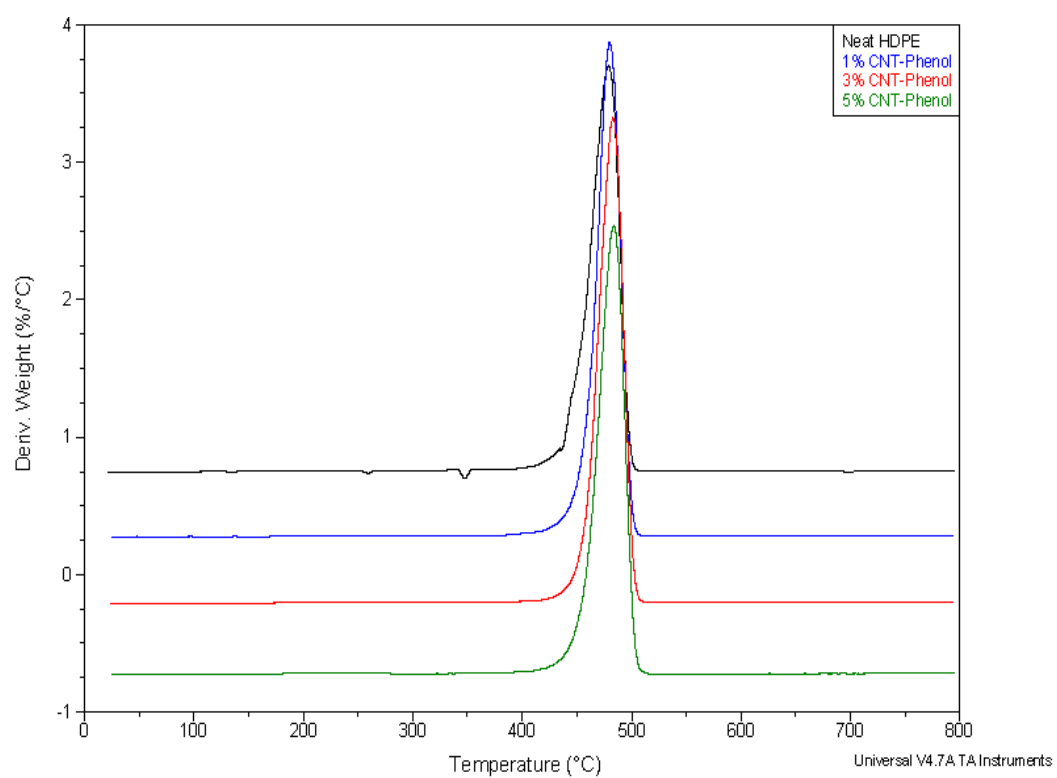


Fig.45.DTG curves of MWCNT-phenol/HDPE nanocomposites.

It is observed that the onset temperatures and degradation temperatures are not greatly affected with addition of MWCNTs and surfactants to HDPE matrix. Table 6 highlights onset temperatures and degradation temperatures in all these nanocomposites.

Table 6. The onset temperatures and degradation temperatures of HDPE nanocomposites.

Composites	T_{onset} °C	T_{degradation} °C
Neat HDPE	408	476
MWCNT/HDPE 1%	427	480
MWCNT/HDPE 3%	431	481
MWCNT/HDPE 5%	438	484
MWCNT-COOH/HDPE 1%	428	480
MWCNT-COOH/HDPE 3%	420	480
MWCNT-COOH/HDPE 5%	440	484
MWCNT-C₁₈/HDPE 1%	423	479
MWCNT-C₁₈/HDPE 3%	416	481
MWCNT-C₁₈/HDPE 5%	434	483
MWCNT-PHENOL/HDPE 1%	422	478
MWCNT-PHENOL/HDPE 3%	430	481
MWCNT-PHENOL/HDPE 5%	420	482

4.6 RHEOLOGICAL PROPERTIES

Rheology is the study of the flow behavior of a material under conditions in which they flow rather than elastic or plastic deformation. It is also concerned with establishing predictions for mechanical behavior (on the continuum mechanical scale) based on the micro or nanostructure of the materials (Prentice P. 1995). The study of rheological response of CNT/polymer nanocomposites have both practical importance related to composite processing and scientific importance as a probe of the composite dynamics and microstructure (Moniruzzaman M, et al. 2006). The rheological properties of CNT/polymer nanocomposites depend on factors such as characteristics of the filler loadings, aspect ratio and dispersion, polymer molecular weight, and the interfacial interaction between the polymer and filler (Liu C et al. 2003, Du F et al. 2004, Huang YY, et al. 2006, Fan Z, et al. 2007, Abbasi S, et al. 2009). The variation of viscosity and storage modulus of nanocomposites as a function of frequency are two commonly used techniques to characterize the rheological properties of CNT/polymer nanocomposites. Figures 46-49 show the complex viscosity of HDPE nanocomposites with different MWCNT and surfactants contents. At low frequencies, the fully relaxed HDPE chain exhibits the typical Newtonian viscosity plateau. The viscosity is lowered at 1wt% loading of low frequencies in all the nanocomposites. However, with the addition of MWCNTs and surfactants, the low frequency complex viscosity significantly increase, whereas the whole trend of viscosity drops with an increase of frequency sweep at a given MWCNTs and surfactants contents indicating that the relaxation of HDPE chain in the

nanocomposites is effectively restrained by the presence of MWCNTs and surfactants. In other words, when the MWCNTs and surfactants more than 1.0wt% are filled in the nanocomposites, the Newtonian plateau region does not exist anymore.

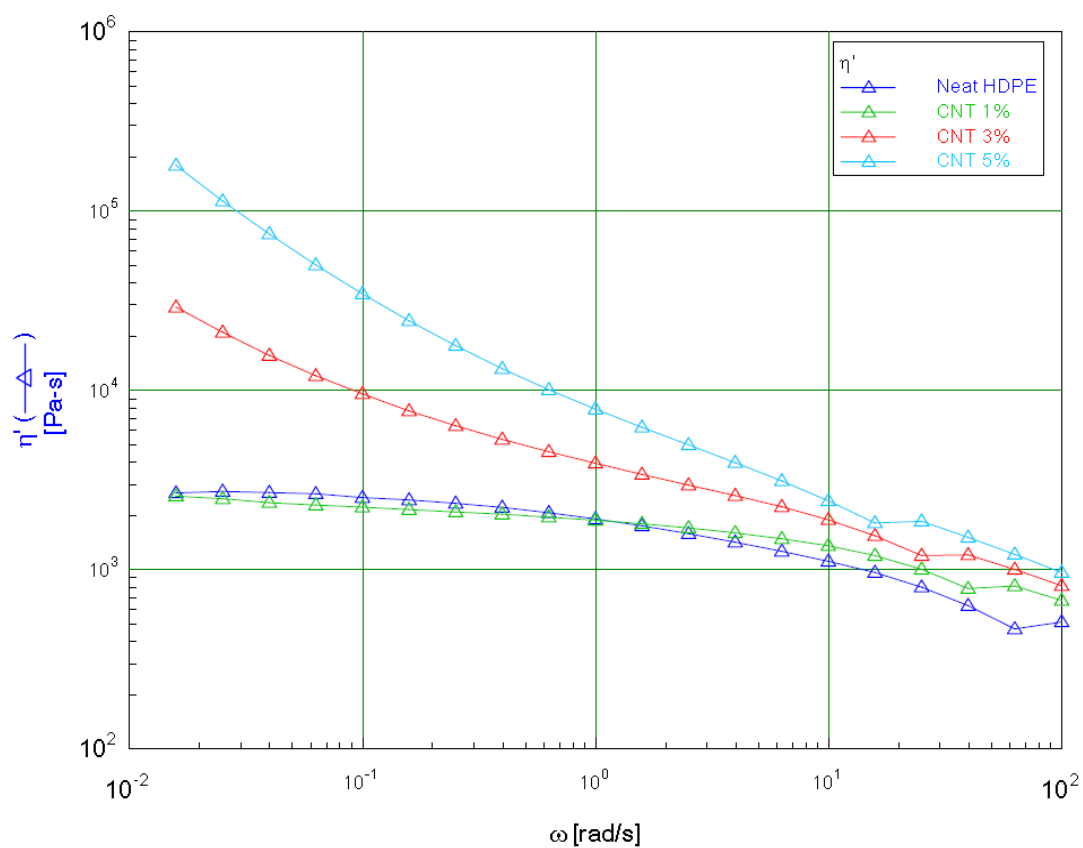


Figure.46.Rheological response: complex viscosity of MWCNT/HDPE nanocomposites as a function of frequency at 200 °C

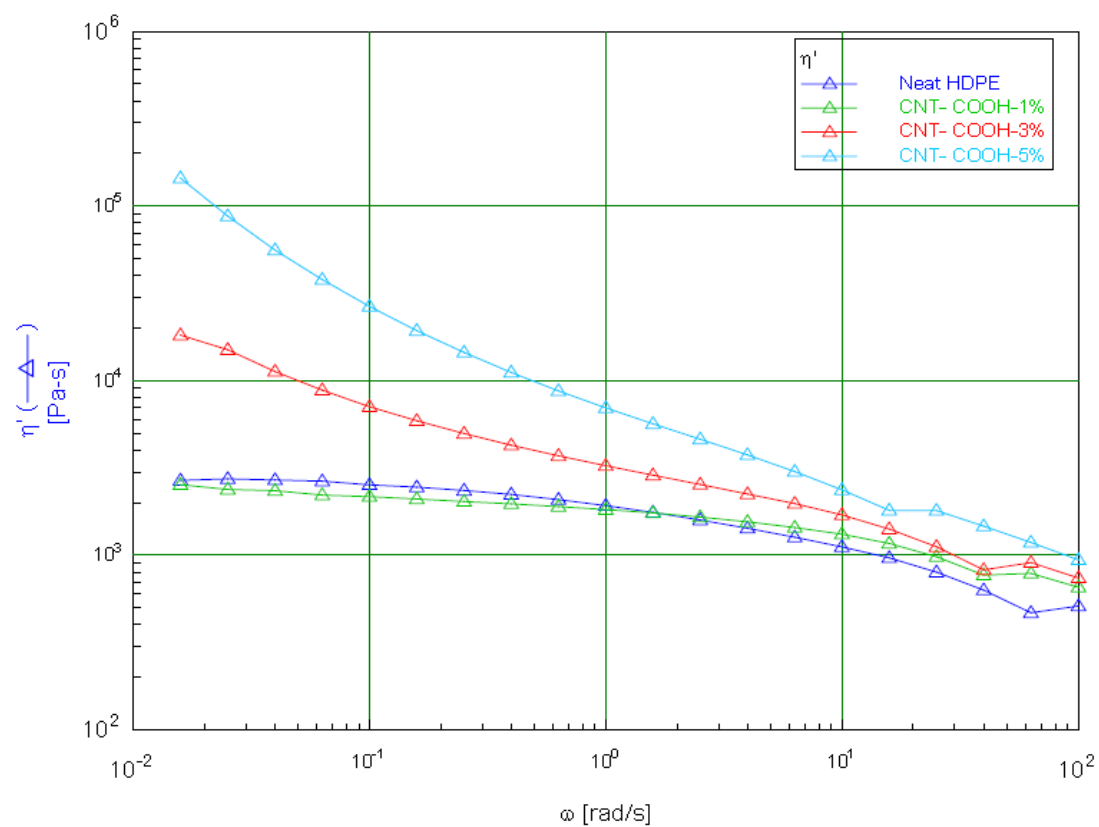


Figure.47.Rheological response: complex viscosity of MWCNT-COOH/HDPE nanocomposites as a function of frequency at 200 °C

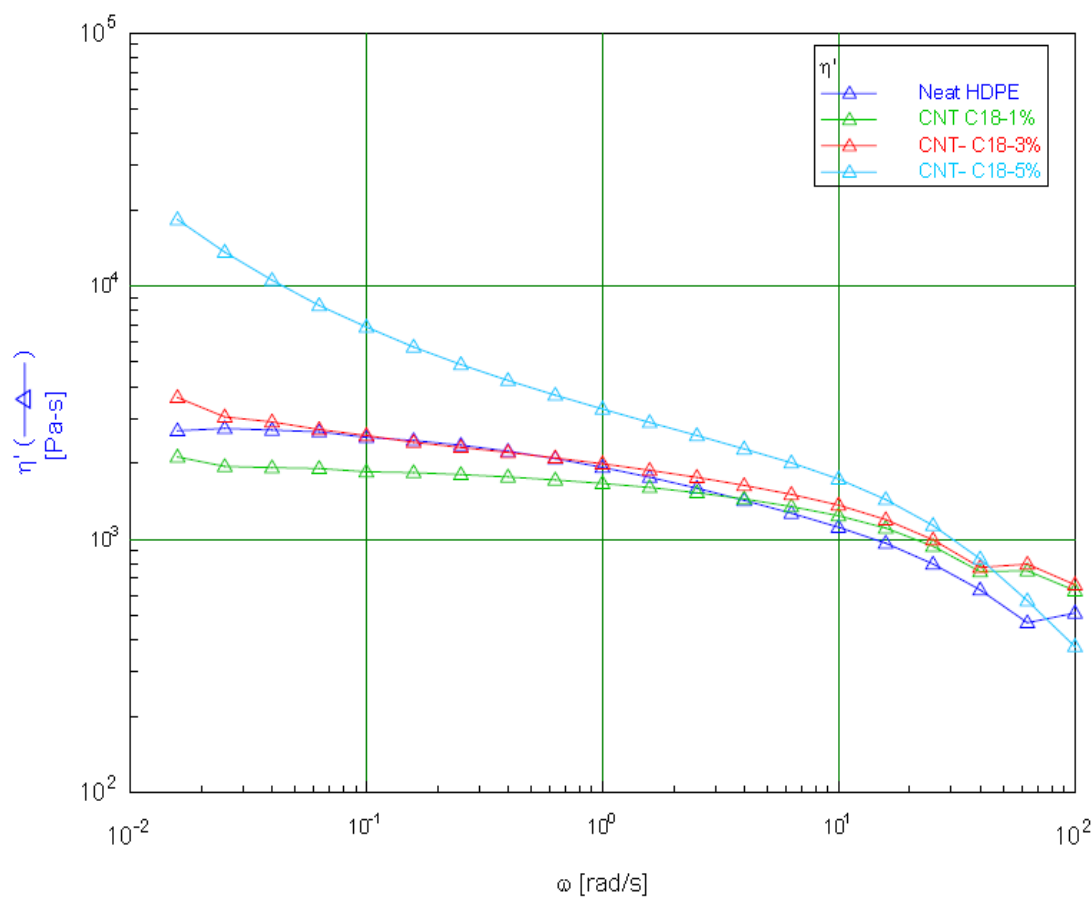


Figure.48.Rheological response: complex viscosity of MWCNT-C₁₈/HDPE nanocomposites as a function of frequency at 200 °C

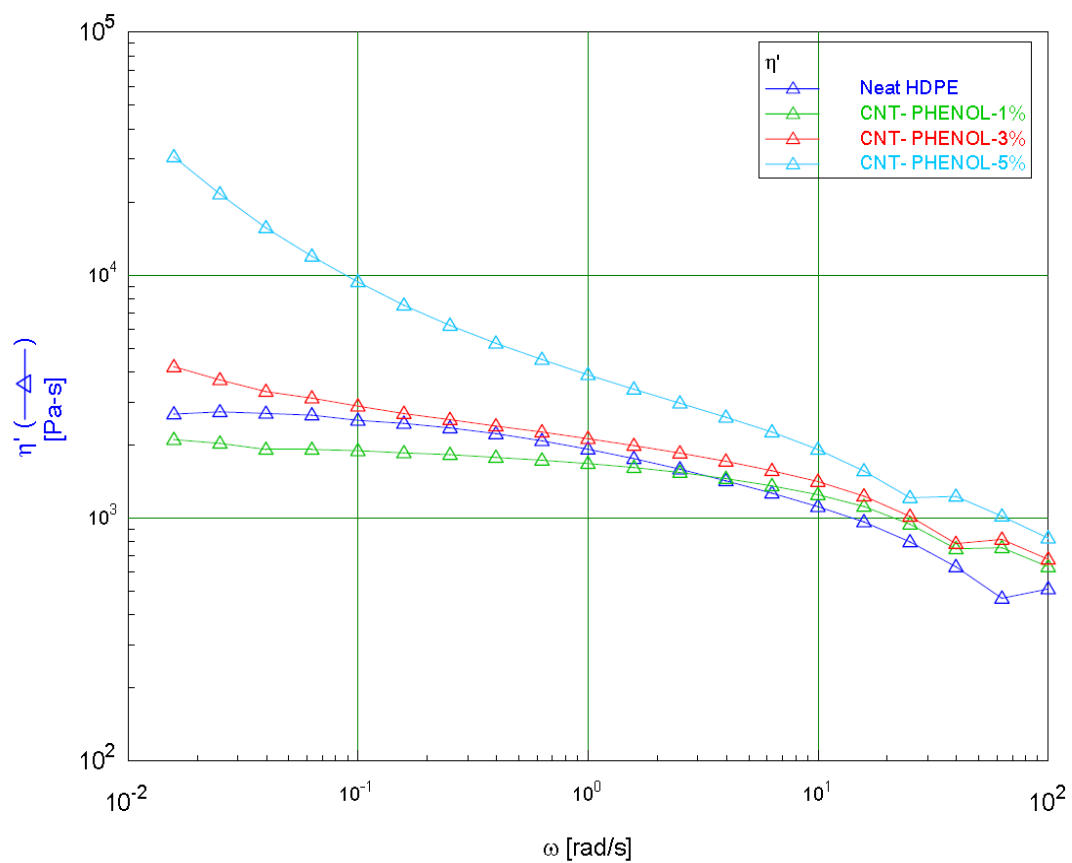


Figure.49.Rheological response: complex viscosity of MWCNT-PHENOL/HDPE nanocomposites as a function of frequency at 200 °C

Conversely, figures 50-53 show that the storage modulus of HDPE nanocomposites gradually increases with increasing frequency and MWCNT as well as surfactants contents, indicating a transition from viscous liquid to solid like behavior. The storage modulus monotonically increases with an increase in the oscillatory frequency. The more MWCNTs and surfactants filled in the HDPE matrices, the higher is the storage modulus obtained. The high aspect ratio and surface area of the MWCNTs cause the formation of the percolation structure, which raises the storage modulus of the nanocomposites. Moreover, it has been reported that particles with very small sizes, like MWCNTs, more easily make strong particle-polymer interaction even at very low filler concentration because the interfacial area between the particle and polymer dramatically increases (Bohm and Nguyen 1995; Chan et al. 2002). Zuiderduin et al. (2003) showed that rheological properties significantly increase with the decreasing size filler, unlike mechanical properties. The enhancement in the rheological properties is considered as a result of physical network structure by the strong MWCNT/surfactants-polymer interaction, which means that rheology can act as a good tool to characterize the interaction between MWCNT and polymer. Similar to the electrical percolation behavior, the rheology of a CNT/polymer nanocomposites also show a transition from a rheological state (where the viscosity or storage modulus changes significantly with increasing filler content) to a solid like behavior (where the viscosity or the storage modulus is insensitive or has only a slight variation with increasing filler content).

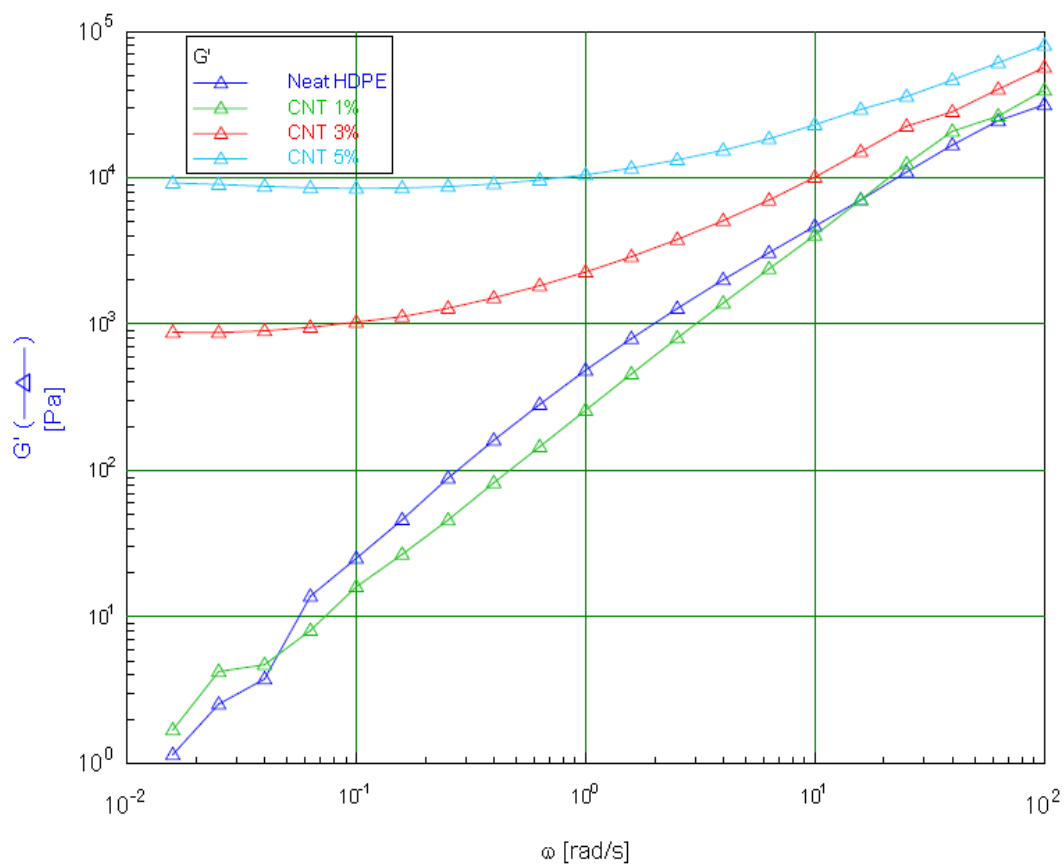


Figure.50. Rheological response: storage modulus of MWCNT/HDPE nanocomposites as a function of frequency at 200 °C.

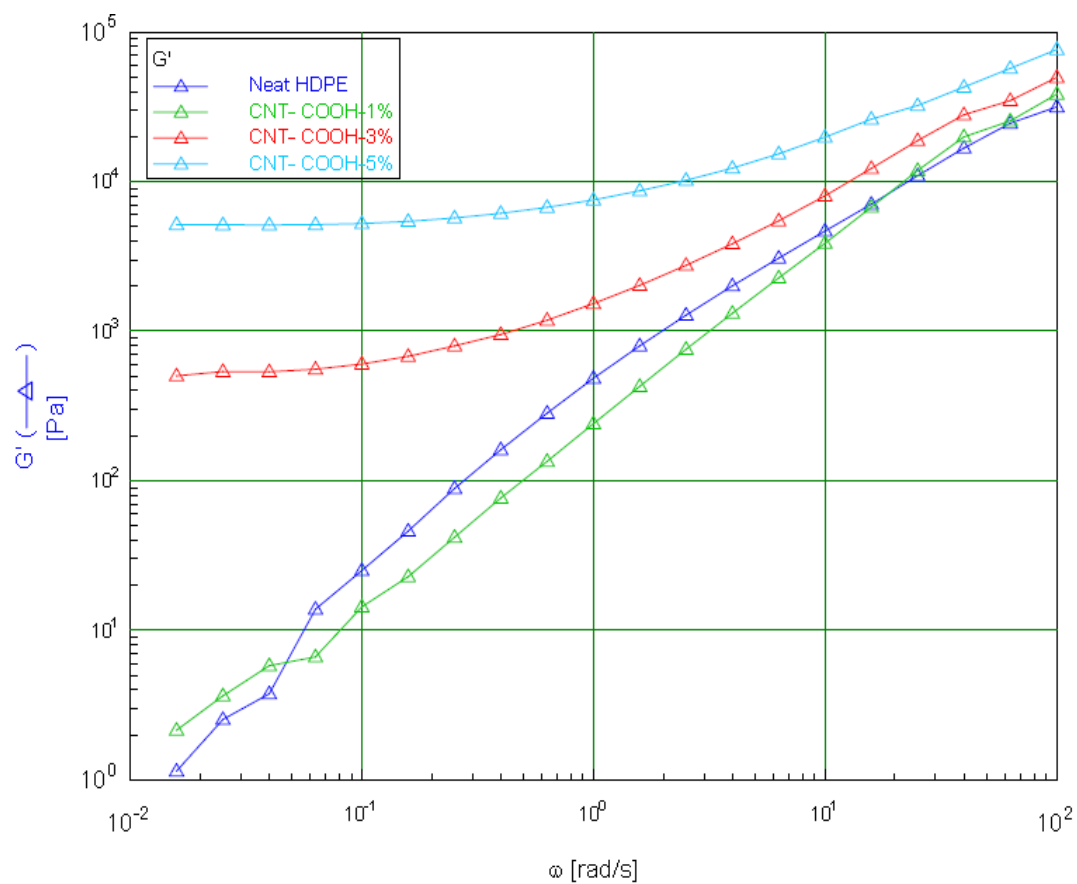


Figure.51. Rheological response: storage modulus of MWCNT-COOH/HDPE nanocomposites as a function of frequency at 200 °C.

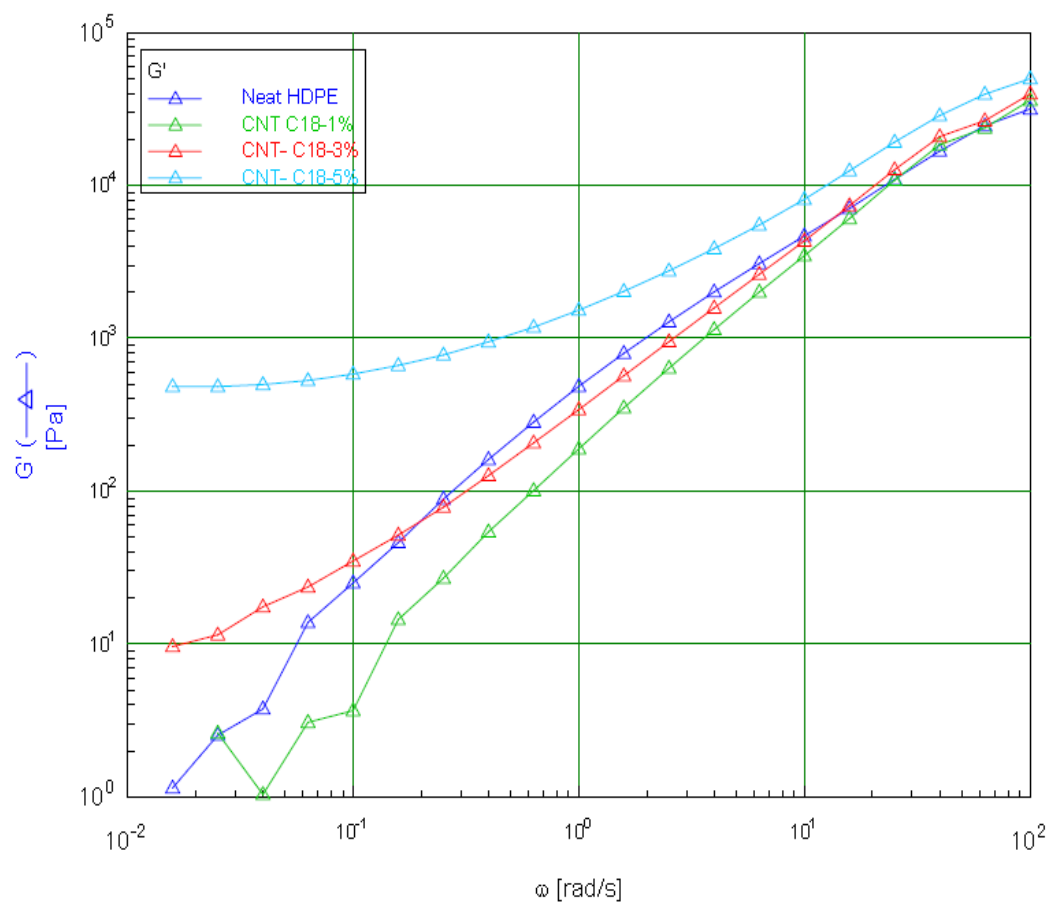


Figure.52. Rheological response: storage modulus of MWCNT-C₁₈/HDPE nanocomposites as a function of frequency at 200 °C.

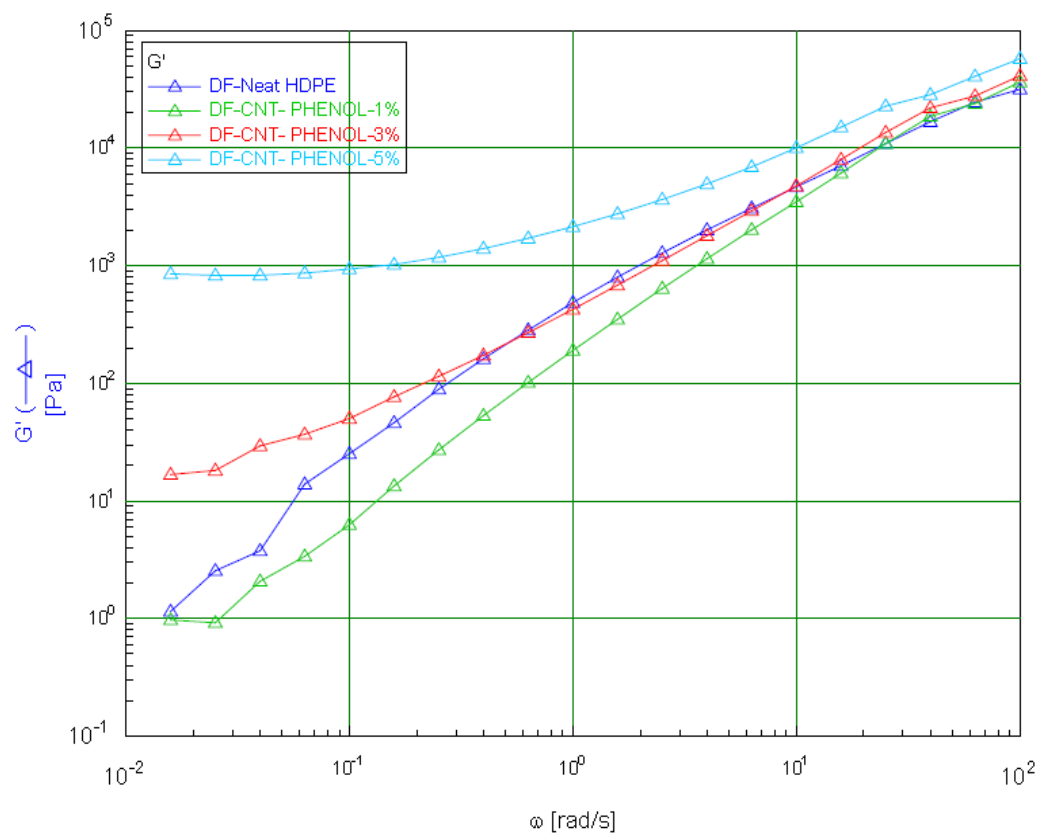


Fig.53. Rheological response: storage modulus of MWCNT-PHENOL/HDPE nanocomposites as a function of frequency at 200 °C.

The corresponding increase in the loss moduli (G'') in all HDPE nanocomposites is much lower than for the storage moduli and there is no evidence for the formation of a plateau, as demonstrated in Figs. 54-57. The loss moduli increased with increasing frequency and MWCNT as well as surfactants contents.

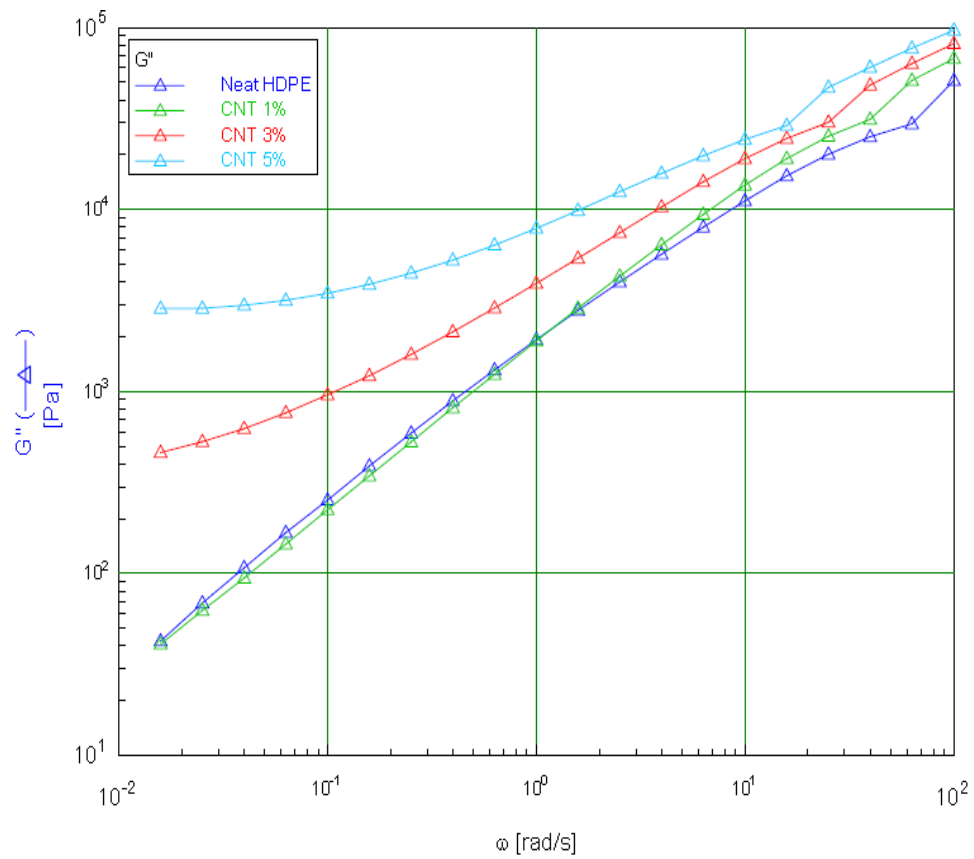


Figure.54.Rheological response: loss modulus of MWCNT/HDPE nanocomposites as a function of frequency at 200 °C.

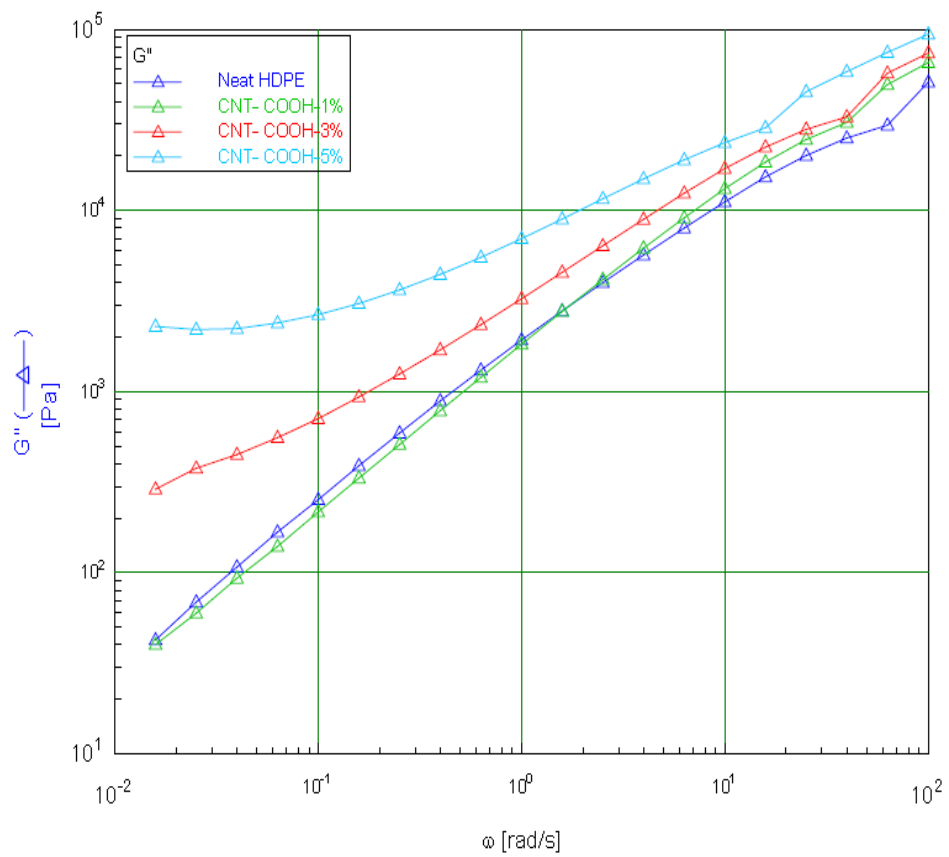


Figure.55. Rheological response: loss modulus of MWCNT-COOH/HDPE nanocomposites as a function of frequency at 200 °C.

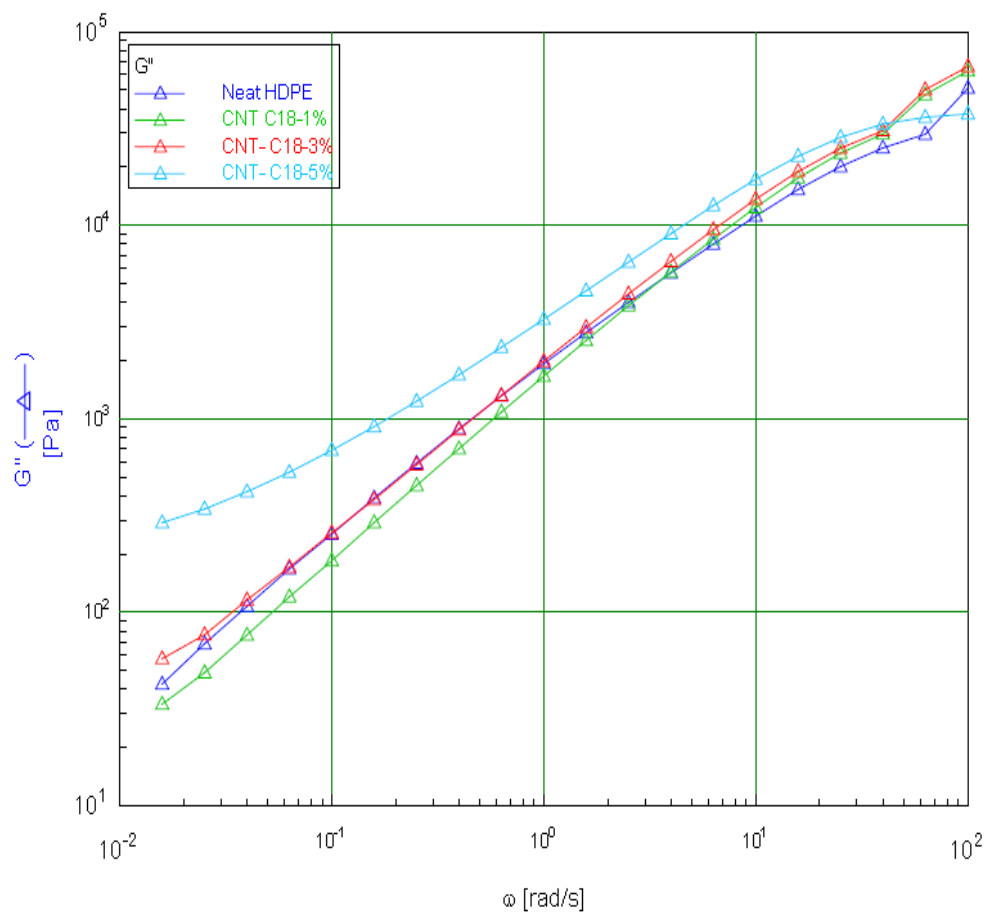


Figure.56. Rheological response: loss modulus of MWCNT-C₁₈/HDPE nanocomposites as a function of frequency at 200 °C.

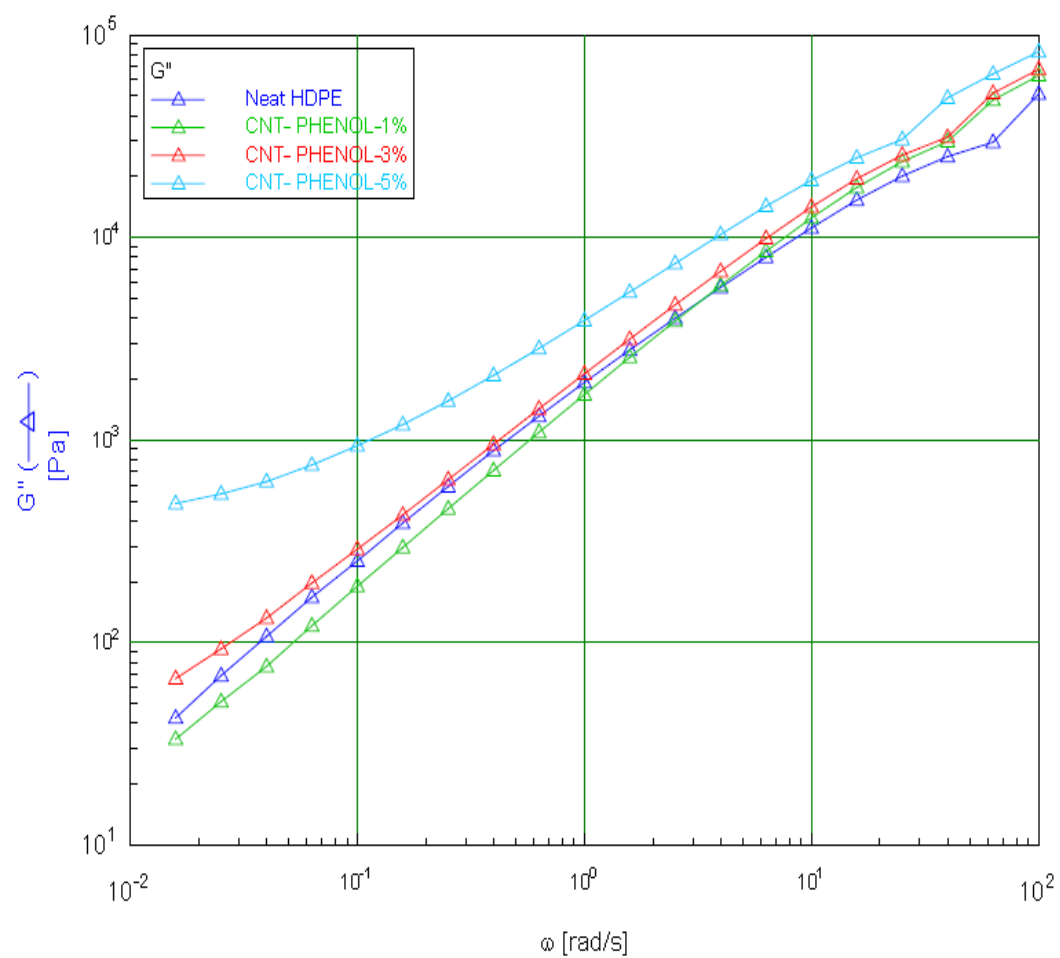


Figure.57. Rheological response: loss modulus of MWCNT-PHENOL/HDPE nanocomposites as a function of frequency at 200 °C.

CHAPTER 5

5.0 CONCLUSIONS AND RECOMMENDATIONS

5.1 CONCLUSIONS

In this work, a melt processing method was used to fabricate MWCNT/HDPE nanocomposites. The same procedure was repeated for the surfactants (COOH, C₁₈, and Phenol) used in this study. SEM images show that the presence of carbon nanotubes are not visible in 1-Octadecanol/HDPE nanocomposites fractured surface, thus, a conclusive remark cannot be drawn due to inability of the scanner to picture the carbon nanotubes from the matrices. The study shows that MWCNTs and surfactants exhibited a remarkable improvement of both mechanical and thermal properties in HDPE matrix. The ultimate strength and Young's modulus increased in all the nanocomposites from 0wt%, 1wt%, 3wt% and 5wt%. However, not much improvement was achieved in HDPE/MWCNT-C₁₈ and HDPE/phenol nanocomposites. This is attributed to inhomogeneous dispersion inefficient loading transfer of MWCNTs in HDPE matrix. The strain at break and toughness decreased in all the nanocomposites because the high ratio of MWCNTs and surfactants act as crack initiators or stress risers in HDPE matrices. Conversely, the degree of crystallinity slightly decreases with the addition of MWCNTs and surfactants in HDPE matrix, however, all the nanocomposites crystallinity increases as compared to neat HDPE. Moreover, the thermal stability of all the nanocomposites is not greatly affected with the loadings of MWCNTs

and surfactants. From the rheological point of view, the complex viscosity (η') was lowered at 1wt% loading and increased with addition of MWCNTs and surfactants above 1wt%. Likewise, the storage modulus (G') was found to increase in all the nanocomposites with increase in MWCNTs and surfactants contents. The corresponding increase in the loss moduli (G'') in all HDPE nanocomposites is much lower than for the storage moduli and there is no evidence for the formation of a plateau.

5.2 RECOMMENDATIONS

The effects of functionalized carbon nanotubes surface modification using carboxylic, 1-octadecanol and phenol on the properties of HDPE/CNT have been investigated. In spite of the enhanced dispersion of the selected nanocomposites and improvement of mechanical and thermal properties of the HDPE matrices, there are still task and challenges required to overcome in order to translate fully the unique properties of CNTs into the polymer matrices. Hence, some challenging future works are recommended below:

1. There is a need to develop tools and techniques for quantitative analysis of degree of dispersion or agglomeration in HDPE matrices, which can directly correlate with a number of material parameters, including the particle size or aspect ratio, CNT surface functionalities and surface energies.
2. An efficient method of attaining controlled functionalization of carbon nanotubes should be investigated so that CNTs can still maintain their properties

and integrity without being damaged.

3. The use of compatibilizer such as HDPE-grafted maleic anhydrides to reduce interfacial energy between the composite materials.

4. The use of DMA to investigate how the surfactants influence the glass transition temperature of HDPE nanocomposites.

5. In order to validate the rheological properties, electrical properties of HDPE nanocomposites should be investigated.

APPENDIX A: Stress-Strain curves of HDPE nanocomposites

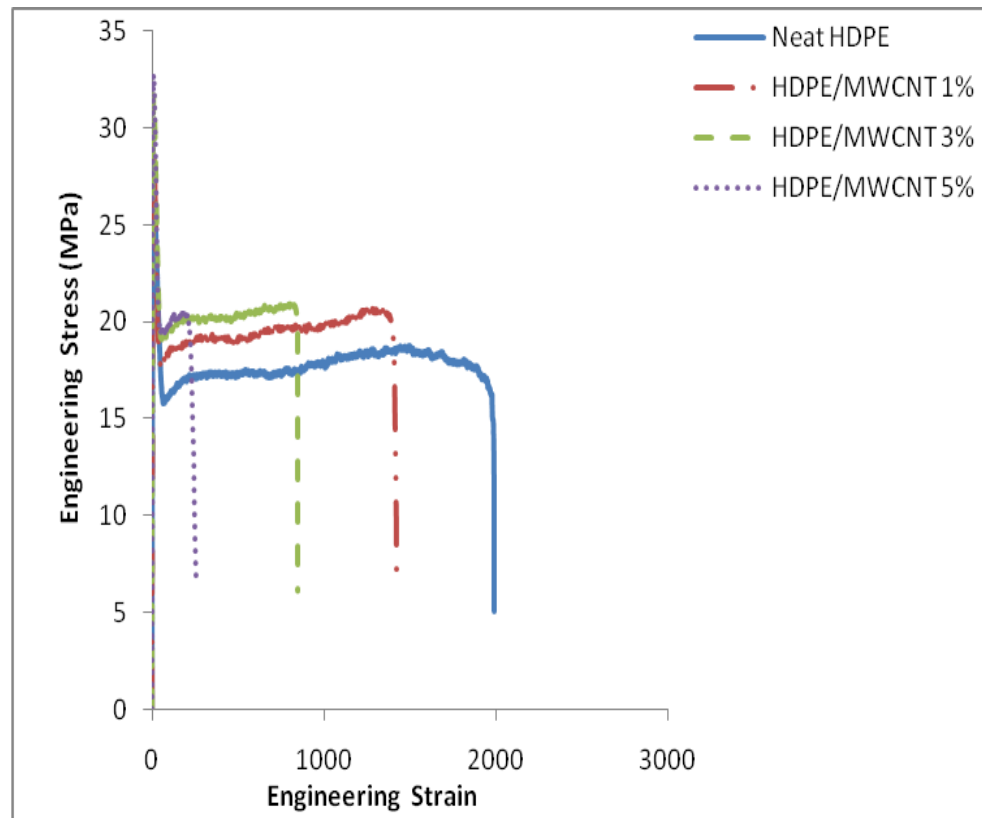


Figure 58: Stress-Strain curves for HDPE/MWCNT nanocomposites

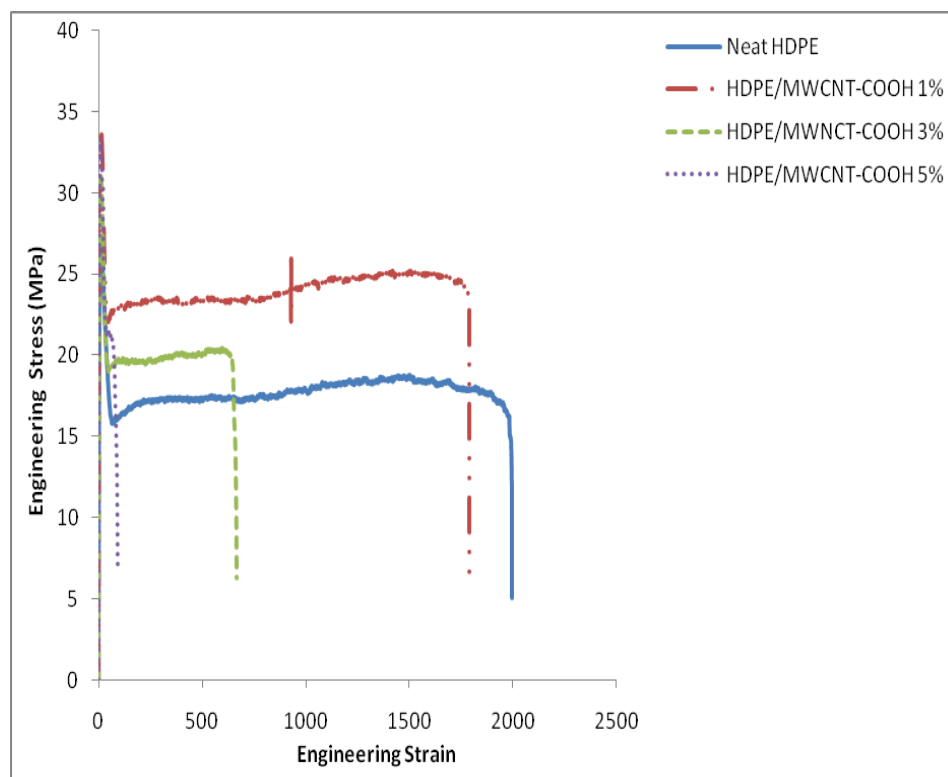


Figure 59: Stress-Strain curves for HDPE/MWCNT-COOH nanocomposites

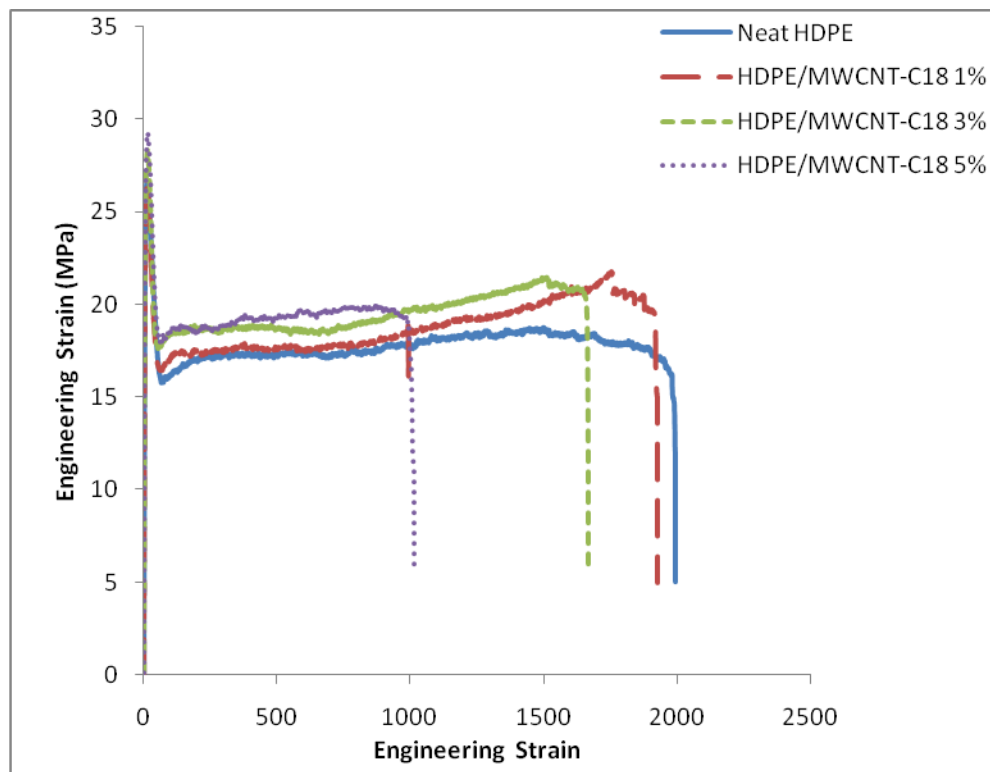


Figure 60: Stress-Strain curves for HDPE/MWCNT-C₁₈ nanocomposites

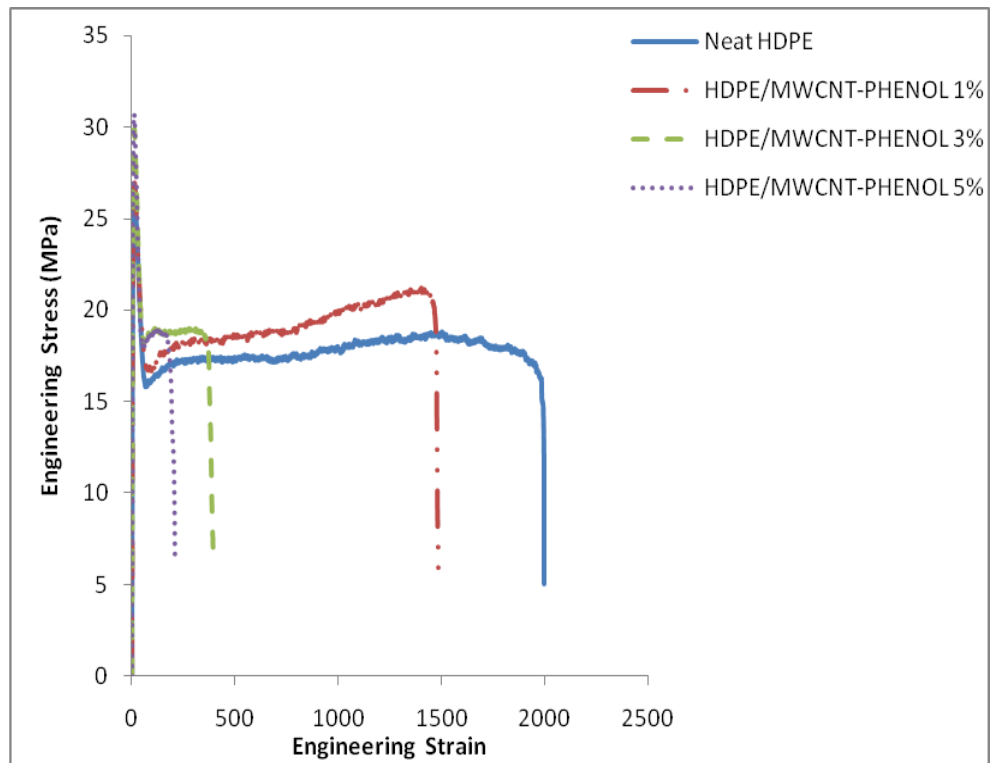


Figure 61: Stress-Strain curves for HDPE/MWCNT-phenol nanocomposites

APPENDIX B: Percentage increase and decrease in mechanical properties of HDPE nanocomposites.

Composites	% increase in ultimate strength	% increase in Young's modulus	% decrease in strain @ fracture	% decrease in toughness
Neat HDPE	0.00	0.00	0.00	0.00
HDPE-MWCNT 1%	5.56	14.42	9.96	6.55
HDPE-MWCNT 3%	19.42	44.34	77.14	75.13
HDPE-MWCNT 5%	21.64	49.77	90.97	90.60
HDPE-MWCNT/COOH 1%	24.05	31.34	65.73	57.78
HDPE-MWCNT/COOH 3%	24.11	32.43	81.89	80.71
HDPE-MWCNT/COOH 5%	26.53	50.60	96.03	95.50
HDPE-MWCNT/C ₁₈ 1%	0.98	1.09	3.77	3.11
HDPE-MWCNT/C ₁₈ 3%	8.20	7.78	15.94	8.15
HDPE-MWCNT/C ₁₈ 5%	9.03	8.16	31.21	28.23
HDPE-MWCNT/PHENOL 1%	0.83	9.72	48.24	46.98
HDPE-MWCNT/PHENOL 3%	10.60	25.76	82.14	81.77
HDPE-MWCNT/PHENOL 5%	19.09	37.71	84.57	83.13

APPENDIX C: Nomenclatures

CNTs	Carbon nanotubes
MWCNTs	Multiwalled Carbon nanotubes
HDPE	High Density Polyethylene
PMMA	Poly methyl methacrylate
ABS	Acrylonitrile Butadiene Styrene
PC	Polycarbonate
PP	Polypropylene
PS	Polystyrene
FTIR	Fourier Transform Infrared Spectroscopy
SEM	Scanning Electron Microscopy
TEM	Transmission Electron Microscopy
DSC	Differential Scanning Calorimetry
TGA	Thermogravimetric Analyzer
PE	Polyethylene
LDPE	Low Density Polyethylene
LLDPE	Linear Low Density Polyethylene
MMD	Molecular Mass Distribution
NMR	Nuclear Magnetic Resonance
MFI	Melt Flow Index
ASTM	American Society for Testing Materials
SWCNTs	Single Walled Carbon nanotubes

CVD	Chemical Vapor Deposition
GNPs	Graphite nanoplatelets
ARES	Advanced Rheometric Expansion System
rpm	radian per minute

REFERENCES

1. Ajayan PM, Schadler LS, Braun PV. Nanocomposite science and technology. Weinheim: Wiley-VCH; 2003.p.77-80.
2. Andrews R, Jacques D, Rao AM, Rantell T, Derbyshire F, Chen Y, et al. Appl Phys Lett 1999;75:1329.
3. Assouline E, Lustiger A, Barber AH, Cooper CA, Klein E, Wachtel E, et al. Nucleation ability of multiwalled carbon nanotubes in polypropylene composites. J Polym Sci, Part B 2003;41:520-7.
4. Awasthi K, Kamalakaran R, Singh AK, Srivastava ON. Ball milled carbon and hydron storage. Int J Hydrogen Energy 2002;27:425-32.
5. Balasubramanian K, Burghard M. Chemically functionalized carbon nanotubes. Small 2005;1:180=92.
6. Bal S, Samal SS. Carbon nanotubes reinforced polymer composites-a state of the art. Bull Mater Sci 2007;30:379-86.
7. Baughman RH, Zakhidov AA, De Heer WA. Science 2002;297:787.
8. Belin T, Epron F. Mater Sci Eng B 2005;119:105.
9. Berber S, KWON Y-K, Tomanek D. Phys Rev Lett 2000;84:4613.
10. Biercuk MJ, Llaguno MC, Radosavljevic M, Hyun JK, Johnson AT, Fisher JE. Appl Phys Lett 2002;80:2767.
11. Bohm GGA, Nguyen MN (1995) Flocculation of carbon black in filled rubber compound. I. Flocculation occurring in unvulcanized compounds during annealing at elevated temperatures. J Appl Poly Sci 55:1041-1050.

12. Breuer O, Sundararaj U. Big returns from small fibers: a review of polymer/carbon nanotube composites. *Polym Compos* 2004;25:630-45.
13. Cadek M, Coleman JN, Barron V, Hedicke K, Blau WJ. Morphological and mechanical properties of carbon nanotubes reinforced semicrystalline and amorphous composites. *Appl Phys Lett* 2000;81(27):5123-5.
14. Che G, Lakshmi BB, Martin CR, Fisher ER, Ruoff RS. *Chem Mater* 1998;10:260.
15. Chen J, Hamon MA, et al. Sidewall functionalization of single-walled carbon nanotubes by addition of dichlorocarbene. *J Am Chem Soc* 2003;125:14893-900.
16. Coleman JN, Cadek M, Blake R, Nicolosi V, Ryan KP, Belton C, et al. High performance nanotube-reinforced plastics: Understanding the mechanism of strength increase. *Adv Funct Mater* 2004;14:791-8.
17. Coleman JN, Khan U, Blau WJ, Gun'ko YK. Small but strong: A review of the mechanical properties of carbon nanotube-polymer composites. *Carbon* 2006;44:1624-52.
18. Coleman JN, Khan U, Gunko YK. Mechanical reinforcement of polymers using carbon nanotubes. *Adv Mater* 2006;18:689-706.
19. Dai HJ, Hafner JH, Rinzler AG, Colbert DT, Smalley RE. *Nature* 1996;384:147.
20. Edidin AA, Kurtz SM. Development of validation of the small punch test for UHMWPE used in total joint replacements. *Funct Biomater* 2001;198:1-40.

21. Esumi K, Ishigami M, Nakajima A, et al. Chemical treatment of carbon nanotubes. *Carbon* 1996;34:279-81.
22. Fiedler B, Gojny FH. Fundamental aspects of nano-reinforced composites. *Compos Sci Technol* 2006;66:3115-25.
23. Frackowiak E, Beguin F. *Carbon* 2002;40:1775.
24. Gao B, Bower C, Lorentzen JD, et al. Enhanced saturation lithium composition in ball-milled single-walled carbon nanotubes. *Chem Phys Lett* 2000;327:69-75.
25. Ge M, Sattler K. *Appl Phys Lett* 1994;67:710.
26. Gibson RF, Ayorinde EO, Wen YF. Vibrations of carbon nanotubes and their composites: a review. *Compos Sci Eng R* 2007;67:1-28.
27. Gong X, Liu J, Baskaran S, Voise RD, Young JS. Surfactant-assisted processing of carbon nanotubes/polymer composites. *Chem Mater* 2000; 12(4):1094-52.
28. Gorga RE, Cohen RE. Toughness enhancement in poly(methyl methacrylate) by addition of oriented multiwall carbon nanotubes. *J Polym Sci, Part B: Polym Phys* 2004;42:2690-702.
29. Gojny FH, Wichmann MHG, Kopke U, Fiedler B, Schulte K. *Compos Sci Technol* 2004;64:2363.
30. Grunlan JC, Mehrabi AR, Bannon MV, Bahr JL. *Adv Mater* 2004;16:150.
31. Hill DE, Lin Y, Rao AM, Allard LF, Sun YP. Functionalization of carbon nanotubes with polystyrene. *Macromolecules* 2002;35:9466-71.

32. Hirsch A. Functionalization of single walled carbon nanotubes. *Angew Chem Int Ed* 2002;41:1853-9.
33. Hirsch A, Vostrowsky O. Functionalization of carbon nanotubes. *Top Curr Chem*
34. Holzinger M, Steinmetz J, Samaille D, et al. [2+1] Cycloaddition for cross-linking SWCNTs. *Carbon* 2004;42:941-7.
35. <<http://www.exakt.com>>, three roll mills, EXAKT company (accessed June 2010).
36. <<http://www.sonifier.com>>, sonifier products, Branson ultrasonic corp (accessed June 2010).
37. Huang JY, Yasuda H, Mori H. Highly curved carbon nanostructures produced by ball-milling. *Chem Phys Lett* 1999;303:130-4.
38. Iijima S. Helical microtubule of graphitic carbon. *Nature* 1991; 354:56-8.
39. Ji XL, Jing JK, Jiang W, Jiang BZ. Tensile modulus of polymer nanocomposites. *Polym Eng Sci* 2002;42(5):983-93.
40. Kelly KF, Chiang IW, Mickelson ET, et al. Insight into the mechanism of sidewall functionalization of single -walled nanotubes: an SMT study. *Chem Phys Lett* 1999;313:445-50.
41. Kim B, Lee J, Yu I.J *Appl Phys* 2003;94:6724.
42. Kim HB, Choi JS, Lee CH, Lim ST, Jhon MS, Choi HJ (2005) Polymer blend/organoclay nanocomposite with poly(ethylene oxide) and poly(methyl methacrylate). *Eur Polym J* 41:679-685

43. Kim JY, Kim SH. Influence of multi wall carbon nanotube on physical properties of poly (ethylene 2,6-naphthalate) nanocomposites. *J Polym Sci B* 2006;44:1062-71.
44. Kim KS, Bae DJ, Kim JR, et al. Modification of electronic structures of a carbon nanotube by hydrogen functionalization. *Adv Mater* 2002;14:1818-21.
45. Kim YA, Hayashi T, Fukai Y, et al. Effect of ball milling on morphology of cup stacked carbon nanotubes. *Chem Phys Lett* 2002;355:279-84.
46. Knupher M. *Surf Sci Rep* 2001;42:1
47. Kong J, Franklin NR, Zhou C, Chapline MG, Peng S, Cho K, et al. *Science* 2000;287:622.
48. Krishnan A, Dujardin E, Ebbesen TW, Yianilos PN, Treacy MMJ. *Phys Rev B* 1998;58:14013.
49. Kroto HW, Heath JR, O'Brien SC, Curl RF, Smalley RE. *Nature* 1985;318:162.
50. Li J, Ma PC, Chow WS, To CK, Tang BZ, Kim JK. Correlations between percolation threshold, dispersion state and aspect ratio of carbon nanotube. *Adv Funct Mater* 2007;17:3207-15.
51. Li YB, Wei BQ, Liang J, et al. Transformation of carbon nanotubes to nanoparticles by ball milling process. *Carbon* 1999;37:493-7.
52. Li WZ, Xie SS, Qian LX, Chang BH, Zou BS, Zhou WY, et al. *Science* 1996;274:1701.
53. Liu C, Fan YY, Liu M, Cong HT, CHENG HM, Dresselhaus MS. *Science* 1999;286:1127.

54. Lu KL, Lago RM, Chen YK, Green MLH, Harris PJF, Tsang SC. Mechanical damage of carbon nanotubes by ultrasound. *Carbon* 1996;34:814-6.
55. Moniruzzaman M, Du FM, Romero N, Winey KI. Increased flexural modulus and strengtgh in SWNT/epoxy composites by a new fabrication method. *Polymer* 2006;47:293-8.
56. Moniruzzaman M, Winey KI. Polymer nanocomposites containing carbon nanotubes. *Macromolecules* 2006;39:5194-205.
57. Mukhopadhyay K, Dwivedi CD, Mathur GN. Conversion of carbon nanotubes to carbon nanofibers by sonication. *Carbon* 2002;40:1373-6
58. Ma PC, Kim JK, Tang BZ. Functionalization of carbon nanotubes using a silane coupling agent. *Carbon* 2006;44:3232-8.
59. Ma PC, Tang BZ, Kim JK. Converting semiconducting behavior of carbon nanotubes using ball milling. *Chem Phys Lett* 2008;458:166-9.
60. Ma PC, Wang SQ, Tang BZ, Kim JK. In situ amino functionalization of carbon nanotubes using ball milling. *J Nanosci Nanotechnol* 2009;9:749-53.
61. Mickelson ET, Huffman CB, Rinzler AG, et al. Fluorination of cup-stacked carbon nanotubes. *Chem Phys Lett* 1998;296:188-94.
62. Odom TW, Huang J-L, Kim P, Lieber CM. *J Phys Chem B* 2000;104:2794.
63. Ogasawara T, Ishikawa T, Yokota R. *Compos A Appl Sci Manuf* 2004;35:67.
64. Ounaies Z, Park C, Wise KE, Siochi EJ, Harrison JS. *Comput Sci Tech* 2003;63:1637.
65. Popov VN, van Doren VE, Balkanski M. *Phys Rev B* 2000;61:3078.

66. Qian D, Dickey EC, Andrews R, Rantell T. Load transfer and deformation mechanism in carbon nanotube-polystyrene composites. *Appl Phys Lett* 2000;76(20):2868-70.
67. Roche S. *Anm Chim Sci Matter* 2000;11:65.
68. Safadi B, Andrews R, Grulke EA. *J Appl Polym Sci* 2002;84:2660.
69. Sandler J, Shaffer MSP, Prasse T, Bauhofer W, Schulte K, Windle AH. Development of a dispersion process for carbon nanotubes in an epoxy matrix and the resulting electrical properties. *Polymer* 1999;40:5967-71.
70. Schmid CF, Klingenberg DJ. Mechanical flocculation in flowing fiber suspensions. *Phys Rev Lett* 2000;84:290-3.
71. Shaffer MSP, Windle AH. Fabrication and characterization of carbon nanotube/poly (vinyl alcohol) composites. *Adv Mater* 1999;11(11):937-41.
72. Sham ML, Kim JK. Surface functionalities of multi-wall carbon nanotubes after UV/ozone and TETA treatments. *Carbon* 2006;44:768-77.
73. Sugie H, Tanemura M, Filip V, Iwata K, Takahashi K, Okuyama F. *Appl Phys Lett* 2001;78:2578.
74. Tagmatarchis N, Prato MJ. Functionalization of carbon nanotubes via 1,3-dipolar cycloadditions. *J MaterChem* 2004;14:437-9.
75. Tai NH, Yeh MK, Liu JH. *Carbon* 2004;42:2774.
76. Tang W, Santare MH, Advani SG. Melt processing and mechanical property characterization of multi-walled carbon nanotube/high density polyethylene (MWCNT/HDPE) composite films. *Carbon* 2003;41:2779-85.

77. Tasis D, Tagmatarchis N, Bianco A, Prato M. Chemistry of carbon nanotubes. *Chem Rev* 2006;106:1105-36.
78. Terrones M. *Annu Rev Mater Res* 2003;33:419.
79. Thostenson ET, Chou TW. Aligned multi-walled carbon nanotube reinforced composites: processing and mechanical characterization. *J Phys D: Appl Phys* 2002;35:L77-80.
80. Thostenson ET, Li C, Chou T-W. *Compos Sci Technol* 2005;65:491.
81. Unger E, Graham A, Kreupl F, et al. Electrochemical functionalization of multi-walled carbon nanotubes for salvation and purification. *Curr Appl Phys* 2002;2:107-11.
82. Villmow T, Potschke P, Pegel S, Haussler L, Kretzschmar B. Influence of twin screw extrusion conditions on the dispersion of multi-walled carbon nanotubes in a poly(lactic acid) matrix. *Polymer* 2008;49:3500-9.
83. Xie S, Li W, Pan Z, Chang B, Sun L. *J Phys Chem Solids* 2000;61:1153.
84. Xie XL, Mai YW, Zhou XP. Dispersion and alignment of carbon nanotubes in polymer matrix: a review. *Mater Sci Eng R* 2005;49:89-112.
85. Yu M-F, Lourie O, Dyer MJ, Moloni K, Kelly TF, Ruoff RS. *Science* 2000;287:637.
86. Yu R, Chen L, Liu Q, Lin J, Tan KL, Ng SC, et al. Platinum deposition on carbon nanotubes via chemical modification. *Chem Mater* 1998;10:718-22.
87. Zhang Q, Rastogi S, Chen D, Lippits D, Lemstra PJ. *Carbon* 2006;44:778.
88. Zhang QH, Chen DJ. Percolation threshold and morphology of composites of conducting carbon black/polypropylene/EVA. *J Mater Sci* 2004;39:1751-7.

89. Zou Y, Feng Y, Wang L, Liu X. Processing and properties of MWCNT/HDPE composites. *Carbon* 2004;42:271-7.
90. Zuiderduin WCJ, Westzaan C, Huetink J, Gaymans RJ (2003) Toughening of polypropylene with calcium carbonate particles. *Polymer* 44:261-275.

VITAE

NAME: Ahmad Akanbi Adewunmi

NATIONALITY: Nigerian

DATE OF BIRTH: September 13, 1980

PLACE OF BIRTH: Ilaro

EMAIL: ahmadadewunmi@yahoo.com

MOBILE: +966535443435

EDUCATION: B.Eng (HONS) Chemical Engineering,
Federal University of Technology, Minna,
Niger State, Nigeria.
2006.

MSc, Chemical Engineering,
King Fahd University of Petroleum & Minerals,
Dhahran 31261, Kingdom of Saudi Arabia.
2011.